Numerical Prediction of the Static Hydrodynamic Derivatives using CFD Techniques

BENZOHRA Abdelmalek

Master Thesis

presented in partial fulfilment

of the requirements for the double degree:

“Advanced Master in Naval Architecture” conferred by University of Liege

"Master of Sciences in Applied Mechanics, specialization in Hydrodynamics, Energetics and Propulsion” conferred by Ecole Centrale de Nantes

developed at "Dunarea de Jos" University of Galati

in the framework of the

Supervisor: Prof. Dan Obreja, "Dunarea de Jos" University of Galati

Lecturer PhD. Oana Marcu, "Dunarea de Jos" University of Galati

Reviewer: Prof. Lionel Gentaz, Ecole Centrale de Nantes

Galati, February 2017

ABSTRACT

Numerical Prediction of the Static Hydrodynamic Derivatives using CFD Techniques

By **BENZOHRA Abdelmalek**

The master thesis was focused on the numerical prediction of the static hydrodynamic derivatives, required to solve the ship manoeuvring problem. The hydrodynamic forces and moments acting on the considered ship (KVLCC2) with the influences of the drift and rudder deflection angles were computed using CFD techniques, in correlation with the standard PMM (Planar Motion Mechanism) static tests. The corresponding hydrodynamic derivatives were calculated and the characteristics of the turning circle and Zig-Zag manoeuvres were estimated on the basis of the simulated ship trajectory.

The master thesis is composed by three main parts:

- The estimation of the preliminary hydrodynamics performance (ship resistance, powering and manoeuvring) using the PHP software platform, developed at the "Dunarea de Jos" University of Galati;
- The computation of the hydrodynamics forces and moments acting on the 1/58 KVLCC2 ship model, during the static drift, static rudder and static drift and rudder motions, using CFD instruments (SHIPFLOW code);
- The simulation of the ship trajectory and the estimation of the turning circle characteristics using the hydrodynamics derivatives obtained on the basis of CFD computation and statistical relations (Clarke, Gedling and Hine).

In the first part, specific methods dedicated to the initial design stage were used: Holtrop-Mennen for ship resistance prediction and propeller series B-Wageningen in order to estimate the hydrodynamic characteristics in open water. From manoeuvrability view point, the Voitkounsky model was used to compute the hydrodynamics of the rudder (including the optimum position of the rudder stock), and the Brix model was dedicated to check the rudder cavitation. Also, Abkowitz model and statistical relations proposed by Lyster and Knights were introduced to estimate the turning circle characteristics.

The second part was dedicated to estimate the hydrodynamics forces and moments acting on the ship with the propeller and rudder deflection influences, using the viscous flow theory (RANS), in deep water condition, for 0.142 Froude number, corresponding to the design speed.

The potential flow theory was applied for wave resistance computation of the bare hull, and the experimental model tests performed by MOERI were used in order to validate this procedure, for a range of Froude numbers between 0.101 and 0.147.

The static drift, static rudder and combined static drift and rudder numerical simulations in viscous flow assumption were done, in the following conditions:

- The static drift angle, β, was varied with 2° step, in the range of -20° to 20°, the rudder being kept in the Center Line;
- The static rudder deflection angle, δ, was varied with 10° step, in the range of -40° to 40°, the hull being kept on the straight ahead course;
- Also, all the static drift and rudder deflection combinations were considered.

The obtained hydrodynamics lateral forces Y were compared with the experimental results provided by MOERI, for static drift and static rudder.

In the last part, the numerical prediction of the static hydrodynamic derivatives and the simulation of the turning circle and Zig-Zag manoeuvres were performed on the basis of two specific codes (POLINEW and PMMPROG) developed at the "Dunarea de Jos" University of Galati. The characteristics of the turning circle and Zig-Zag manoeuvres were determined, the IMO criteria being used to establish the manoeuvring performance of the ship.

In conclusion, the CFD techniques may be introduced in the design process in order to increase the quality of the hydrodynamic performance prognosis, including the manoeuvrability characteristics.

KEY WORDS: ship manoeuvring; static hydrodynamic derivatives; CFD Techniques; KVLCC2 model.

ACKNOWLEDGEMENTS

First I would like to express my gratitude to our coordinator Prof. Philippe RIGO, for giving me the chance to be one of EMShip students.

I would like to give special thanks to my supervisors Prof. Dan Obreja and Lecturer PhD. Oana Marcu, from University of Galati.

I would like also to give special thanks to my supervisor Dipl. Eng. Adrian Presura, from SHIP DESIGN GROUP, Galati, Romania.

I express my enormous gratitude for the scientific team and all professors from EMShip.

I dedicate the following Master Thesis to all parts of my family (my Mother and Sister), my Romanian family (C. Valentina and Darius) and especially, to my uncle Mohammed.

This thesis was developed in the frame of the European Master Course in "Integrated Advanced Ship Design" named "EMSHIP" for "European Education in Advanced Ship Design", Ref.: 159652-1-2009-1-BE-ERA MUNDUS-EMMC.

CONTENTS

List of Figures

List of Tables

DECLARATION OF AUTHORSHIP

I BENZOHRA Abdelmalek declare that this thesis and the work presented in it are my own and have been generated by me as the result of my own original research.

“Numerical Prediction of the Static Hydrodynamic Derivatives using CFD Techniques”

Where I have consulted the published work of others, this is always clearly attributed.

Where I have quoted from the work of others, the source is always given. With the exception of such quotations, this thesis is entirely my own work.

I have acknowledged all main sources of help.

Where the thesis is based on work done by myself jointly with others, I have made clear exactly what was done by others and what I have contributed myself.

This thesis contains no material that has been submitted previously, in whole or in part, for the award of any other academic degree or diploma.

I cede copyright of the thesis in favor of the “Dunarea de Jos” University of Galati.

1. INTRODUCTION

It is known that Very Large Crude Carrier (VLCC) has some problems with manoeuvring characteristics because of their high block coefficient and large inertia forces.

The prediction of the hydrodynamics derivatives necessary to solve the ship manoeuvring problem becomes essential, beginning at the early design stage or the basic design. As a naval architect viewpoint, the manoeuvring problems are closely related to a marine disaster. As a consequence, the prediction of ship manoeuvring trajectory with good accuracy is very important, in order to increase the ship safety in sea conditions and to fulfill the manoeuvring performance standards proposed by the International Maritime Organization (IMO).

To solve manoeuvring problems, different convenient methods may be used, based on:

- Statistics data;
- Model tests results or sea trials at full scale;
- Numerical simulations.

The statistics relations (Lyster and Knights) can be applied to estimate the course keeping and manoeuvring performance at the early design stage, on the basis of ship main dimensions, but the results accuracy depends of the ship type and characteristics.

An expensive method is based on the model tests results obtained in a manoeuvring basin, at basic design stage, or on the basis of sea trials at full scale.

The numerical simulation method can be useful at the early design stage or basic design, because can easily reflect the variation of manoeuvring performances due to the change of hull form, rudder or propeller characteristics. In this case, different hydrodynamics models can be used to express the manoeuvring motions in horizontal plane, based on the hydrodynamic forces and moments acting on the ship hull, rudder and propeller.

The following three main parts were analysed on this thesis:

- Theoretical prediction of the ship resistance, powering and manoeuvring performances of the KVLCC2 ship, typically in the initial design stage was performed on the basis of PHP software platform, developed at “Dunarea de Jos” University of Galati; The hydrodynamic derivatives used in the Abkowitz linear manoeuvring model were calculated using the statistics relations proposed by Clarke, Gedling and Hine;
- Computational Fluid Dynamic (CFD) techniques were applied to calculate the hydrodynamic forces and moments acting on the KVLCC2 hull model, with the influences of the drift and rudder deflection angles, in correlation with typically PMM static tests;

- On the basis of the hydrodynamics forces and moments acting on the KVLCC2 hull model, the static hydrodynamics derivatives were calculated. Also, the ship trajectories during the turning circle and Zig-Zag tests were simulated, using the non-linear Abkowitz model and the specific manoeuvring characteristics were estimated and compared with IMO criteria.

1.1. General information

KRISO (Korea Research Institute for Ships and Ocean Engineering) Very Large Crude Carrier 2, named KVLCC2 is a ship who is selected for the investigation of hydrodynamic forces and moments acting on hull, with the influences of the drift and rudder deflection angles. Generally, the KVLCC2 hull form was used for the investigation of flow physics around hull and for CFD validations of modern tanker ships with bulbous bow [1].

Nowadays, a lot of CFD researchers use this ship type, because of the availability of the existing towing tank model tests results (resistance, powering and manoeuvring).

1.2. Main characteristic and hull geometry

The main characteristics and geometry information can be found using the link mentioned on the references [2]. The model used for the numerical and CFD calculation was proposed and built by MOERI (Maritime and Ocean Engineering Research Institute).

The following tables contain the used information.

Table 1.1 Main ship description and characteristics

Hull Characteristics	Notation & Unity	Full scale	Experimental MOERI model (1/58 scale)
Length between perpendiculars	L_{PP} [m]	320,0	5,52
Length of waterline	L_{WL} [m]	325,5	5,61
Beam	B [m]	58	1
Depth	D [m]	30	0,52
Draught	T [m]	20,8	0,36
Volumetric displacement	[m^3]	312622	1,60
Bare hull wetted surface	S [m^2]	27194	8,08
Block coefficient	C_B	0,8098	0,8098
Midship section coefficient	C_M	0,998	0,998
Longitudinal center of buoyancy from amidships: (+Ahead)	LCB % of LWL	3,48	3,48

Table 1.2 Rudder, propeller characteristics and test conditions

Characteristics	Notation & Unity	Full scale	Experimental MOERI model
Rudder	-	-	-
Type	-	Horn	Horn
Rudder surface	[m²]	273,3	0,081
Lateral area	[m²]	136,7	0,041
Turn rate	[deg/s]	2,34	17,8
Propeller	-	-	-
Type	-	FP	FP
Number of blades	-	4	4
Diameter	[m]	9,86	0,17
Pitch ratio at 0,7 R	-	0,721	0,721
Rotation	-	Right Hand	Right Hand
Hub ratio	-	0,155	0,155
Test Condition	-	-	-
Draught	T [m]	20,8	0,36
Volumetric displacement	[m^3]	312622	1,60
Area including the rudder	S [m²]	27467,3	8,17
Longitudinal center of gravity	LCG [m]	11,1	0,192
GM: Initial metacentric height	[m]	5,71	0,099
Roll radius of gyration	k_{xx}/B [-]	0,4	0,400
Yaw radius of gyration	k_{zz}/L_{PP} [-]	0,25	0,250
Ship Speed			
Design speed	Full scale [Kn], model [m/s]	15,5	1,05
Froude number	-	0,142	0,142

KVLCC2 Hull's form is taken into consideration for the study. Hence, a lines plan must be generated to go further.

1.3.Hull geometry & lines plan

KVLCC2 is selected for the current study. A body lines plan will be generated based on the IGES file for the ship model [2], by the use of Rhino and AutoCAD software.

1.3.1. Generality

Before starting the lines plan drawing a definition of the rule length must be taking into account

It exist two definitions:

- According to Load Lines Regulation (1966)
  a. The length (L) shall be taken as 96% of the total length on a waterline at 85% of the least moulded depth measured from the top of the keel, or as the length from the fore side of the stem to the axis of the rudder stock on that waterline, if that be greater.
  b. For ships without a rudder stock, the length (L) is to be taken as 96% of the waterline at 85% of the least moulded depth.
- According to bureau VERITAS Regulation part B, Ch 1, Sec 2, symbols and definitions
  a. The rule length L is the distance, in m, measured on the summer load waterline, from the fore-side of the stem to the after side of the rudder post, or to the centre of the rudder stock where there is no rudder post. L is to be not less than 96% and need not exceed 97% of the extreme length on the summer load waterline.
  b. In ships without rudder stock (e.g. ships fitted with azimuth thrusters), the rule length L is to be taken equal to 97% of the extreme length on the summer load waterline.
- The length between perpendiculars is taken 97% of the extreme length on the summer load waterline. It is taken according to BV rules definition.

1.3.2. Lines plan

As a naval architect point of view a lines plan drawing is needed to:

- Represent a hull geometry;
- Know the mains dimension;
- Have an overview of some hull coefficients and ratios (geometric ratio);
- Take a look on the smoothness of the hull;
- Have view on the general arrangement (machinery room, spaces for cargo and their arrangement);
- Recognize the efficient hydrodynamic draft;
- Create 3D hull surface and calculate the hydrostatics parameters.

At early design stage, changes are regular to obtain the level for the approval process, going further from the early design stage step and after modifications, the lines plan will become the base of all the design, numerical predictions and CFD calculations.

In general, the geometry created based on the lines plan needs to obey for some requirements. It need to:

- Be convenient and beneficial regarding the incoming flow around the propeller zone and hull resistance;
- Be able to adjust the rudder geometry with required clearances;
- General overview about the seakeeping and manoeuvrability.

The 3-D hull model of the KVLCC2 ship is presented in the following picture and the drawing of the body lines plan is showed on the next page (Figure 1-1).

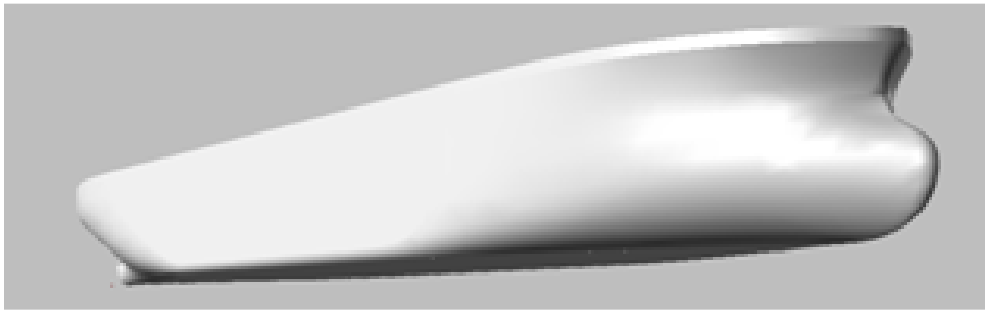

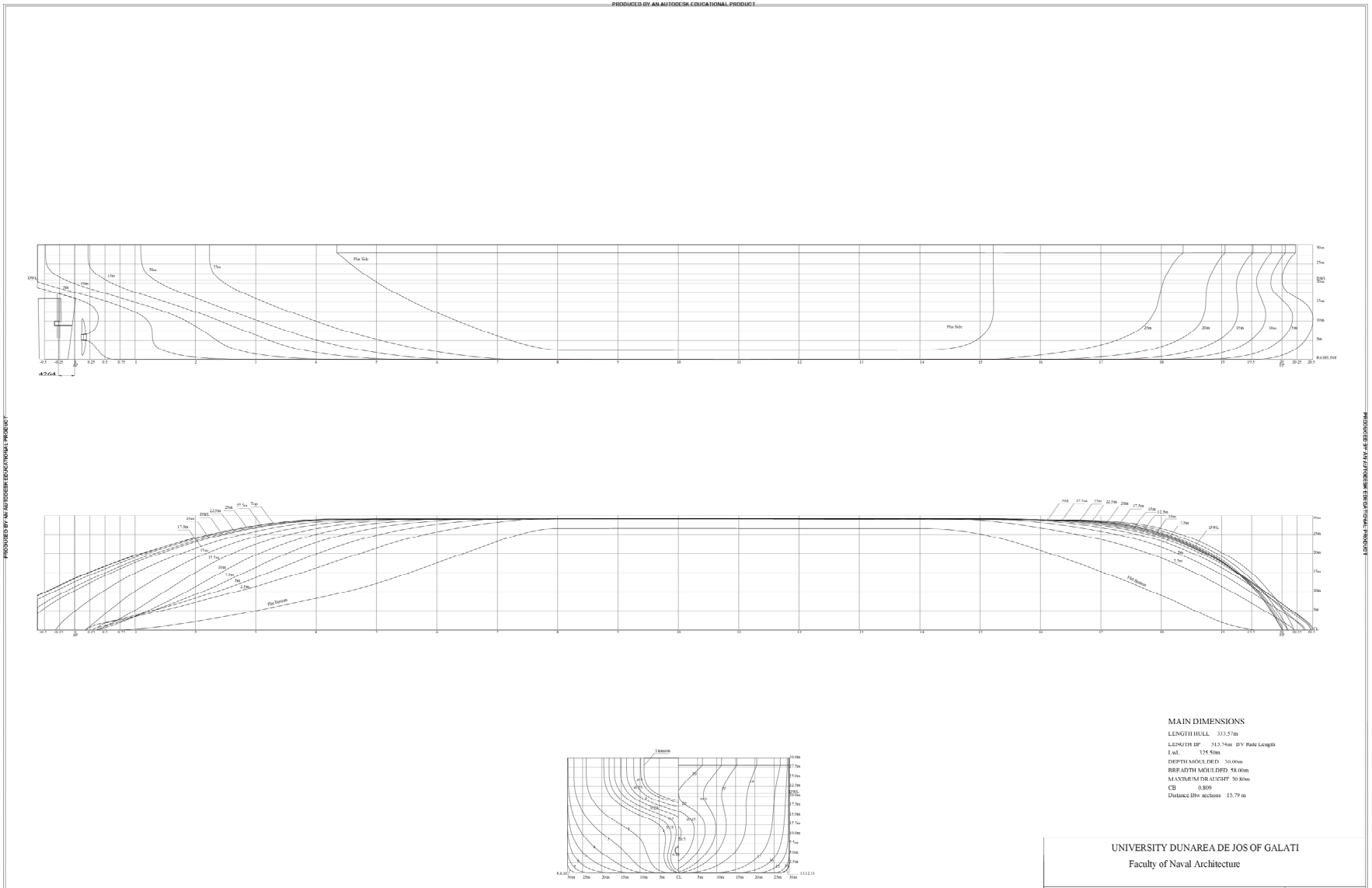

Figure 1-1 Lines plan KVLCC2

1.4. Hull geometry and calculation under NAPA software

1.4.1. Introduction

Hydrostatics calculation and Bonjean curve will be computed using NAPA software. To do that, a 3D hull surface made based on the lines plan using Rhino software will be introduced as IGES file to NAPA. It should be mentioned here that is necessary to know the main particularities of the ship.

Based on ship dimension and the hull introduced to NAPA software, the calculation can be done easily.

Observations:

- The draft taking for this study is the same mentioned in the references, T=20.8m;
- The obtained information for hydrostatics parameters will be represented and checked with references;
- Bonjean curve will be computed at the end.

1.4.2. Hydrostatics parameters calculation under NAPA software

NAPA software is divided on different subsystems. To calculate hydrostatics parameters under NAPA, it is needed to pass by the following steps:

- Import the IGES geometry under **geometry (GM)** application subsystem;
- Input geometry parameters and main dimensions under **ship model (SM)** application subsystem;
- Calculate the hydrostatics parameter under **hydrostatics (HD)** application subsystem.

The subsystem used for the hydrodynamics calculations contains all the function necessary for plotting different parameters calculated from the hull form introduced under **geometry (GM)** application subsystem.

The results are obtained by varying draft with fixed step of 0.4 m, from initial draft of 0.4 m to final draft of 26 m.

The hydrostatics parameters are calculated taking into consideration that:

- The ship is in upright position;
- The heel is fixed at zero;
- The trim is fixed at zero (no trim).

The displacement, the longitudinal centre of buoyancy and other hydrostatics parameters are calculated and presented in the following tables.

Table 1.3 Hydrostatic parameters -1-

T	Disp	LCB[m]	CB	WLA	Cw	LCF	VOLT
0,4	4746	177,11	0,6067	11774,3	0,6323	176,84	4630,3
0,8	9693,6	176,92	0,6275	12322,7	0,6621	176,68	9457,2
1,2	14829,5	176,82	0,6427	12711,7	0,6831	176,63	14467,8
1,6	20106,9	176,76	0,6549	13019	0,6997	176,55	19616,5
2	25497,7	176,71	0,6653	13267,3	0,7131	176,5	24875,8
2,4	30980,7	176,67	0,6742	13469,7	0,724	176,44	30225,1
2,8	36539,9	176,63	0,682	13640,3	0,7332	176,4	35648,7
3,2	42165,1	176,60	0,6889	13790,8	0,7413	176,36	41136,6
3,6	47848,7	176,57	0,6952	13925,9	0,7486	176,34	46681,6
4	53584,6	176,54	0,7009	14049,1	0,7552	176,33	52277,7
4,4	59368,8	176,52	0,7061	14161,4	0,7613	176,31	57920,7
4,8	65197,3	176,50	0,7109	14264,7	0,7668	176,29	63607,1
5,2	71066,4	176,48	0,7155	14360,1	0,772	176,25	69333
5,6	76973,5	176,45	0,7197	14448,8	0,7767	176,21	75096,1
6	82915,5	176,43	0,7236	14531,5	0,7812	176,15	80893,2
6,4	88890,5	176,41	0,7274	14608,7	0,7853	176,07	86722,5
6,8	94896,5	176,38	0,7309	14681,4	0,7893	175,97	92581,9
7,2	100930,8	176,35	0,7343	14750,3	0,793	175,86	98469
7,6	106992,7	176,32	0,7374	14816,1	0,7965	175,72	104383,1
8	113081,5	176,29	0,7405	14880	0,7999	175,56	110323,4
8,4	119196,3	176,25	0,7434	14941,9	0,8033	175,37	116289,1
8,8	125336,5	176,20	0,7462	15002,2	0,8065	175,17	122279,5
9,2	131501,4	176,15	0,7489	15061,3	0,8097	174,93	128294
9,6	137690,5	176,09	0,7515	15119,6	0,8128	174,68	134332,2
10	143903,5	176,02	0,7541	15177,2	0,8159	174,4	140393,7
10,4	150139,6	175,95	0,7565	15235	0,819	174,08	146477,7
10,8	156399	175,87	0,7589	15292,4	0,8221	173,74	152584,4
11,2	162682,8	175,78	0,7612	15349,7	0,8252	173,36	158714,9
11,6	168989,9	175,68	0,7635	15407,2	0,8283	172,95	164868,2
12	175320,3	175,57	0,7657	15464,9	0,8314	172,52	171044,2
12,4	181674,3	175,46	0,7679	15523,2	0,8345	172,05	177243,2
12,8	188052	175,34	0,77	15581,6	0,8377	171,57	183465,4
13,2	194453,5	175,20	0,7721	15640,8	0,8409	171,05	189710,7
13,6	200879,1	175,06	0,7742	15699,7	0,844	170,51	195979,6

Table 1.4 Hydrostatic parameters -2-

T	Disp	LCB[m]	CB	WLA	Cw	LCF	VOLT
14	207329,2	174,91	0,7762	15758,7	0,8472	169,93	202272,4
14,4	213803,5	174,75	0,7782	15818,1	0,8504	169,32	208588,8
14,8	220302,3	174,58	0,7802	15878,6	0,8536	168,67	214929,1
15,2	226826,4	174,40	0,7822	15939,9	0,8569	168,01	221294
15,6	233375,4	174,21	0,7842	15999,6	0,8601	167,34	227683,3
16	239948,5	174,02	0,7861	16061,9	0,8635	166,64	234096,1
16,4	246547,3	173,81	0,7881	16123,4	0,8668	165,95	240534
16,8	253171,7	173,59	0,79	16183,2	0,87	165,27	246996,8
17,2	259822	173,37	0,7919	16243,3	0,8732	164,6	253484,9
17,6	266493,6	173,14	0,7938	16306,5	0,8766	163,91	259993,8
18	273187	172,91	0,7956	16371,2	0,8801	163,25	266523,9
18,4	279911,9	172,67	0,7975	16435,2	0,8836	162,63	273084,8
18,8	286664	172,43	0,7994	16498,3	0,887	162,05	279672,2
19,2	293441	172,18	0,8012	16558,6	0,8902	161,51	286283,9
19,6	300241,2	171,93	0,8031	16612,3	0,8931	161,06	292918,3
20	307062,4	171,69	0,8049	16660,9	0,8957	160,69	299573,1
20,4	313902,8	171,44	0,8067	16705,1	0,8981	160,38	306246,7
20,8	320760,2	171,20	0,8085	16745,5	0,9003	160,12	312936,8
21,2	327633,5	170,97	0,8102	16781,8	0,9022	159,91	319642,4
21,6	334520,9	170,74	0,812	16815	0,904	159,74	326361,8
22	341421,3	170,52	0,8136	16845,8	0,9057	159,61	333094
22,4	348334	170,30	0,8153	16874,2	0,9072	159,53	339838
22,8	355257,9	170,09	0,8169	16900,7	0,9086	159,48	346593,1
23,2	362192,3	169,89	0,8185	16925,5	0,91	159,45	353358,3
23,6	369136,5	169,69	0,8201	16948,6	0,9112	159,46	360133,2
24	376089,8	169,50	0,8216	16970	0,9124	159,49	366916,9

Notations:

T	Draught, moulded	[m]
Disp	Total displacement in salt water 1.025 t/cum	[t]
LCB	Longitudinal centre of buoyancy from FR0	[m]
C_B	Block coefficient	--
WLA	Wetted surface area	[m²]
C_W	Waterplane area coefficient	--
LCF	Longitudinal centre of flotation	[m]
VOLT	Volumetric displacement	[m^3]

1.4.3. Hydrostatics parameters checking

A comparison between the hydrostatics characteristics at design draught obtained by NAPA software and the benchmark is presented in the following table.

Table 1.5 Comparison between NAPA and benchmark

Main particulars	NAPA	Benchmark	Error
Disp (m3)	312936,8	312622,0	-0,10%
S –without- rudder (m2)	27302,0	27194,0	-0,40%
CB	0,8085	0,8098	0,16%
CM	0,9980	0,9980	0,00%
LCB (%)	3,442	3,480	1,09%

The results obtained by NAPA software regarding the main particulars of the ship are suitable. The hydrostatic drawings are represented in Figure 1-2.

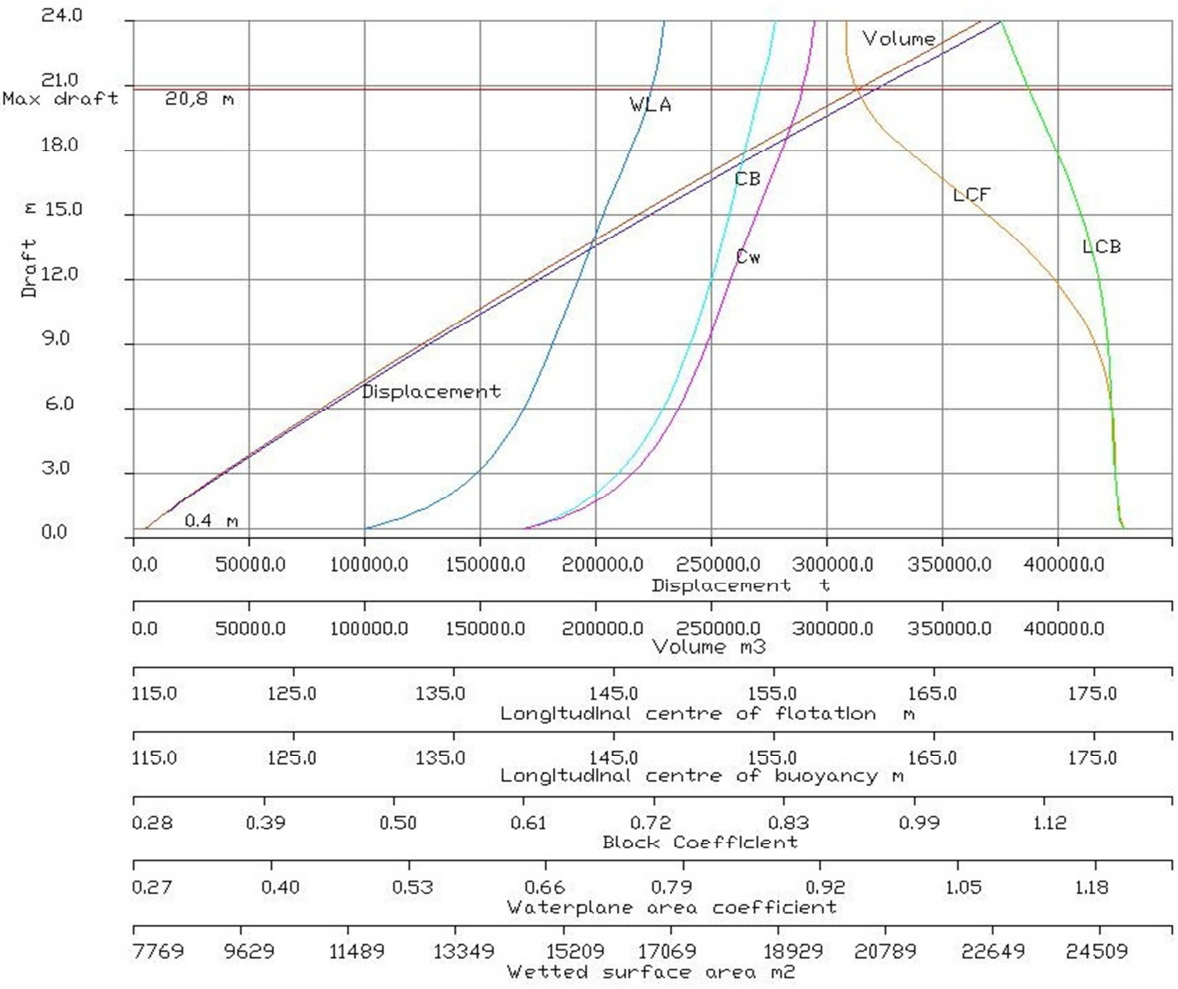

Figure 1-2 Hydrostatic parameters KVLCC2

The hydrostatics analysis contains, also, the Bonjean curves which are generated at each station corresponding to the ship design grid, showing the area variation with draft.
The results are represented on the Figure 1.3.

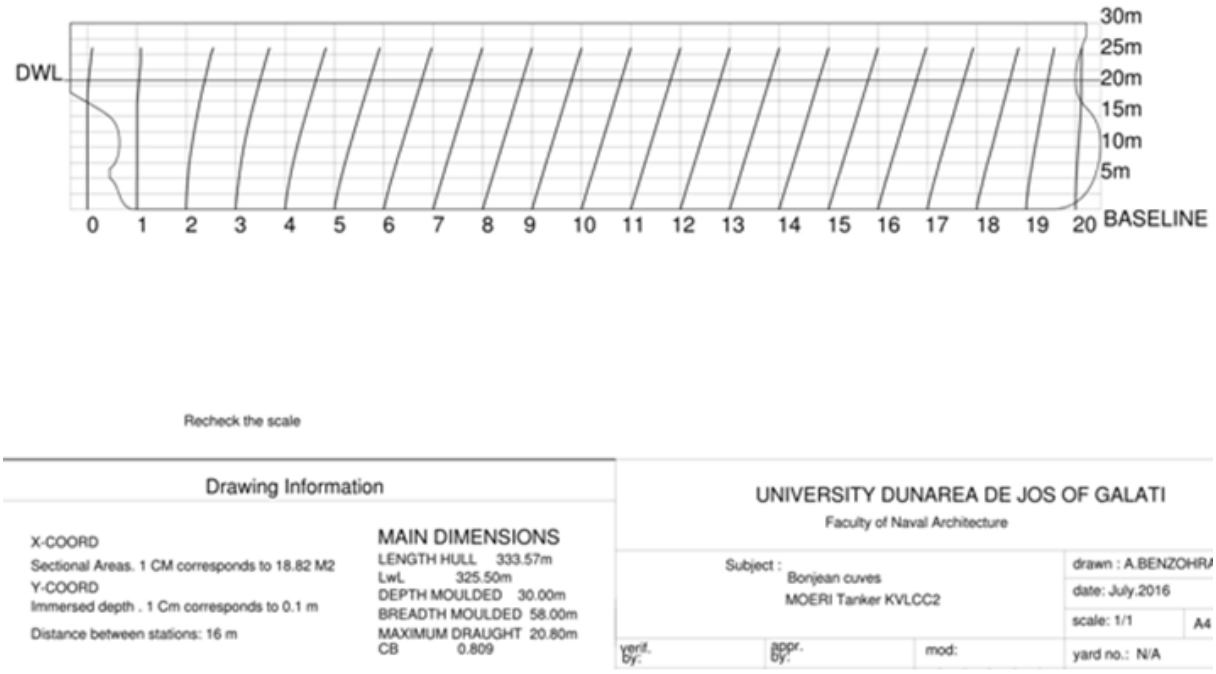

Figure 1-3 Bonjean curves drawing

It should be mentioned here that the numerical data are represented on the **APPENDIX 1.1 Bonjean curves numerical results**.
Also, the Bonjean diagram is represented on the **APPENDIX 1.2 Bonjean curves drawing**.

2. PRELIMINARY HYDRODYNAMICS PERFORMANCES (PHP) SOFTWARE PLATFORM

Ship resistance, powering and manoeuvring are the most important hydrodynamics performances which are necessary to be estimated, with good accuracy, beginning with initial design stage.

The *ship resistance* can be defined as the total force that the ship overcomes as is moves through the water.

In the early design stage, it would be impossible to determine the ship resistance on the basis of the experimental model tests in towing tanks, due to the lack of parameters on this step of design and the expensive prices of the model tests. As a consequence, in order to estimate the ship resistance a lot of software platforms were developed in the world, different methods being applied, depending of the ship type, hull forms, speed domain, etc.:

- Traditional and standard series methods (Taylor, Ayre, Guldhammer-Harvald, Series 60, SSPA, Japanese, Coaster series, etc.);
- Regression methods (Scott, Holtrop);
- Computational Fluid Dynamic (CFD).

Regarding the *propeller characteristics*, the Wageningen B-series, Gawn series or ducted propellers can be applied in order to define the hydrodynamics characteristics in open water condition.

On the basis of ship resistance and propeller characteristics, the *ship powering performance* may be estimated and the delivered power or brake power can be calculated according with MS (service margins) and MCR (maximum continuous rating) conditions.

Regarding the *manoeuvring information*, the rudder hydrodynamics performances, the ship stability on route and the manoeuvring performances are necessary to be known beginning with the early design stage.

A *preliminary hydrodynamic performance software platform (PHP)* was developed at University of Galati, in order to determine ship hydrodynamic performances (ship resistance, open water propeller characteristics, powering and manoeuvring) at initial design stage. It's necessary to analyse the main characteristics of the ship for the selection of a suitable method.

2.1.PHP Resistance (Holtrop-Mennen)

The prediction of the resistance is done based on statistical methods for the majority of large ships and VLCC. In order to predict KVLCC2 ship resistance at early design stage, the **Holtrop-Mennen method** was selected.

a. Holtrop- Mennen restrictions

The **Holtrop-Mennen** method used for ship resistance calculation has some restrictions. To start the calculations with **Holtrop-Mennen** method, it is necessary to check if the KVLCC2 ship data fulfil these restrictions, presented in the following table.

Table 2.1 Holtrop-Mennen method restrictions regarding KVLCC2

Ship Type	Froude number limitation	Cp		L_{WL}/B		B/T	
		Min	Max	Min	Max	Min	Max
Tanker and bulk carriers	Fn<=0,24	0,73	0,85	5,10	7,10	2,40	3,20
Container ships and destroyers	Fn<=0,45	0,55	0,67	6,00	9,50	3,00	4,00
Trawlers, coastal ships and tugs	Fn<=0,38	0,55	0,65	3,90	6,30	2,10	3,00
KVLCC2	0,142	0,81		5,61		2,79	

Observations:

- All the restrictions are fulfilled in the case of KVLCC2 ship;
- It should mention, here, that the statistical methods results cannot replace the experimental model tests results, which have the best accuracy referring the ship resistance prognosis;
- The statistical ship resistance methods give a lot of theoretical results necessary to advance further calculations referring the powering the manoeuvring characteristics.

b. KVLCC ship resistance prediction using Holtrop-Mennen method

Taking into consideration the method restrictions, our project is suitable for the use of the **Holtrop-Mennen** method. Consequently, to advance in preliminary ship resistance calculation we employ the main dimensions and hydrostatic parameters for KVLCC2, to estimate the total ship resistance using the **Holtrop-Mennen** method, from PHP software platform (see the relation 2.1). The input data are presented in Table 2.2 and the output data in Tables 2.3-2.5. Figure 2.1 depicts the total ship resistance versus Froude number.

Table 2.2 Input data for ship resistance (Holtrop-Mennen method) using PHP software platform

Hydrostatics parameters		
HULL CHARACTERISTICS	Input	Notation & Unity
Length of waterline	325,50	L_{WL} [m]
Beam	58,00	B [m]
Draught	20,80	T [m]
Fore draught	20,80	TF [m]
Aft draught	20,80	TA [m]
Longitudinal center of buoyancy from amidships: (+Ahead)	3,44%	LCB % of LWL
Volumetric displacement	312936,80	V [m3]
Waterplane coefficient	0,887	C_W
Longitudinal prismatic coefficient	0,810	C_P
Transom wetted area	13,90	ATR [m²]
Bare hull wetted surface	27302,00	S [m²]
Half entrance angle	52,00	iE [deg]
Stern shape coefficient : U-shaped sections	7	cpp
Bulb transverse area at F.P.	173,20	ABT [m²]
Height of bulb centroid from B.L.	9,10	hB [m]
APPENDAGES CHARACTERISTICS		
Rudder behind stern		
Area	136,70	[m²]
Form factor	1,50	
PROPULSION TYPE		
Single screw with conventional stern		
Propeller diameter	9,86	[m]
Blade area ratio	0,431	
SHIP SPEED		
Minimum speed	10,00	[Knots]
Design speed	15,50	[Knots]
Maximum speed	18,00	[Knots]
Speed increment	0,50	[Knots]
WATER PROPERTIES		
Water density	1.025	[t/m^3]
Kinematic viscosity	1.18831E-6	[m²/s]

Remarques:

- It should be mentioned that zero trim was considered in calculation;
- Regarding the propeller blade area ratio, A_e/A_0, we take into consideration the codes limitation, the minimum input blade ratio area is 0.55.

Table 2.3 Ship resistance coefficients .vs. speed, using PHP Resistance (Holtrop-Mennen)

V [kn]	V [m/s]	Fn	Rn(*10^-9)	C_F	C_{PV}	C_W	C_A
10	5,14	0,091	1,409	0,001467	0,000509	0	0,000228
10,5	5,4	0,096	1,48	0,001459	0,000506	0,000001	0,000228
11	5,66	0,1	1,55	0,001451	0,000503	0,000001	0,000228
11,5	5,92	0,105	1,621	0,001443	0,000501	0,000002	0,000228
12	6,17	0,109	1,691	0,001436	0,000498	0,000003	0,000228
12,5	6,43	0,114	1,761	0,001428	0,000496	0,000006	0,000228
13	6,69	0,118	1,832	0,001422	0,000493	0,000009	0,000228
13,5	6,95	0,123	1,902	0,001415	0,000491	0,000013	0,000228
14	7,2	0,127	1,973	0,001409	0,000489	0,00002	0,000228
14,5	7,46	0,132	2,043	0,001403	0,000487	0,000028	0,000228
15	7,72	0,137	2,114	0,001398	0,000485	0,000039	0,000228
15,5	7,97	0,141	2,184	0,001392	0,000483	0,000054	0,000228
16	8,23	0,146	2,255	0,001387	0,000481	0,000072	0,000228
16,5	8,49	0,15	2,325	0,001382	0,00048	0,000094	0,000228
17	8,75	0,155	2,396	0,001377	0,000478	0,000121	0,000228
17,5	9	0,159	2,466	0,001373	0,000476	0,000154	0,000228
18	9,26	0,164	2,536	0,001368	0,000475	0,000193	0,000228

Notations:

- Fn = Froude number;
- Rn = Reynolds number;

Ship resistance coefficients

- C_F = friction resistance coefficient;
- C_{PV} = viscous pressure resistance coefficient ;
- C_W = wave resistance coefficient;
- C_A = model-ship correlation resistance coefficient.

Table 2.4 Decomposition of KVLCC2 ship resistance (Holtrop-Mennen)

V[kn]	*V*[m/s]	R_F[kN]	R_{PV}[kN]	R_{APP}[kN]	R_W[kN]	R_B[kN]	R_{TR}[kN]	R_A[kN]
10	5,14	543,43	188,56	4,08	0,11	19,41	13,05	84,8
10,5	5,4	595,59	206,66	4,47	0,24	21,82	13,02	93,49
11	5,66	650	225,54	4,88	0,51	24,34	12,8	102,61
11,5	5,92	706,63	245,19	5,31	0,99	26,96	12,36	112,15
12	6,17	765,48	265,61	5,75	1,84	29,69	11,68	122,11
12,5	6,43	826,54	286,8	6,21	3,25	32,51	10,75	132,5
13	6,69	889,8	308,75	6,68	5,52	35,4	9,54	143,32
13,5	6,95	955,25	331,46	7,17	9,03	38,38	8,04	154,55
14	7,2	1022,87	354,92	7,68	14,27	41,42	6,23	166,21
14,5	7,46	1092,67	379,14	8,21	21,91	44,51	4,09	178,3
15	7,72	1164,63	404,11	8,75	32,72	47,66	1,61	190,8
15,5	7,97	1238,74	429,83	9,3	47,68	50,85	0	203,74
16	8,23	1315,01	456,29	9,88	67,94	54,07	0	217,09
16,5	8,49	1393,41	483,49	10,47	94,85	57,33	0	230,87
17	8,75	1473,95	511,44	11,07	129,97	60,61	0	245,08
17,5	9	1556,61	540,12	11,69	175,07	63,91	0	259,71
18	9,26	1641,39	569,54	12,33	232,14	67,22	0	274,76

Notations:

Ship resistance

- R_F = friction resistance;
- R_{PV} = viscous pressure resistance;
- R_{APP} = appendages resistance;
- R_W = wave resistance;
- R_B = additional fore bulb's resistance;
- R_{TR} = additional wetted transom's resistance;
- R_A = model-ship correlation resistance;
- R_T = total ship resistance, computed using the following relation:

$$R_T = R_F(1+k_1) + R_{APP} + R_W + R_B + R_{TR} + R_A \tag{2.1}$$

where, $1+k_1 = 1.5$ represents the form factor.

Ship Propulsion

- P_E = effective power;
- w = wake fraction;

- t = thrust deduction fraction;
- ETAH = hull efficiency;
- ETAR = relative rotative efficiency.

Table 2.5 Total resistance, effective power and propulsion coefficients

v[kn]	v[m/s]	RT[kN]	Thrust[kN]	PE[kW]	w	t	ETAH	ETAR
10	5,14	853,44	1103,63	4390,46	0,451	0,227	1,408	1,021
10,5	5,4	935,3	1209,5	5052,2	0,451	0,227	1,407	1,021
11	5,66	1020,67	1319,89	5775,87	0,45	0,227	1,406	1,021
11,5	5,92	1109,59	1434,89	6564,48	0,45	0,227	1,405	1,021
12	6,17	1202,17	1554,6	7421,39	0,449	0,227	1,404	1,021
12,5	6,43	1298,56	1679,25	8350,46	0,449	0,227	1,404	1,021
13	6,69	1399,01	1809,15	9356,3	0,449	0,227	1,403	1,021
13,5	6,95	1503,88	1944,76	10444,43	0,448	0,227	1,402	1,021
14	7,2	1613,61	2086,66	11621,6	0,448	0,227	1,401	1,021
14,5	7,46	1728,83	2235,65	12896,09	0,448	0,227	1,4	1,021
15	7,72	1850,28	2392,71	14277,96	0,448	0,227	1,4	1,021
15,5	7,97	1980,14	2560,64	15789,4	0,447	0,227	1,399	1,021
16	8,23	2120,28	2741,86	17452,24	0,447	0,227	1,398	1,021
16,5	8,49	2270,42	2936,02	19272,09	0,447	0,227	1,398	1,021
17	8,75	2432,11	3145,12	21270,18	0,446	0,227	1,397	1,021
17,5	9	2607,11	3371,41	23471,21	0,446	0,227	1,397	1,021
18	9,26	2797,38	3617,46	25903,73	0,446	0,227	1,396	1,021

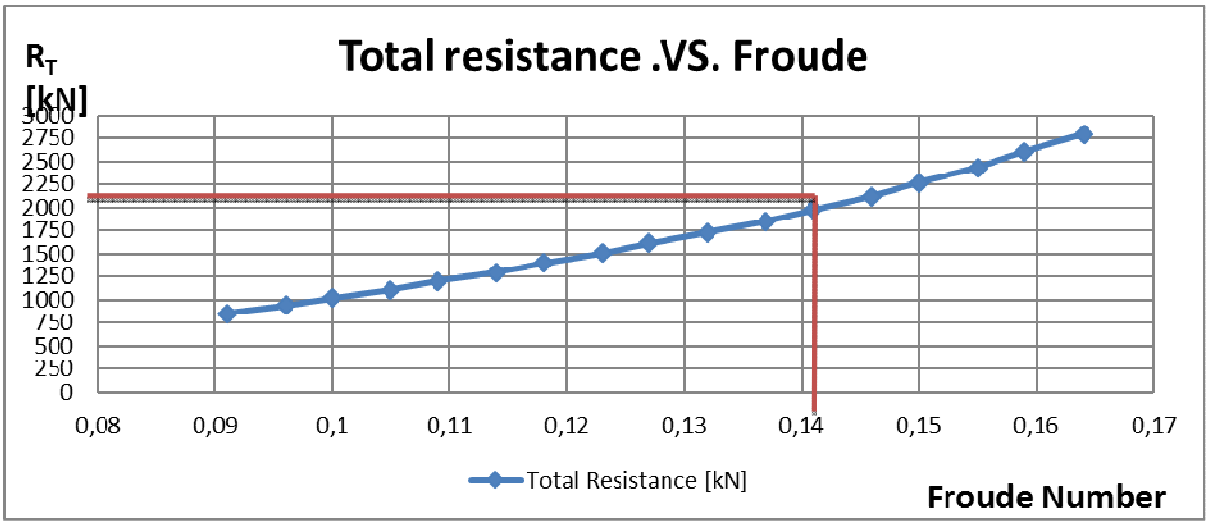

Figure 2-1 Total ship resistance .vs. Froude number

Discussion:

- The graph above represents the estimated total ship resistance using **Holtrop-Mennen** prediction;

- For the design speed of 15.5 Knots (Froude number equal to 0.141) the predicted ship resistance is about 1980.14 kN.

In the next step, in correlation with benchmark and only for preliminary design stage, the total ship resistance may be evaluated using the design margins condition M_D=0.1 [7], in order to increase the estimation accuracy of the total ship resistance (see Figure 2-2).

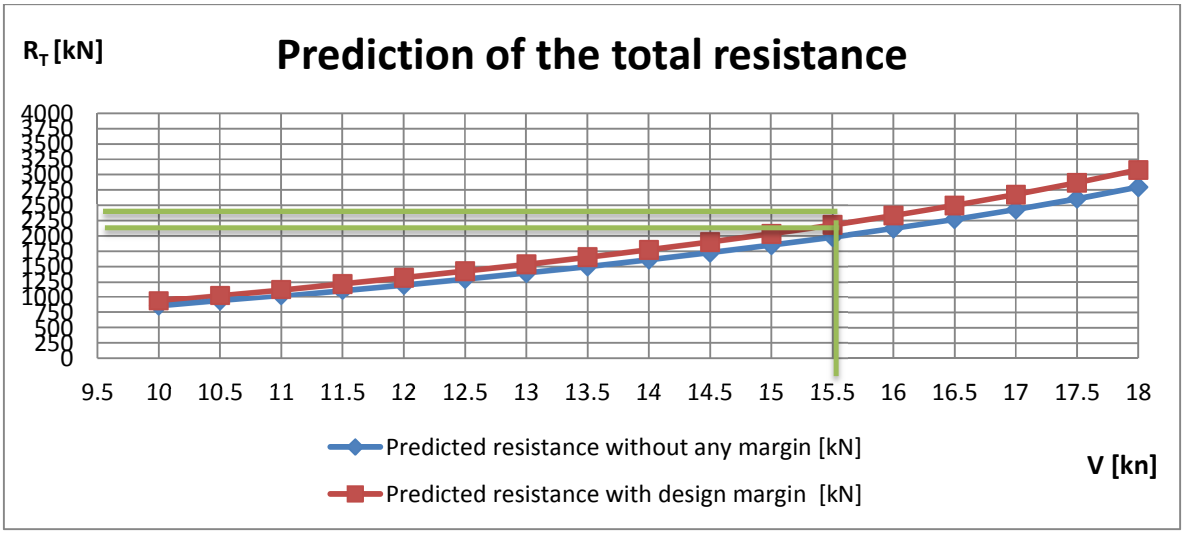

Figure 2-2 Predicted total resistance with and without design margin (full scale model)

Table 2.6 Total resistance using the design margin

V[kn]	R_T[kN]	Service margin	R_T[kN] with design margin
10	853,44	85,344	938,784
10,5	935,3	93,53	1028,83
11	1020,67	102,067	1122,737
11,5	1109,59	110,959	1220,549
12	1202,17	120,217	1322,387
12,5	1298,56	129,856	1428,416
13	1399,01	139,901	1538,911
13,5	1503,88	150,388	1654,268
14	1613,61	161,361	1774,971
14,5	1728,83	172,883	1901,713
15	1850,28	185,028	2035,308
15,5	1980,14	198,014	2178,154
16	2120,28	212,028	2332,308
16,5	2270,42	227,042	2497,462
17	2432,11	243,211	2675,321
17,5	2607,11	260,711	2867,821
18	2797,38	279,738	3077,118

2.2. PHP Powering

One of the main problems at the preliminary design stage is the determination of the propulsive power of the ship. For that raison, at this design stage it is essential for the naval architect to settle the power required for the ship to overcome its resistance. The power required to maintain the ship design speed through the water relies on the resistance given by the water and the air [3].

a. Preliminary hydrodynamics performance (PHP) powering software

To go further in the power prediction calculations, it's essential to use the ship resistance results, obtained using Holtrop-Mennen method, as input data (see Table 2.7). Also, the additional PHP Powering input data are presented in the Table 2.8. The output data are presented in the Table 2.9.

Table 2.7 PHP Powering input data (ship with one propeller)

V [KN]	V [m/s]	F_n	R_T [kN]	w	t	etaH	etaR
10	5,144	0,091	853,438	0,451	0,227	1,408	1,021
10,5	5,402	0,096	935,304	0,451	0,227	1,407	1,021
11	5,659	0,1	1020,673	0,45	0,227	1,406	1,021
11,5	5,916	0,105	1109,594	0,45	0,227	1,405	1,021
12	6,173	0,109	1202,169	0,449	0,227	1,404	1,021
12,5	6,431	0,114	1298,56	0,449	0,227	1,404	1,021
13	6,688	0,118	1399,015	0,449	0,227	1,403	1,021
13,5	6,945	0,123	1503,877	0,448	0,227	1,402	1,021
14	7,202	0,127	1613,614	0,448	0,227	1,401	1,021
14,5	7,459	0,132	1728,827	0,448	0,227	1,4	1,021
15	7,717	0,137	1850,275	0,448	0,227	1,4	1,021
15,5	7,974	0,141	1980,138	0,447	0,227	1,399	1,021
16	8,231	0,146	2120,277	0,447	0,227	1,398	1,021
16,5	8,488	0,15	2270,421	0,447	0,227	1,398	1,021
17	8,746	0,155	2432,113	0,446	0,227	1,397	1,021
17,5	9,003	0,159	2607,108	0,446	0,227	1,397	1,021
18	9,26	0,164	2797,379	0,446	0,227	1,396	1,021

Table 2.8 PHP Powering additional input data

Propeller diameter (Dp)	9,86 [m]
Blades number (z)	4
Expanded blade area ratio (Ae/A0)	0,55
Pitch ratio (P/D)	0,69
Shaft efficiency (η_{ax})	0,97

Gear efficiency (η_{red})	1,00
Service margin (M_S)	0,15
Design margin (M_D)	0,10
Maximum continuous rating (MCR):	100 %

Term used for the calculation:

- w = Wake fraction;
- t = Thrust deduction fraction;
- etaH = Hull efficiency;
- etaR = Relative rotative efficiency;
- eta0 = Propeller efficiency in open water;
- etaD = Quasipropulsiv coefficient.

Regarding the propulsion term:

- P_E = Effective Power;
- P_D = Delivered Power;
- P_B = Break Power.

Table 2.7 PHP Powering output data (effective, delivered and break power)

V [Kn]	V [m/s]	Fn	eta0	etaD	RPM [rpm]	P_E[kW]	P_D [kW]	P_B [kW]
10	5,144	0,091	0,482	0,694	47,283	4829,509	6963,719	8445,991
10,5	5,402	0,096	0,484	0,695	49,515	5557,421	7997,953	9700,368
11	5,659	0,1	0,485	0,696	51,741	6353,46	9126,932	11069,657
11,5	5,916	0,105	0,486	0,697	53,964	7220,932	10355,337	12559,536
12	6,173	0,109	0,487	0,698	56,185	8163,528	11688,598	14176,59
12,5	6,431	0,114	0,488	0,699	58,408	9185,511	13133,237	15928,729
13	6,688	0,118	0,489	0,7	60,639	10291,928	14697,28	17825,688
13,5	6,945	0,123	0,49	0,701	62,882	11488,87	16390,747	19879,62
14	7,202	0,127	0,49	0,701	65,145	12783,764	18226,214	22105,778
14,5	7,459	0,132	0,491	0,702	67,437	14185,695	20219,44	24523,275
15	7,717	0,137	0,491	0,701	69,769	15705,755	22390,059	27155,924
15,5	7,974	0,141	0,491	0,701	72,172	17368,337	24783,427	30058,735
16	8,231	0,146	0,49	0,7	74,669	19197,459	27444,454	33286,179
16,5	8,488	0,15	0,489	0,698	77,248	21199,301	30383,998	36851,422
17	8,746	0,155	0,487	0,695	79,923	23397,196	33646,558	40808,439
17,5	9,003	0,159	0,486	0,692	82,711	25818,336	37284,981	45221,323
18	9,26	0,164	0,483	0,689	85,627	28494,101	41361,508	50165,564

Remarques:

- It has been assumed that the gear box does not exist and the main engine is used for both ahead and astern speed;
- The wake fraction (w) and the thrust deduction coefficients (t) were performed by Holtrop-Mennen method;
- The following relations were applied in order to calculate the powering components:

$$P_E = R_T \cdot v \cdot (1 + M_D) \tag{2.2}$$

$$P_D = \frac{P_E}{\eta_D} \tag{2.3}$$

$$P_B = \frac{P_D}{\eta_{ax} \cdot \eta_{red} \cdot (1 - M_S)} \tag{2.4}$$

where, v is the ship speed and η_D is the quasipropulsiv coefficient.

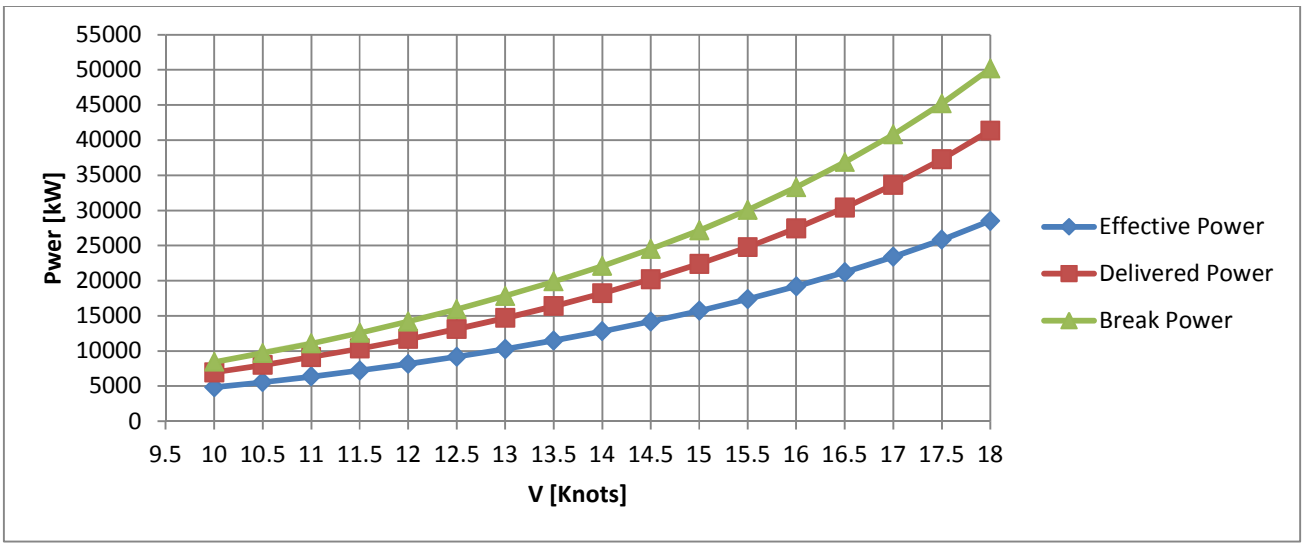

Figure 2-3 Effective, delivered and break power of the ship

Discussion:

Using the PHP software platform for power prediction, we found that for the design speed of 15.5 Knots:

- The break power is P_B = 30058,735 [kW];
- The delivered power is P_D =24783,427 [kW];
- The effective power is P_E =17368,337 [kW].

A linear regression method is done in order to check the suitability of the results.

b. Regression method

In order to check the range of break power needed to maintain required speed, for such kind of big ships, a linear regression method was applied.

1. Ships selection

Four ships having similar characteristics (speed, length and deadweight) were used in order to determine the brake power data (see **APPENDIX 2.1 Ship Selection (regression method)**). The diagram of the brake power depending of the ship speed was depicted in the following figure.

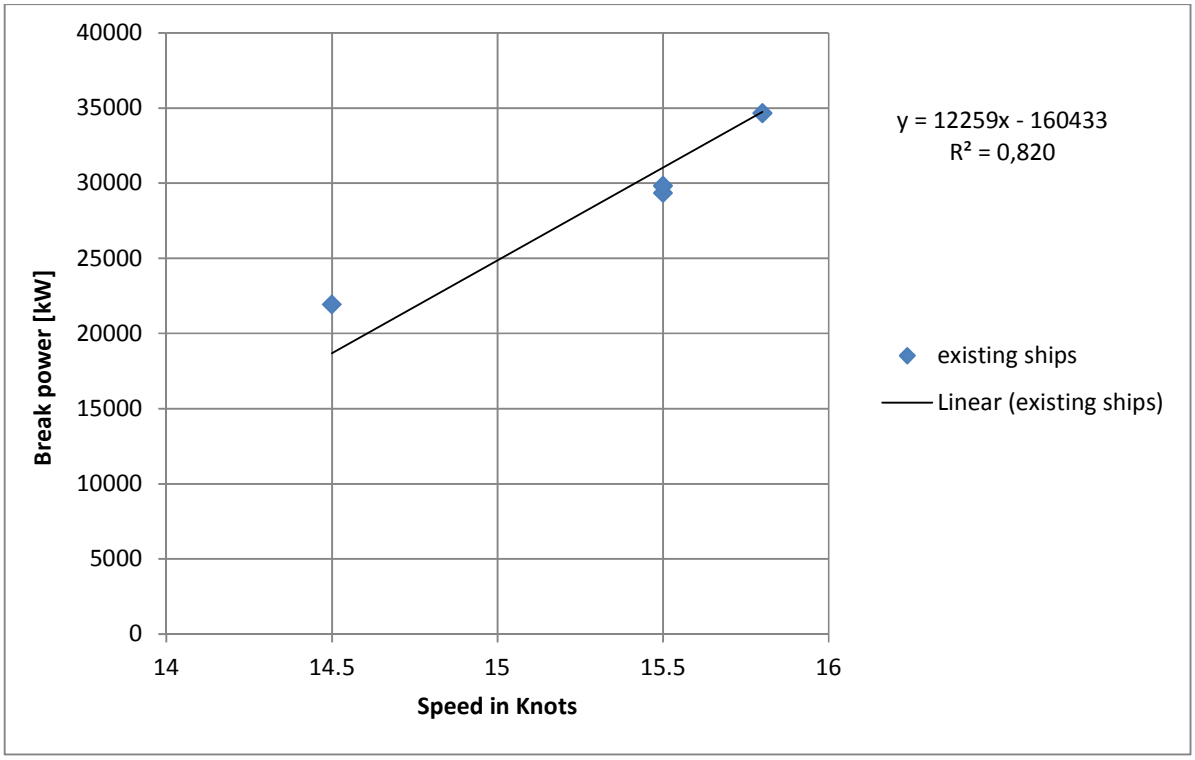

Figure 2-4 Graphic representation of the regression method - brake power .vs. speed in knots

Discussion:

- From the graph results the linear regression fits with 82 %;
- The linear relation for existing ships (break power [kW] .vs. speed [knots]) can be used to estimate the break power on the KVLCC2;

- Using the KVLCC2 service speed of 15.5 Knots as an input in the linear relation, an estimated value of the break power P_B=29581,5 kW was determined.
- A good agreement between PHP Powering software and regression method results may be observed in the following table.

Table 2.8 Comparison between Regression method and PHP software platform results

Regression method [kW]	PHP prediction [kW]	Error
P_B=29581,50	P_B=30058,74	1,59%

- The Holtrop-Mennen method used in order to compute the KVLCC2 ship resistance and propulsive coefficients is suitable and provides reliable results for initial ship design stage.

2.3. PHP Rudder hydrodynamics

According to Oxford dictionaries definitions, a rudder is a flat piece hinged vertically near the stern of a boat or ship for steering.

Rudders are commonly used for different types of ships. The height of the rudder can be usually comprise between 40 cm, for the case of an underwater vehicle and about 9 m (with weight over 80 tonnes) for a large container ships [4].

Rudder objective

The main role of rudder is to provide course-keeping ad manoeuvering performances.

2.3.1. Rudder design and characteristics

A rudder is a hydrodynamic profile which turns about a vertical axis. Conventionally, it is located in the stern of the ship in order to use the incoming water flow from the propeller to produce a transverse force and turning moment about the ship centroid.

Rudders are adapted for each distinct ship, because its designed geometry and characteristics have significant effect on the ship manoeuvering performances.

a. Rudder characteristics:

- The semi-balanced rudder profile developed by MOERI is NACA 0018;
- The scale factor for model is 1/58;
- Additional rudder characteristics were summarized on the following table.

Table 2.9 Rudder characteristics

Full scale rudder			
Rudder area	A_R	136.7	[m^2]
Percentage of lateral area	A_R/LT	2.02	[%]
Movable rudder area	A_M	111.43	[m^2]
Rudder height	b	15.8	[m]
Mean chord length	c_m	8.65	[m]
Mean thickness	t_m	1.55	[m]
Geometric aspect ratio	λ	1.83	[-]
Thickness ratio	t_m/c_m	0.18	[-]
Degree of twist	α	0	[°]

b. Rudder aspect ratio:

An important hydrodynamic characteristic of the rudder is the ratio between the rudder span and the chord (named aspect ratio, λ). For the case of KVLCC2 rudder profile, the value of the aspect ratio is equal with λ=1.83 and can ensure an adequate magnitude of the rudder hydrodynamics forces and moments.

The rudder hydrodynamic performances will be calculated in the next step, after the rudder design stage.

c. Rudder design

More details about the rudder drawing were presented in the **Appendix 2.2 Rudder drawing**.

Observation:

Usually, the distance between the upper part of the rudder and the aft part of the ship (clearance) must be very small. This is done in order to realize the mirror effect on the rudder, which increase the lateral hydrodynamics forces at a given deflection angle of the rudder.

If the clearance will be small, the effective aspect ratio will be modified and will be almost double of the geometric aspect ratio.

From manoeuvring point of view, adding a hydrodynamic fixed foil between the upper part of the rudder and the aft part of the ship, in order to realize a small clearance, the hydrodynamic performance of the rudder will be increase on the basis of the large increasing of the effective aspect ratio.

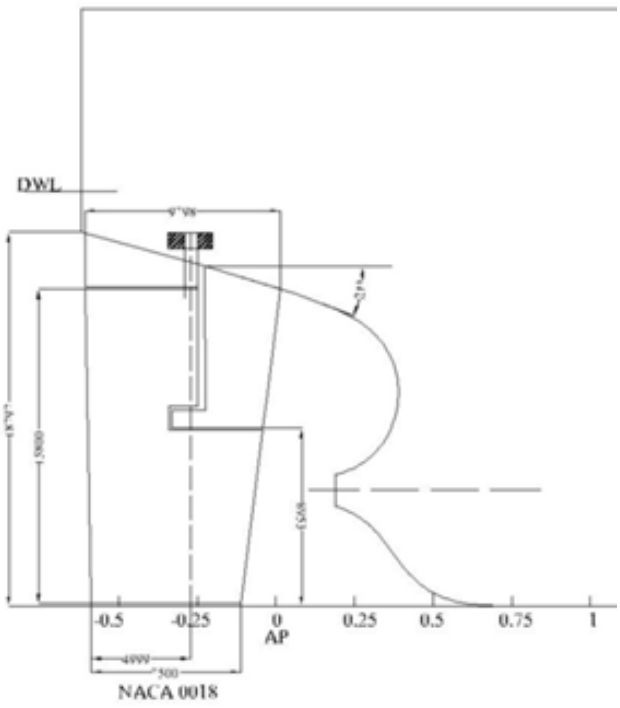

Figure 2-5 Rudder detail drawing

2.3.2. Rudder hydrodynamics calculation

In the case of the rudder hydrodynamics analyses at initial design stage, the PHP software platform was used, and rudder calculation module was running.

2.3.2.1. Method used

- The hydrodynamic calculations of the rudder were performed based on the method proposed by Y.I. Voitkounsky (1985) ([25], [7]) (see **Appendix 2.5 Rudder hydrodynamics calculation**).
- Ahead and astern ship motions were considered for the calculations.
- Estimation of the rudder hydrodynamic forces and moments generated on the rudder, both for ahead and astern motions, as well as the optimum position of the rudder stock were determined.
- The estimation of the maximum value of the torque against the rudder stock was performed, in order to be able to select the steering gear and to compute the rudder stock diameter.
- Preliminary checking of the rudder cavitation risk was performed, by using the Brix method [7].

2.3.2.2. Input data

The input data concerning the rudder design are presented in the Table 2.12 and Figure 2-6. It's already mentioned that:

- The rudder used is of semi-balanced type, with pintle;
- The rudder profile is NACA 0018.

Also, it's necessary to mention the direction of propeller rotation (right). Other input data are presented in the Table 2.13.

Table 2.10 Distances used for hydrodynamic calculations

H [m]	hi [m]	hs [m]	bi [m]	bs [m]	Spi [m]	Sps [m]
17,26	0,1	8,85	8,75	7,05	71,2	37,5

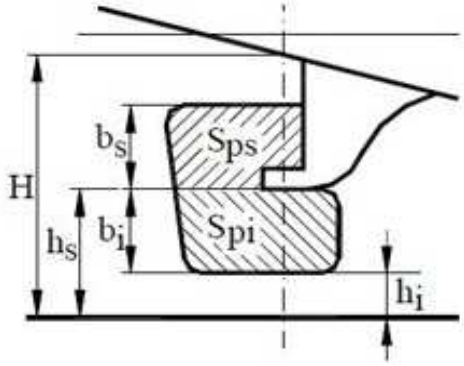

Figure 2-6 Rudder type used (representation)

Table 2.11 Ahead and astern motions rudder inputs

Rudder characteristics- ahead motion	Input	Notation & Unity
Wake coefficient	0,205	w
Advance speed	6,341	VA [m/s]
Propeller disc area	76,356	A0 [m²]
Flow speed on the rudder	8,917	Vr [m/s]
Load coefficient of the propeller	1,627	Ct
Coefficient of the propeller thrust	0,184	Kt
Coefficient of the propeller torque	0,032	Kq
Advance coefficient	0,536	J
Maximum deviation angle of the flow	45,65	alphaR0 [Deg]
Flow deviation angle for the rudder section situated in the propeller's jet	-3,332	alphaEm [Deg]
Average deviation angle of the propeller jet	-2,001	alphaRe [Deg]

Ship speed	7,970	V[m/s]
Water density	1,025	ro [t/m3]
Propeller thrust	2560,64	Tp [kN]
Propeller diameter	9,86	Dp [m]
Propeller revolution	72	nP [rpm]
Propeller efficiency	0,491	eta0
Rudder area	136,700	Ar [m²]
Area of the rudder section placed in the propeller jet	82,109	Spcj [m²]
Average height (span) of the rudder	15,800	b [m]
Average geometric chord of the rudder	8,650	c [m]
Aspect ratio of the rudder	1,830	lambda
Relative aspect ratio of the rudder section situated in the propeller jet	1,184	lambdaPcj
Coefficient n1, depending on the ratios b /D and d /R	0,900	n1
Coefficient n2, depending on the ratios b /D and d /R	0,200	n2
Rudder characteristics-astern motion	Input	Notation & Unity
Astern ship speed	2,881	Vb [m/s]
Distance from the propeller disc to the rudder leading edge	3,000	x [m]
Load coefficient of the propeller	1,627	Ct
Coefficient for stern motion	0,618	kb
Flow speed on the rudder in astern motion	2,586	Vpb[m/s]
Fluid's axial speed before entering the propeller disc	0,215	Vab [m/s]
Flow speed on the rudder with the influence of the propeller	2,801	Vpb1 [m/s]
Wake coefficient in the astern motion	0,102	w_b

2.3.2.3.Output data

Ahead motion results

As a first output for ahead motion, the obtained results are: the rudder coefficients versus the rudder angle of attack, the results obtained are showed on the table below.

Table 2.12 Drag, lift and moment coefficients .vs. rudder angle of attack, ahead motion

delta [deg]	0	5	10	15	20	25	30	35	40
alfa [deg]	-1,844	2,92	7,684	12,447	17,211	21,975	26,739	31,502	36,266
coefCx	0,0075	0,034	0,0423	0,0565	0,0994	0,1623	0,2646	0,3861	0,5037
coefCy	0	0,206	0,4196	0,6338	0,791	0,9025	0,9242	0,8459	0,7486
coefCm	0	0,0301	0,0696	0,1195	0,171	0,2121	0,2483	0,3213	0,3303

Notations:

Rudder deflection angle	delta	[Deg]
Rudder angle of attack	alfa	[Deg]
Drag coefficient of the rudder	coefCx	-
Lift coefficient of the rudder	coefCy	-
Hydrodynamic torque coefficient from the rudder leading edge	coefCm	-

Figures 2-7, 2-8 and 2-9 are graphic representations of the rudder hydrodynamics coefficients (drag, lift and hydrodynamic torque respectively), in ahead motion.

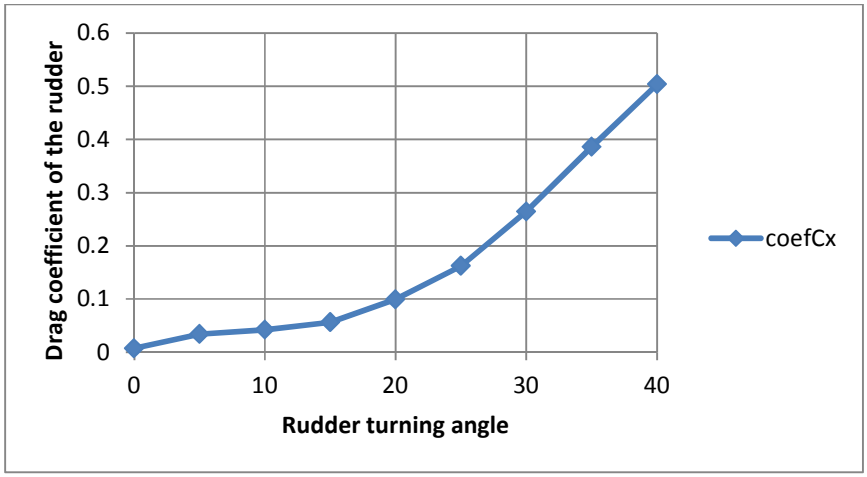

Figure 2-7 Drag coefficient of the rudder (ahead motion)

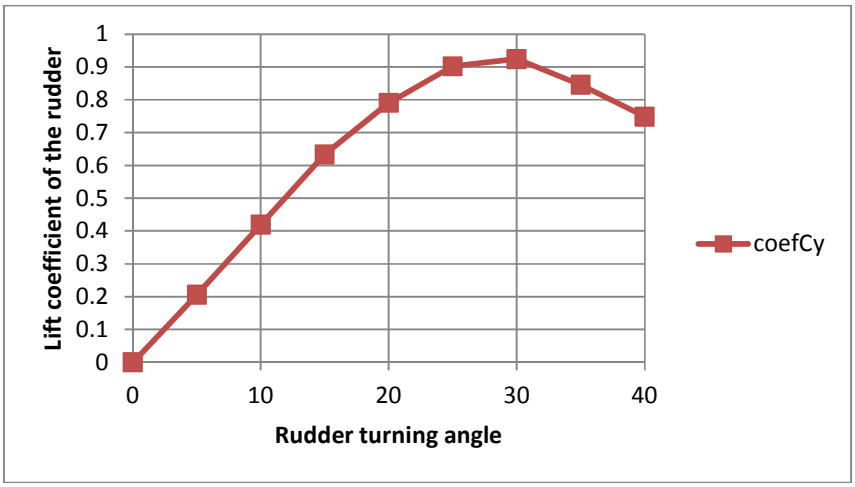

Figure 2-8 Lift coefficient of the rudder (ahead motion)

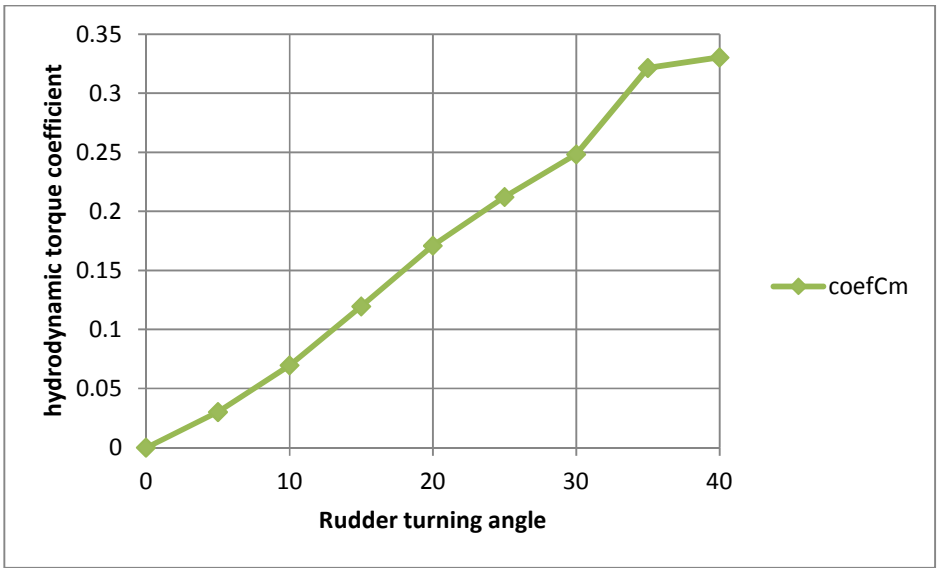

Figure 2-9 Hydrodynamic torque coefficient of the rudder (ahead motion)

Other outputs for the case of ahead motion, concerning the normal force parameters were described in the Table 2.15 and Figure 2-10. The diagram of the normal force acting on rudder is depicted in Figure 2-11.

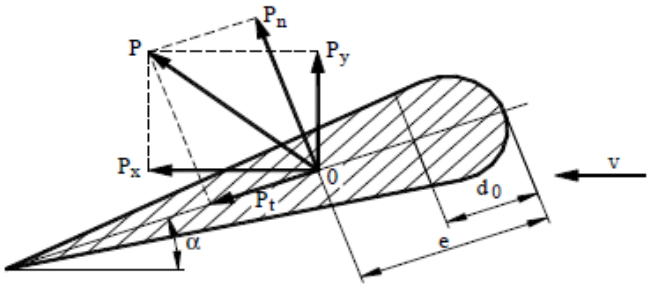

Figure 2-10 Rudder forces decomposition

Table 2.13 Rudder forces and moment .vs. rudder angle of attack (ahead motion)

alfa[deg]	0	5	10	15	20	25	30	35	40
Cn	0	0,208	0,421	0,627	0,777	0,887	0,933	0,914	0,897
Pn [kN]	0	1159,422	2342,719	3492	4330,32	4938,487	5195,626	5093,606	4998,264
M [kNm]	0	1450,221	3355,478	5757,964	8240,536	10222,475	11966,059	15483,466	15918,19
e [m]	0	1,251	1,432	1,649	1,903	2,07	2,303	3,04	3,185

Notations:

Normal force coefficient acting on rudder	Cn	-
Normal force acting on rudder	Pn	[kN]
Hydrodynamic moment from the rudder leading edge	M	[kNm]
Distance of center of pressure from rudder leading edge	e	[m]
Distance of the rudder stock from leading edge	d	[m]

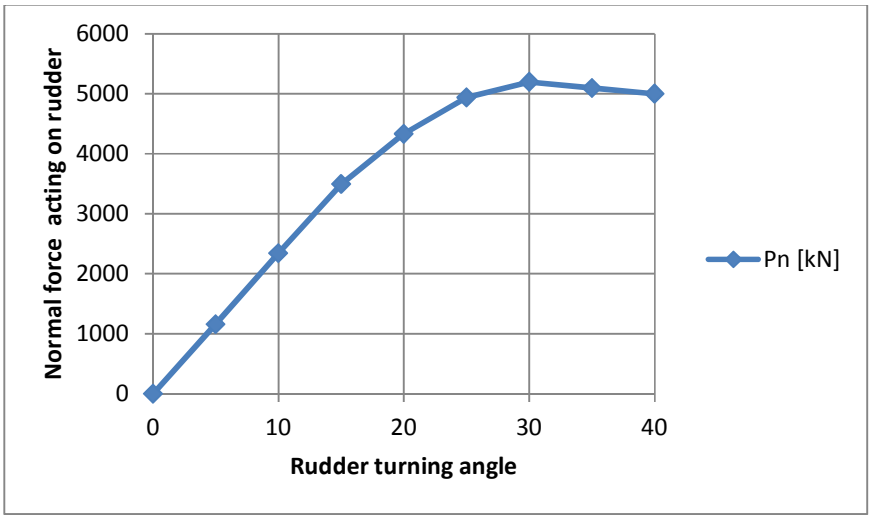

Figure 2-11 Normal force acting on rudder (ahead motion)

The next step is to estimate the optimum position of the rudder stock to the leading edge. The hydrodynamic torque to the rudder stock (Mr) was determined, by using five virtual distances, d, from the rudder stock to the leading edge, comprised between 0.15 and 0.35 from medium chord of the profile. The diagram of the hydrodynamic torque to the rudder stock, for all five virtual distances is presented in Figure 2-12.

Table 2.14 Hydrodynamic torque for five virtual distances of the rudder stock from leading edge

d (m)	Mr [kNm]								
1,298	0	-54,129	315,799	1227,094	2621,945	3814,788	5224,733	8874,512	9432,942
1,73	0	-555,579	-697,427	-283,196	749,081	1678,892	2977,625	6671,527	7271,192
2,163	0	-1057,029	-1710,653	-1793,486	-1123,782	-457,004	730,517	4468,542	5109,443
2,595	0	-1558,479	-2723,879	-3303,776	-2996,646	-2592,900	-1516,592	2265,558	2947,693
3,028	0	-2059,929	-3737,105	-4814,065	-4869,51	-4728,795	-3763,7	62,573	785,944

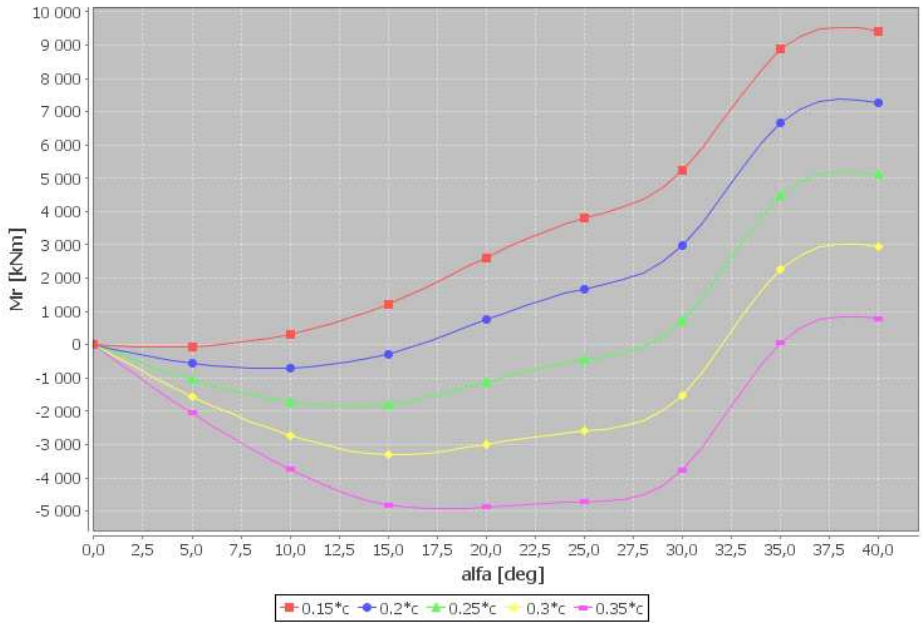

Figure 2-12 Hydrodynamic torque with virtual distances from the rudder stock to the leading edge

Discussion:

- From the figure 2.12 it's seen that the rudder torque decrease with the increase of the distance d, between rudder stock and leading edge.

The optimum distance (d0) was determined at the intersection point of the red curve, containing maximum values of the hydrodynamic torque, with the blue curve containing the minimum values of the hydrodynamic torque (see Figure 2-13).

Finally, the optimal hydrodynamic torque in ahead motion and the optimal distance from the rudder stock to the leading edge were presented in the following table.

Table 2.15 Optimal hydrodynamic torque and distance for ahead motion

Ahead motion results	
Optimal distance from the rudder stock to the leading edge(d0)	2,553 [m]
Optimal hydrodynamic torque to the rudder stock(MrOpt)	4546,542 [kNm]

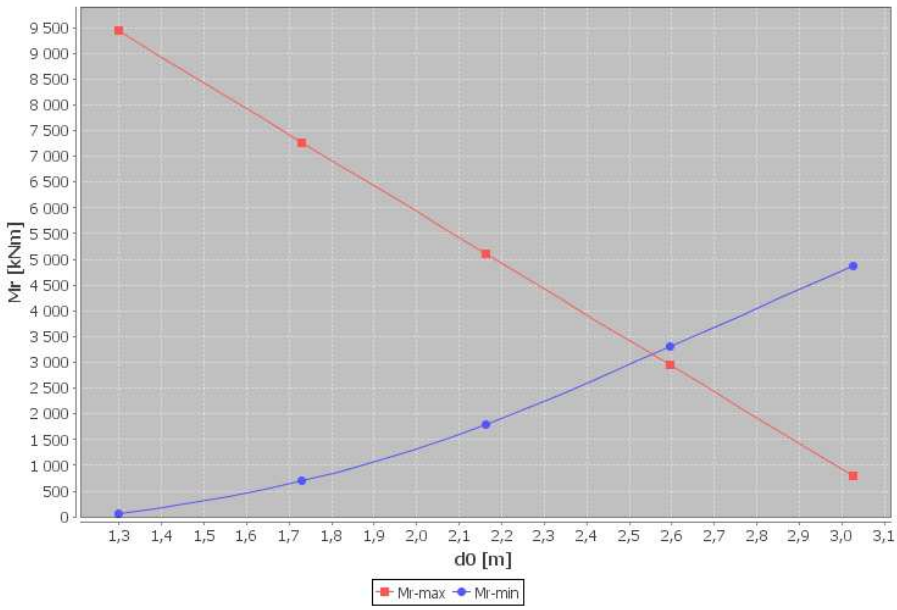

Figure 2-13 Optimal distance and hydrodynamic torque to the rudder stock

It was observed that:

- In the case of the rudder developed by MOERI, the compensation factor is 40 %;
- In the case of the PHP software platform results, regarding the optimum position of the rudder stock, the compensation factor is 30 %. As a consequence, in this case the hydrodynamic torque related to the rudder stock will be greater than the case of the rudder developed by MOERI.

Astern motion results

Regarding astern motion, the same method was used. The rudder coefficients versus the rudder angle of attack, obtained in the case of astern motion are showed on the following table.

Table 2.16 Drag, lift and moment coefficients .vs. rudder angle of attack, in astern motion

delta [deg]	0	5	10	15	20	25	30	35	40
coefCxb	0,007	0,068	0,093	0,145	0,203	0,296	0,408	0,539	0,65
coefCyb	0	0,296	0,493	0,651	0,812	0,953	1,049	0,97	0,877
coefCmb	0	-0,155	-0,232	-0,303	-0,359	-0,415	-0,467	-0,449	-0,483

Notations:

Rudder deflection angle	delta	[Deg]
Drag coefficient of the rudder in astern motion	coefCxb	-
Lift coefficient of the rudder in astern motion	coefCyb	-
Hydrodynamic torque coefficient from the rudder leading edge	coefCmb	-

Figures 2-14, 2-15 and 2-16 are graphic representations of the rudder coefficients (drag, lift and hydrodynamic torque respectively) in astern motion.

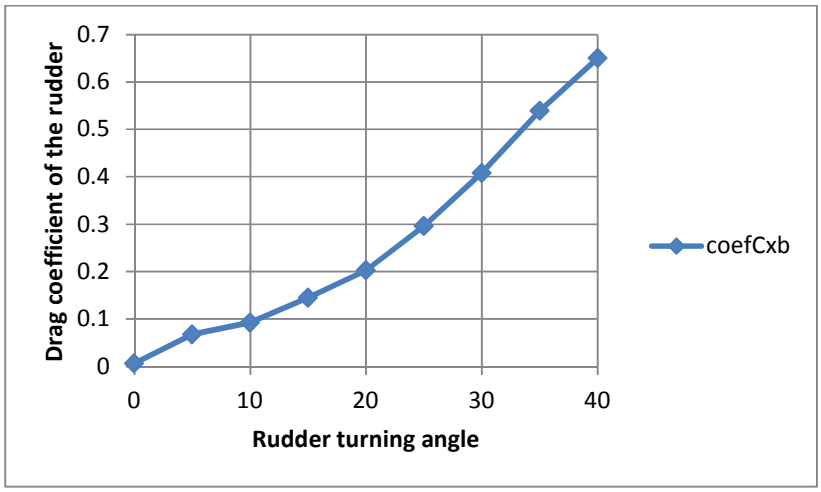

Figure 2-14 Drag coefficient of the rudder (astern motion)

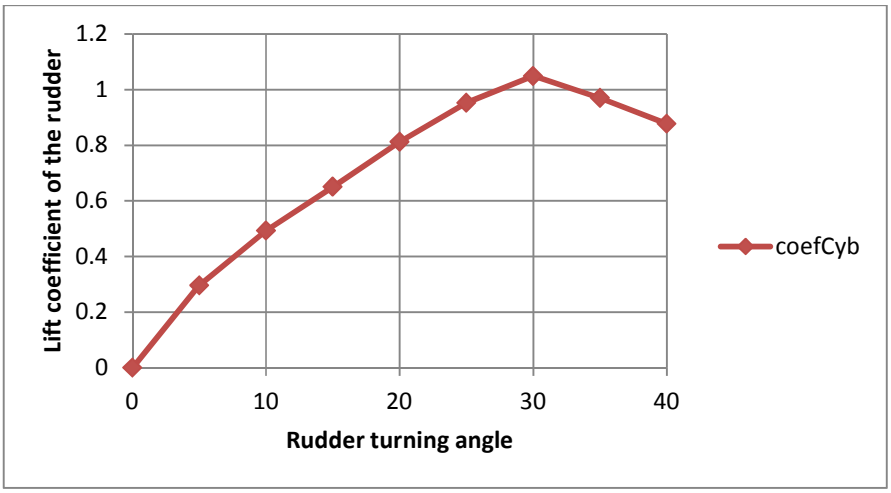

Figure 2-15 Lift coefficient of the rudder (astern motion)

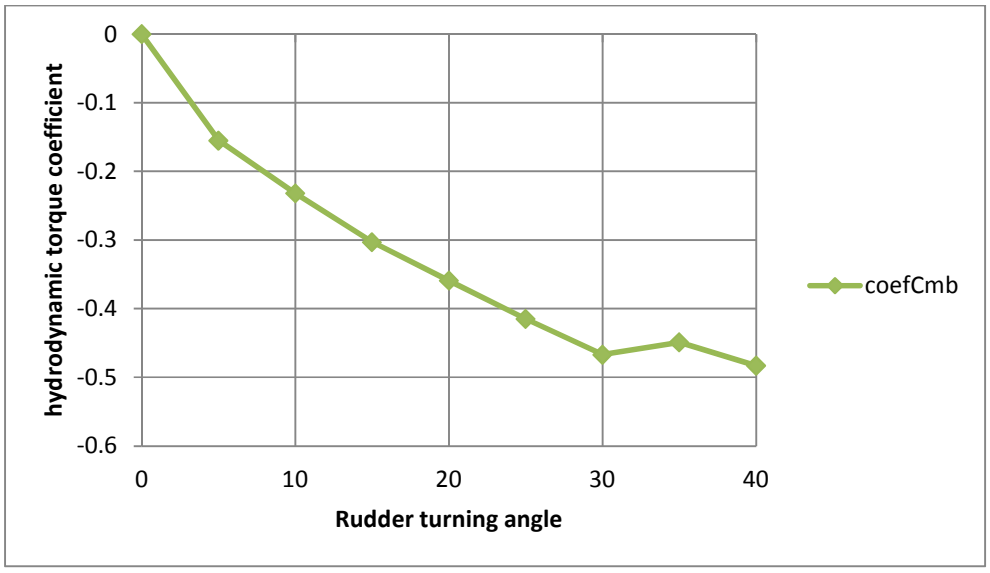

Figure 2-16 Hydrodynamic torque coefficient of the rudder (astern motion)

The normal forces and moments calculated for astern motion are showed in the table below.

Table 2.17 Rudder forces and moments vs. rudder angle of attack, in astern motion

alfa [deg]	0,00	5,00	10,00	15,00	20,00	25,00	30,00	35,00	40,00
Cnb	0,00	0,30	0,50	0,67	0,83	0,99	1,11	1,10	1,09
Pnb [kN]	0,00	165,48	275,87	366,01	457,57	543,57	611,24	606,76	599,04
Mb [kNm]	0,00	-737,79	-1103,88	-1442,30	-1708,01	-1973,14	-2219,17	-2133,44	-2296,38

Notations:

Normal force coefficient	Cnb	-
Normal force acting on rudder	Pnb	[kN]
Hydrodynamic moment from the rudder leading edge	Mb	[kNm]
Rudder angle of attack	alfa	[Deg]

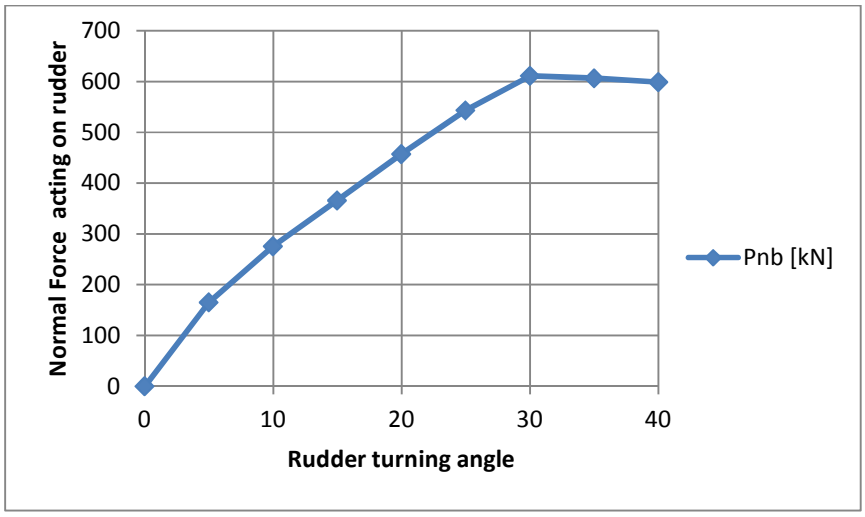

Figure 2-17 Normal force acting on rudder (astern motion)

Finally, the optimal hydrodynamic torque to the rudder stock, in astern motion was determined and presented in the following table.

Table 2.18 Optimal hydrodynamic torque for astern motion

Astern motion results		
Distance from the rudder stock to the trailing edge of the rudder (df):	-6,097	[m]
Optimal hydrodynamic torque to the rudder stock in astern motion (MrbOpt):	1952,515	[kNm]

Optimal rudder hydrodynamic torque

After estimating rudder hydrodynamics for both ahead and astern motions, a maximum hydrodynamic torque should be selected. In the case of KVLCC2 ship, the maximum hydrodynamic torque is corresponding to the one obtained at ahead motion.

In order to obtain the total torque, an additional friction torque is added. This component is equal about 20 % of the maximum hydrodynamic torque, obtained in ahead motion case.

At the end, the total torque may be obtained, by summing the hydrodynamic component with friction component (about 5455.85 kNm, see Table 2.21).

Table 2.19Total torque

Maximum hydrodynamic torque	4546,542	kNm
Supplementary torque due to the friction	909,308	kNm
Total torque	5455,85	kNm

Remarque:

The selection of the steering gear for a preliminary design will be based on the total torque result.

2.3.3. Rudder force and torque calculation according to BV rules

Calculation of the force and torque acting on rudder are done, also, according to BV rules.

a. Calculation procedure for the force and torque acting on rudder

On the basis of the calculation procedure details (presented in the **Appendix 2.4 Force and torque acting on rudder according to BV Rules**) the rudder hydrodynamic force and torque were determined and presented in the following table.

Table 2.20 Rudder force and torque results

Name	Notation	Ahead	Astern	Unity
Rudder force	C_R	3979,69	723,58	[N]
Rudder torque	M_{TR}	4495,01	1605,59	[kN.m]

As results from calculation details, only for the ahead condition, the minimum rudder torque is to be taken not less than the following value: $M_{TR,MIN} = 3442,97$ kN.m

b. Comparison and discussion

A comparison between PHP software platform and BV results, concerning the rudder torque value is presented in Table 2.23.

Table 2.21 Rudder torque comparison

Name	Ahead	Astern	Unity
Optimal hydrodynamic torque (PHP software platform)	4546,542	1952,515	[kN.m]
Torque calculations (Bureau Veritas)	4495,01	1605,59	[kN.m]
Error	1,13%	17,77%	

Concerning the results, it's seen that:

- The optimal torque estimation, using PHP software platform, in ahead motion is well estimated, comparing to BV calculations;
- The optimal torque estimation, using PHP software platform, in astern motion is overestimated comparing to BV calculations;
- From the point of view of steering gear selection, the important forces and moments are the ones obtained in the case of ahead motion.

2.4. PHP Rudder cavitation

In addition to the propeller cavitation, rudder cavitation may occur, which leads to a decrease in rudder performances and sometimes may cause the damage or the loss of the rudder situated behind the propeller jet.

The preliminary checking of the rudder cavitation risk was performing, by running the same PHP software platform, with specialized module for rudder cavitation, performed on the basis of Brix method [4].

2.4.1. Rudder cavitation input data

The input data are presented in Table 2.24 and are based on MOERI rudder geometry and the resistance and powering results, obtained on the basis of PHP software platform.

Table 2.22 Rudder cavitation input data

Rudder characteristics	Input	Notation & Unity
Ship speed	15,5	V [Knots]
Rudder profile	NACA0018	-
Wake coefficient	0,447	w
Thrust deduction fraction	0,227	t
Propeller diameter	9,860	Dp [m]
Propeller thrust	2560,640	Tp [kN]
Propeller efficiency	0,491	eta0
Relative rotation efficiency	1,021	etaR
Propeller revolution	72,000	np [rpm]
Distance from the propeller disc to the rudder leading edge	3,000	x [m]
Distance between top of rudder and propeller axis	10,100	h1 [m]
Distance between the propeller axis and the water surface	15,000	h2 [m]
Water density	1,025	ro [t/m3]
Chord length of the rudder	8,650	c [m]

2.4.2. Rudder cavitation output data

The checking of the cavitation risk on the rudder profile can be done at the preliminary design phase, based on a method proposed by Brix, presented in **Appendix 2.6 Rudder cavitation checking**. The output parameters were presented in Table 2.25 and Table 2.26. It's observed that no risk of cavitation is possible, because the total pressure (the sum between the static pressure and dynamic pressure) is positive.

Table 2.23 Rudder cavitation results

alfa[deg]	pSt [kPa]	pDyn [kPa]	pTot [kPa]
11	221.3	-56,1	165,2 > 0
18	221.3	-104,4	116,9 > 0
22	221.3	-142,9	78,4 > 0

Notations:

Attack angle	alfa	[deg]
Static pressure	pSt	[kPa]
Dynamic pressure	pDyn	[kPa]
Total pressure	pTot	[kPa]

Table 2.24 Rudder cavitation output data

Rudder characteristics	output	Notation & Unity
Advance speed	4,410	vA [m/s]
Load coefficient of the propeller	3,365	Ct
Hull efficiency	1,398	etaH
Propulsive efficiency	0,701	etaD
Delivered power	22523,5	Pd [kW]
Propeller torque	2987,3	Q [kN,m]
Coefficient of the propeller torque	0,022	kq
Advance coefficient	0,373	J
Wake coefficient radius increases	4,543	r+Dr [m]
Corrected wake coefficient speed	8,529	Vcor [m/s]
Axial velocity	10,22	vx [m/s]
Slipstream radius	4,150	rx [m]
Maximum axial speed	10,71	vmax [m/s]
Static pressure	220,45	Pstatic [kPa]
Distance between the respective point of rudder and the water surface	11,68	H [m]

2.5. Manoeuvring performance estimation

The manoeuvring performances of the KVLCC2 ship tanker (the turning circle and the stability on route) have been estimated on the base of Abkowitz linear model or statistical formulas and checked with IMO criteria.

2.5.1. Standard manoeuvres and IMO criteria

On the basis of IMO resolution MSC.137 (76), adopted on 4 December 2002, the standard manoeuvres of the ship may be defined and the manoeuvring characteristics of a given ship can be evaluated.

The main standard manoeuvres in sea trials are: turning circle test, spiral manoeuvres, pull-out manoeuvre, Zig-Zag manoeuvre, stopping trial and man-overboard manoeuvre or Williamson turn (see **APPENDIX 2.3 Standards for ship manoeuvrability**).

2.5.2. Abkowitz mathematical model

The mathematical model used on this master thesis is the Abkowitz model [6], based on the Taylor expansion series applied on the hydrodynamic forces and moments acting on the ship, in order to obtain the hydrodynamic derivatives. The coordinate system is presented in the following figure. Was noted with ψ the heading angle of the ship, β is the drift angle of the ship and δ is the rudder deflection angle.

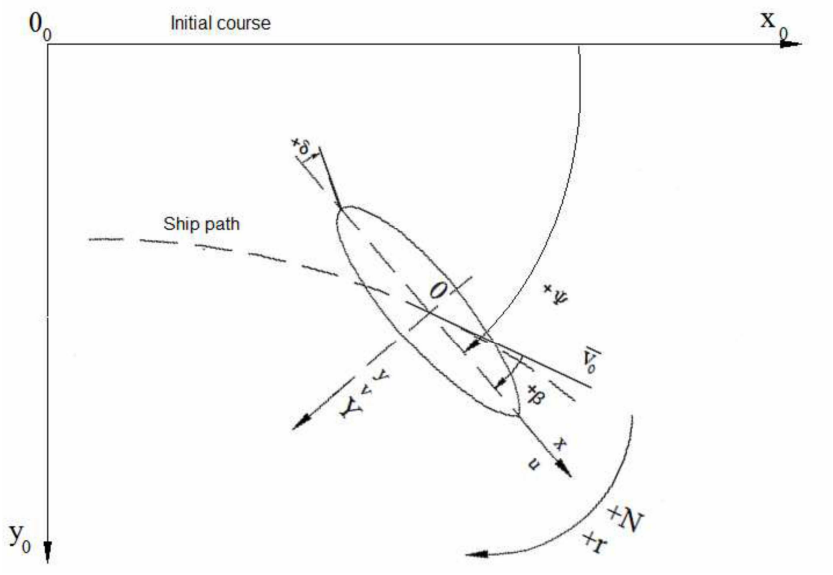

Figure 2-18 Axis system

Ship motion equations in horizontal plane

In order to study the ship motion in still water, in horizontal plan, the following remarks must be considered [6]:

- The ships is a rigid body;
- The origin of the local coordinate system *Oxyz* is fixed at the midship section;
- The longitudinal *x*-axis, positive forward is situated in the centerline plane, usually parallel to the keel or the still water plane;
- The transverse *y*-axis, positive to starboard is perpendicular to the plane of symmetry;
- The vertical *z*-axis, positive downward is perpendicular to the still water plane.

Looking forward from the ship bridge:

- Roll motion about the *x*-axis is positive clockwise;
- Pitch motion about the *y*-axis is positive bow-up;
- Yaw motion about the *z*-axis is positive turning-starboard.

In order to analyze the ship motions for a body moving with six degrees of freedom, the mass of the body was taken constant on time.

If r_G is the vector radius of the centre of gravity, v_0 is the ship speed in the origin of the coordinate system and ω is the ship angular velocity, the following relations highlight the components of these vectors:

$$\begin{aligned} \bar{r}_G &= x_G \cdot \bar{i} + y_G \cdot \bar{j} + z_G \cdot \bar{k} \\ \bar{v}_0 &= u \cdot \bar{i} + v \cdot \bar{j} + w \cdot \bar{k} \\ \bar{\omega} &= p \cdot \bar{i} + q \cdot \bar{j} + r \cdot \bar{k} \end{aligned} \tag{2.4}$$

The general form of the equations of motion for a rigid body, considering all six degrees of freedom is obtained by using the linear momentum theorem and the angular momentum theorem. The following equations of the ship motion in horizontal plan may be obtained [7]:

$$X = m \cdot \left[\frac{\partial u}{\partial t} + qw - rv + \frac{dq}{dt} z_G - \frac{dr}{dt} y_G + (qy_G + rz_G)p - (q^2 + r^2)x_G \right]$$

$$Y = m \cdot \left[\frac{\partial v}{\partial t} + ru - pw + \frac{dr}{dt} x_G - \frac{dp}{dt} z_G + (rz_G + px_G)q - (r^2 + p^2)y_G \right] \tag{2.5}$$

$$Z = m \cdot \left[\frac{\partial w}{\partial t} + pv - qu + \frac{dp}{dt} y_G - \frac{dq}{dt} x_G + (px_G + qy_G)r - (p^2 + q^2)z_G \right]$$

$$
\begin{aligned}
K &= \frac{\partial p}{\partial t}\cdot I_{xx} + rq\cdot\left(I_{zz}-I_{yy}\right)+\\
&+ m\left[y_G\left(\frac{\partial w}{\partial t}+pv-qu\right)- z_G\left(\frac{\partial v}{\partial t}+ru-pw\right)\right]\\
M &= \frac{\partial q}{\partial t}\cdot I_{yy} + pr\cdot\left(I_{xx}-I_{zz}\right)+\\
&+ m\left[z_G\left(\frac{\partial u}{\partial t}+qw-rv\right)- x_G\left(\frac{\partial w}{\partial t}+pv-qu\right)\right]\\
N &= \frac{\partial r}{\partial t}\cdot I_{zz} + pq\cdot\left(I_{yy}-I_{xx}\right)+\\
&+ m\left[x_G\left(\frac{\partial v}{\partial t}+ru-pw\right)- y_G\left(\frac{\partial u}{\partial t}+qw-rv\right)\right].
\end{aligned}
\tag{2.6}
$$

where I_{xx}, I_{yy} and I_{zz} represent the components of the inertia moments and m is the ship mass.
The left parts of the equations contain the components of the hydrodynamics forces (X, Y, Z) and moments (K, M, N) acting of the ship. A simplification of the problem has been done respecting the following assumptions:

- The vertical motion, the roll and pitch motions are negligible;
- Assuming that the center of gravity lies in the centerline plane, than y_G=0.

Thus, the equations of motion become:

$$
\begin{aligned}
X &= m\left(\frac{\partial u}{\partial t}- rv - r^2 x_G\right)\\
Y &= m\left(\frac{\partial v}{\partial t}+ ru + \frac{dr}{dt}x_G\right)\\
N &= \frac{\partial r}{\partial t} I_{zz} + m x_G\left(\frac{\partial v}{\partial t}+ru\right)
\end{aligned}
\tag{2.7}
$$

Linear mathematical model

Typically for the manoeuvring models, using the Taylor expansion series, the hydrodynamics forces and moments can be writing depending of the hydrodynamics derivatives. In the case of the linear model, the equations system (2.7) becomes:

$$
\begin{aligned}
&X_e + X_u u + X_{\dot u}\dot u = m\dot u \\
&Y_e + Y_v v + Y_r r + Y_{\dot v}\dot v + Y_{\dot r}\dot r = m\left(\dot v + rU + \dot r x_G\right) \\
&N_e + N_v v + N_r r + N_{\dot v}\dot v + N_{\dot r}\dot r = I_{zz}\dot r + m x_G\left(\dot v + rU\right).
\end{aligned}
\tag{2.8}
$$

where X_e, Y_e, N_e are the components of the external forces and moments acting on the ship, generated by the rudder-propeller system, depending by the rudder deflection angle δ. The hydrodynamic derivatives X_u, $X_{\dot u}$, Y_v, Y_r, $Y_{\dot v}$, $Y_{\dot r}$, N_v, N_r, $N_{\dot v}$ and $N_{\dot r}$ indicate the action of the fluid motion on the ship.

On the basis of the linear Abkowitz model, the ship stability parameter C (related to the ship stability on route) may be determined, by using the following expression:

$$
C = Y_v\left(N_r - m x_G U\right) + N_v\left(mU - Y_r\right) > 0\,. \tag{2.9}
$$

where U is the ship speed. If C>0, than the ship will be stable on route.

Also, the turning circle radius R and the drift angle β may be determined, using the relations:

$$
R = \frac{U}{r} = \frac{UC}{\delta\left(N_v Y_\delta - Y_v N_\delta\right)} \tag{2.10}
$$

$$
\beta = -\frac{v}{U} = -\frac{\delta}{UC}\left[\left(m x_G U - N_r\right)Y_\delta + \left(Y_r - mU\right)N_\delta\right]. \tag{2.11}
$$

Remarque:

- The results obtained by using the linear model must be regarded with great attention, due to the minimum number of the hydrodynamics derivatives.
- As a consequence, non-linear models must be developed in order to increase the level of accuracy of the manoeuvring prediction.

Non- linear mathematical model

A non-linear mathematical model based on Taylor expansion series of the hydrodynamics forces and moments including terms up to third order have been used ([7], [8]).

The following differential equations of motions have been obtained:

$$
\begin{aligned}
\left(m - X_{\dot u}\right)\dot u &= X_u u + f_1\left(u, v, r, \delta\right) \\
\left(m - Y_{\dot v}\right)\dot v + \left(m x_G - Y_{\dot r}\right)\dot r &= Y_v v + \left(Y_r - mU\right)r + f_2\left(u, v, r, \delta\right) \\
\left(m x_G - N_{\dot v}\right)\dot v + \left(I_{zz} - N_{\dot r}\right)\dot r &= N_v v - \left(N_r - m x_G U\right)r + f_3\left(u, v, r, \delta\right)
\end{aligned}
\tag{2.12}
$$

where the general forms of the nonlinear functions f_1, f_2, f_3 are:

$$f_1(u,v,r,\delta)=\frac{1}{2}\left(X_{uu}u^2+X_{vv}v^2+X_{\delta\delta}\delta^2\right)+\left(\frac{1}{2}X_{rr}+mx_G\right)r^2+$$
$$+X_{v\delta}v\delta+X_{r\delta}r\delta+\left(X_{vr}+m\right)vr+\frac{1}{6}X_{uuu}u^3 \tag{2.13}$$

$$f_2(u,v,r,\delta)=Y_u\,u+Y_\delta\delta+Y_{\delta u}\delta u+\frac{1}{6}\left(Y_{vvv}v^3+Y_{rrr}r^3+Y_{\delta\delta\delta}\delta^3\right)+$$
$$+\frac{1}{2}\left(Y_{vrr}vr^2+Y_{rvv}rv^2+Y_{\delta vv}\delta v^2+Y_{v\delta\delta}v\delta^2+Y_{r\delta\delta}r\delta^2\right)+ \tag{2.14}$$
$$+\frac{1}{2}Y_{\delta rr}\delta r^2+Y_{vr\delta}vr\delta$$

$$f_3(u,v,r,\delta)=N_u u+N_\delta\delta+N_{\delta u}\delta u+\frac{1}{6}\left(N_{vvv}v^3+N_{rrr}r^3+N_{\delta\delta\delta}\delta^3\right)+$$
$$+\frac{1}{2}\left(N_{vrr}vr^2+N_{rvv}rv^2+N_{\delta vv}\delta v^2+N_{v\delta\delta}v\delta^2+N_{r\delta\delta}r\delta^2\right)+ \tag{2.15}$$
$$+\frac{1}{2}N_{\delta rr}\delta r^2+N_{vr\delta}vr\delta.$$

In order to simulate the ship trajectory during the standard manoeuvres (see Chapter 4), the following specific functions (f_1, f_2, f_3) of the mathematical model was introduced and applied:

$$f_1(u,v,r,\delta)=\frac{1}{2}\left(X_{uu}u^2+X_{vv}v^2+X_{\delta\delta}\delta^2\right)+X_{v\delta}v\delta+\frac{1}{6}X_{uuu}u^3$$

$$f_2(u,v,r,\delta)=Y_\delta\delta+\frac{1}{6}\left(Y_{vvv}v^3+Y_{rrr}r^3+Y_{\delta\delta\delta}\delta^3\right)+\frac{1}{2}\left(Y_{\delta vv}\delta v^2+Y_{v\delta\delta}v\delta^2\right) \tag{2.16}$$

$$f_3(u,v,r,\delta)=N_\delta\delta+\frac{1}{6}\left(N_{vvv}v^3+N_{rrr}r^3+N_{\delta\delta\delta}\delta^3\right)++\frac{1}{2}\left(N_{\delta vv}\delta v^2+N_{v\delta\delta}v\delta^2\right)$$

On the basis of the non-linear mathematical model, the following characteristics can be obtained, in time domain (t):

- The coordinates of the path of the origin of the ship, relative to the fixed axis

$$\begin{aligned}x_0(t+\Delta t)&=x_0(t)+\Delta t\left[u(t)\cos\psi(t)-v(t)\sin\psi(t)\right]\\ y_0(t+\Delta t)&=y_0(t)+\Delta t\left[u(t)\sin\psi(t)+v(t)\cos\psi(t)\right]\end{aligned} \tag{2.17}$$

- The radius of the turning circle

$$R(t) = \frac{\sqrt{u^2(t) + v^2(t)}}{r(t)} \tag{2.18}$$

where

$$\begin{aligned} u(t+\Delta t) &= u(t) + \Delta t \cdot \dot{u}(t) \\ v(t+\Delta t) &= v(t) + \Delta t \cdot \dot{v}(t) \\ r(t+\Delta t) &= r(t) + \Delta t \cdot \dot{r}(t). \end{aligned} \tag{2.19}$$

- The heading angle

$$\psi(t+\Delta t) = \psi(t) + \Delta t \cdot r(t) \tag{2.20}$$

- The drift angle

$$\beta(t) = -arctg\frac{v(t)}{U} \tag{2.21}$$

The accuracy of the simulated trajectory depends of the value of the time interval Δt.

In order to obtain the practical solutions of the ship manoeuvring equations, it is necessary to know the hydrodynamic derivatives, which can be determined on the basis of theoretical or experimental methods. In the next chapters, the hydrodynamics derivatives will be determined by using the CFD Technics and statistical relations.

2.5.3. PHP manoeuvering performance

The manoeuvering performances of the KVLCC2 ship were estimated in this chapter by using the specific instruments for the initial ship design stage. The PHP software platform for manoeuvring performance was used, under the deep and unlimited water assumptions.

Manoeuvering performance input data

The input data are presented in Table 2.27. The close stern was considered for KVLCC2.

Table 2.25 Input data in PHP Manoeuvring Performance

Ship Data	Input	Notation & Unity
Length of waterline	325,5	Lwl [m]
Beam	58	B [m]
Draught	20,8	T [m]
Bow profile area	104,52	Ab [m²]
Total rudder area	136,7	Ar [m²]
Rudder deflection angle	35	delta [deg]

Ship speed	15,5	V [m/s]
Longitudinal center of gravity	171,2	xG [m]
Block coefficient	0.797	C_B [-]
Water density (salt water, 15 degree Celsius)	1025	ro [kg/m3]

Manoeuvering performance output data

The hydrodynamics derivatives presented in Table 2.28 and Table 2.29 were obtained based on Clarke, Gedling and Hine relations.

Table 2.26 Hydrodynamics derivatives based on statistical relations

Yv'	-0.024232
Yvpoint'	-0.015313
Yr'	0.004247
Yrpoint'	-0.001202
Nv'	-0.008382
Nvpoint'	-0.001048
Nr'	-0.003322
Nrpoint'	-0.000799

Table 2.27 Rudder derivatives

YdeltaPrime	0.003871
NdeltaPrime	-0.001935

On the basis of the linear Abkowitz model, the following value of the ship stability parameter C was obtained and presented in Table 2.30.

Table 2.28 Ship stability parameter

C	1.953E-4

Remarque:

- It should be mentioned that the value of C is positive, that means the ship will be stable on route.

Also, the characteristic diagram for the spiral manoeuvre was obtained (Figure 2-19), the values of the stady turning radius R and drift angle (beta) being presented in Table 2.31, depending of the rudder deflection angle (delta).

Figure 2-19 Rate of turn vs. rudder angle

Remarque:

- The obtained curve for rate of turn vs. rudder angle is not a hysteresis curve. Hence, the ship will be stable on route.

Table 2.29 Rudder angle, radius and drift angle

Delta [deg.]	R [m]	Beta [deg.]
-35.0	1311.636	13.748
-30.0	1530.242	11.784
-25.0	1836.290	9.820
-20.0	2295.363	7.856
-15.0	3060.484	5.892
-10.0	4590.726	3.928
-5.0	9181.452	1.964
-4.0	11476.815	1.571
-3.0	15302.420	1.178
-2.0	22953.629	0.786
-1.0	45907.259	0.393
0.0	--	0.000

Delta [deg.]	R [m]	Beta [deg.]
0.0	--	0.000
1.0	-45907.259	-0.393
2.0	-22953.629	-0.786
3.0	-15302.420	-1.178
4.0	-11476.815	-1.571
5.0	-9181.452	-1.964
10.0	-4590.726	-3.928
15.0	-3060.484	-5.892
20.0	-2295.363	-7.856
25.0	-1836.290	-9.820
30.0	-1530.242	-11.784
35.0	-1311.636	-13.748

Remarque:

- The steady turning diameter has a very large value (STD = 2623.3 m) for rudder deflection angle delta = 35 deg. Seems to be a wrong estimation, due to the linear form of the mathematical model used in this computer program.

Linear evaluation of tuning ability on the basis of Lyster and Knights relations

Also, this computer program provides the characteristics of the turning circle, calculated on the basis of the statistical relations proposed by Lyster and Knights and presented in the following table.

Table 2.30 Turning circle and tuning ability on the basis of Lyster and Knights relations

STD / L	2.837	STD	923.428 [m]
TD / L	3.458	TD	1125.493 [m]
AD / L	3.125	AD	1017.046 [m]
TR / L	1.653	TR	538.212 [m]
Vt / Va	0.405	Vt	6.276 [knots]

Notations:

Steady turning diameter	STD	[m]
Tactical diameter	TD	[m]
Advance diameter	AD	[m]
Transfer radius	TR	[m]
Ship speed at tuning circle	Vt	[knots]
Initial ship speed	Va	[knots]
Length of waterline	L	[m]

2.6. Conclusions

Comparing the manoeuvring characteristics with IMO standard criteria, the following general observations can be done:

- The characteristics of the turning circle, computed on the basis of Lyster and Knights statistical relations, fulfill the IMO standard criteria;
- The KVLCC2 ship will be stable in route, because the spiral manoeuvre diagram is linear and monotone (without hysteresis) and C parameter is positive;
- The linear Abkowitz model gives too large value for steady turning diameter;
- Non-linear mathematical models and CFD techniques must be used to increase the prediction accuracy of the manoeuvring characteristics, in initial ship design or basic design.

3. CFD BASED HYDRODYNAMICS PERFORMANCE

Starting from the conclusions of the first two chapters that the empirical methods which are considered in the first design stages are not so accurate and should be regarded with fair attention and from the recently proven fact [9] that the numerical methods can be used even in the preliminary design stages in order to determine the hydrodynamic performances of the ship, the master thesis has as main purpose to solve the ship manoeuvring problem by applying CFD based techniques. Thus, the hydrodynamics forces and moments acting on the KVLCC2 hull during the static PMM motions may be determined by using CFD instruments. Then, the static derivatives can be obtained and the ship trajectory during the standard manoeuvres may be simulated.

As a first step, made towards pursuing the presented objective, the ship resistance calculation is aimed to validate the numerical methodology that stands for the longitudinal force determination. For the transversal force and yaw moment acting on the ship hull, during the static manoeuvring motions, the validation is based on the numerical simulation of static PMM tests (static rudder and static drift). In this respect, the commercial SHIPFLOW code was considered, both potential and viscous flow methods have been used as follows: potential and viscous flow methods for the ship resistance tests and viscous methods for the static PMM tests.

3.1.Mathematical Model

As a starting point, it must be mentioned that the accuracy of the numerical analysis highly depends on the selection of the convenient mathematical model which must properly capture the physical phenomena that describe the flow around the ship hull.

For the present thesis, the CFD results are obtained by the use of a potential flow solver and a viscous flow solver, the fundamental equations of fluid dynamics: the continuity equation and the Navier-Stokes equations have been applied for the mathematical modeling of the free-surface viscous flow developed around the KVLCC2 tanker hull.

3.1.1. Potential Flow

The potential flow solver of the SHIPFLOW code is used in order to determine the KVLCC2 ship wave resistance. The governing equations and the assumptions that are underlying the mathematical description of the free-surface flow are given below [10].

It is assumed that the fluid is inviscid, irrotational and incompressible.

For incompressible flows, in Cartesian coordinates, the continuity equation is:

$$\frac{\partial u}{\partial x}+\frac{\partial v}{\partial y}+\frac{\partial w}{\partial z}=0 \qquad (3.1)$$

For a flow fulfilling the given assumptions, a scalar function named the velocity potential ϕ can be defined. Thus, the velocity vector can be expressed as the gradient of the velocity potential function:

$$u=\frac{\partial \phi}{\partial x}\ v=\frac{\partial \phi}{\partial y}\ w=\frac{\partial \phi}{\partial z} \qquad (3.2)$$

Based on the previous relations, the Laplace equation – the governing equation of the potential flow, is obtained:

$$\frac{\partial^2 \phi}{\partial x^2}+\frac{\partial^2 \phi}{\partial y^2}+\frac{\partial^2 \phi}{\partial z^2}=0 \qquad (3.3)$$

In order to obtain the solution of the flow, the problem of the boundary condition must be properly considered.

3.1.1.1.Potential Flow Boundary Conditions

For the potential flow computation, the boundary conditions are:

- ***Boundary conditions on the hull***

  Imposed on the hull surface, the boundary condition requires that no fluid particle penetrates the hull surface - $\frac{\partial \phi}{\partial n}=0$.

- **Boundary conditions on the free surface**

  At the free-surface level, the boundary conditions are ([11, [12]):

- The kinematic boundary condition which assumes that the particle at the surface should remain at the surface all the time;
- The free-surface pressure must be equal to the atmospheric pressure presumed constant;
- At infinity, the upstream disturbance generated by the moving ship vanishes;
- The radiation condition imposed to avoid upstream waves.

3.1.2. Viscous Flow

The viscous flow solver of the SHIPFLOW code is used in order to determine the KVLCC2 viscous resistance (frictional resistance and viscous pressure resistance) and the forces and moments acting on the ship hull during static PMM motions (longitudinal force, transversal force, yaw moment).

In order to solve the viscous flow problem, it is necessary to numerically integrate the incompressible Reynolds averaged Navier Stokes equations. The governing equations and the assumptions that are underlying the mathematical description of the viscous flow are given below ([10], [11]).

For the assumed incompressible flow, the continuity equation which states that the mass is conserved can be written as follows:

$$\frac{\partial U_i}{\partial x_i} = 0 \tag{3.4}$$

The Navier Stokes equations are given by:

$$\rho \frac{\partial U_i}{\partial t} + \rho \frac{\partial \left(U_i U_j \right)}{\partial x_j} = \rho R_i + \rho \frac{\partial \sigma_{ij}}{\partial x_j} \tag{3.5}$$

where σ_{ij} is the total stress.

The velocity and the pressure components can be written as a function of time mean velocity and time mean pressure plus their fluctuations in relation with time:

$$U_i = \bar{U}_i + u_i^{'} = u_i + u_i^{'} \tag{3.6}$$

$$P = \bar{P} + p^{'} = p + p^{'} \tag{3.7}$$

Thus, the time averaged continuity equation and the Navier-Stokes equations for incompressible flow can be written as follows:

$$\begin{aligned} &\frac{\partial u_i}{\partial x_i} = 0 \\ &\frac{\partial u_i}{\partial t} + \frac{\partial \left(u_j u_i + \overline{u_j^{'} u_i^{'}} \right)}{\partial x_j} = \overline{R_i} - \frac{1}{\rho} \frac{\partial p}{\partial x_i} + \frac{\partial}{\partial x_j} \left(\upsilon \left(\frac{\partial u_i}{\partial x_j} + \frac{\partial u_j}{\partial x_i} \right) \right) \end{aligned} \tag{3.8}$$

Although, system (3.7) gives the final form of the RANS equations, the difference between the number of equations and the number of unknowns introduces the so called “closure” problem, an additional number of relations being necessary in order to solve the problem.

3.1.2.1.Turbulence Modelling

For the present thesis, the EASM turbulence model of Gatski and Speziale [12] is chosen, a number of nonlinear terms being introduced. Though intricate, the EASM model gives the explicit solution of the Reynolds stresses at each computational iteration having, thereby, an advantage. The Reynolds stress tensor is given by the following relation [11]:

$$\rho\overline{u_i^{"}u_j^{"}} = \frac{2}{3}\rho k\delta_{ij} - \mu_T\left(S_{ij} + a_2a_4\left(S_{ik}W_{kj} - W_{ik}S_{kj}\right)\right) - a_3a_4\left(S_{ik}S_{kj} - \frac{1}{3}S_{mn}S_{mn}\delta_{ij}\right) \quad (3.9)$$

where

$\upsilon_T = \max\left(-k\alpha_1\frac{0.0005k}{\beta^{'}\omega}\right)$ is the turbulent viscosity and $\alpha_1, \beta^{'}, \alpha_2, \alpha_3, \alpha_4$ are numerical coefficients of the model, while W_{ij} is the rotation-rate.

3.1.2.2.Viscous Flow Boundary Conditions

As presented in Figure 3-1, for the viscous flow computation, Dirichlet and Neumann boundary conditions expressed in terms of pressure, velocity, turbulent kinetic energy and turbulent frequency are imposed on every boundary face of the 3D computational domain.

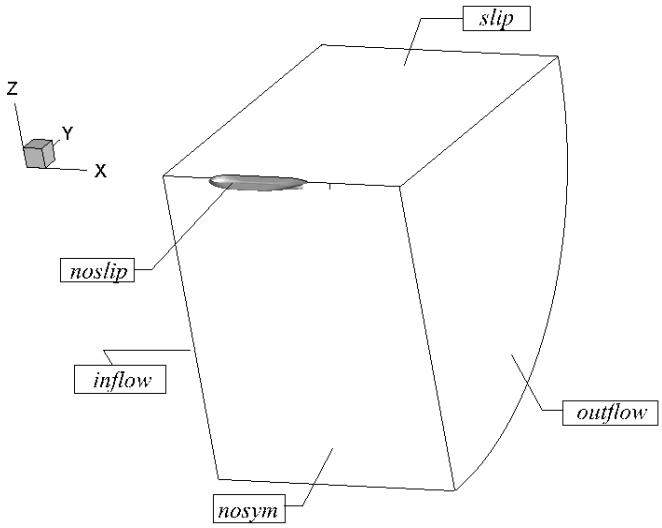

Figure 3-1 Viscous flow boundary conditions

Imposed on the hull surface, the *no-slip* boundary condition assumes:

- Dirichlet type boundary conditions for velocity, turbulent kinetic energy and turbulent frequency;
- Neumann type boundary condition for pressure

$$u_i = 0;\ \frac{\partial p}{\partial \zeta_B} = 0;\ k = 0;\ \omega = f\left(u_T, ...\right) \quad (3.10)$$

For the fluid entering the domain, the *inflow* boundary condition is declared on the upstream frontier imposing:

- Dirichlet type boundary conditions for velocity, turbulent kinetic energy and turbulent frequency;
- Neumann type boundary condition for pressure

$$u = cst;\ \frac{\partial p}{\partial \zeta_B} = 0;\ k = cst;\ \omega = cst \tag{3.11}$$

Regarding the fluid exiting the domain, the *outflow* boundary condition is declared on the downstream frontier as follows:

- Neumann type boundary conditions for velocity, turbulent kinetic energy and turbulent frequency;
- Dirichlet type boundary condition for pressure

$$\frac{\partial u_i}{\partial \zeta_B} = 0;\ p = 0;\ \frac{\partial k}{\partial \zeta_B} = 0;\ \frac{\partial \omega}{\partial \zeta_B} = 0 \tag{3.12}$$

At the free-surface level, the *slip* boundary condition implies Neumann type boundary conditions for all the variables:

$$u_i n_i = 0, \frac{\partial u_i}{\partial \zeta_B} = 0;\ \frac{\partial p}{\partial \zeta_B} = 0;\ \frac{\partial k}{\partial \zeta_B} = 0;\ \frac{\partial \omega}{\partial \zeta_B} = 0 \tag{3.13}$$

3.1.2.3.Propeller Model

In order to study and analyze the manoeuvring performances taking into consideration the effect of the propeller, a "body force" approach has been used. The propeller forces and moments are obtained based on the lifting line theory that replaces the blades with a number of bound vortices extended from the hub to the tip [13]. Free vortices that depend on the intensity of the bound vortices are also shed. In an interactive manner, the program that computes the propeller load is coupled with the viscous CFD solver, the hull-propeller interaction have been taken into consideration on the CFD investigation, for determination of the forces and moment acting on the KVLCC2 hull model.

3.2. Computational Domain

In order to solve both potential and viscous flow problems it is mandatory to properly choose the limits of the computational domain. Also, for a precise capture of all the geometrical changes that describe the surface of the hull influencing the velocity and pressure gradients and for better revealing the evolution of the flow field, it is necessary to pay enough attention to the grid generation process. In the present research, two SHIPFLOW modules were used with respect to

the computational domain: a panel generator for the potential flow computation and a 3D grid generator for the viscous part. It should be mentioned that the 3D grid used for the viscous flow analysis was chosen based on a grid convergence study presented in [14], the numerical uncertainty being assessed by considering the ITTC Recommended Procedures and Guidelines ([15], [16]) for both ship resistance and static PMM tests computation.

3.2.1. Potential Flow Panelization

For the potential flow computation, the mesh generator module of SHIPFLOW code was used to create the panelization on the ship hull and at the free-surface level (see Figures 3-2 and 3-3).

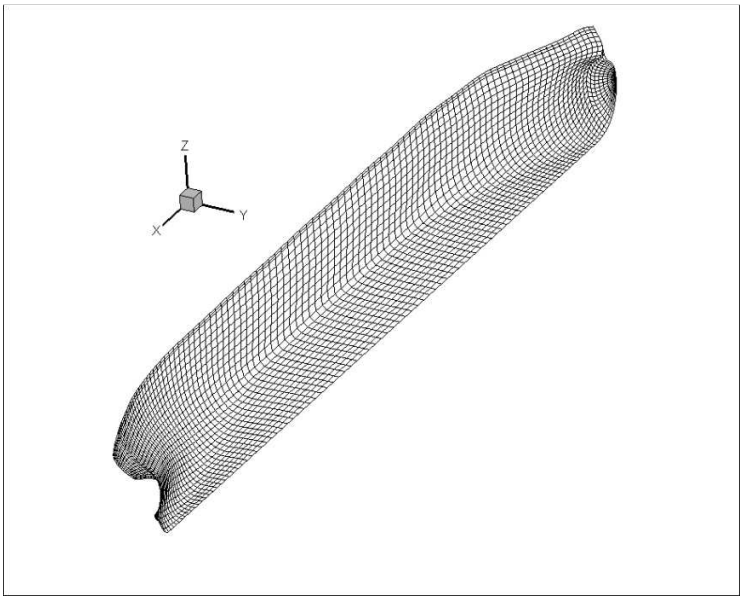

Figure 3-2 KVLCC2 Hull panelization

As Figure 3-4 shows, the free-surface which was decomposed in three major parts upstream, along and downstream the hull, was extended between 0.75 ship length upstream, 2.5 ship length downstream and 0.7 ship length in transversal direction.

The origin of the coordinates system, *Oxyz*, is placed at the waterline level, at the intersection of the aft perpendicular with the Center Line. The *Ox*, *Oy* and *Oz* axes are oriented towards aft, starboard and upwards.

For obtaining the free-surface panelization, every part was divided by a number of stations (in longitudinal direction) and points (in transverse direction). The longitudinal distribution was based on the best practices that recommend a number of 25-30 panels on wave length, whereas for the transversal division 25 panels have been chosen. The mesh was streched towards the aft

and fore part of the hull as well as towards the hull surface in transverse direction ensuring by this increased density a greater capability to capture the phenomena in these areas of interest.

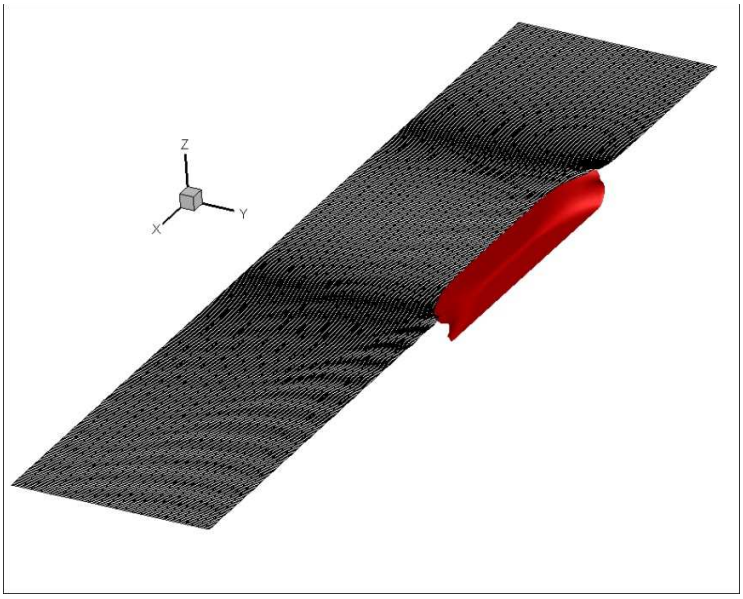

Figure 3-3 Free-surface panelization

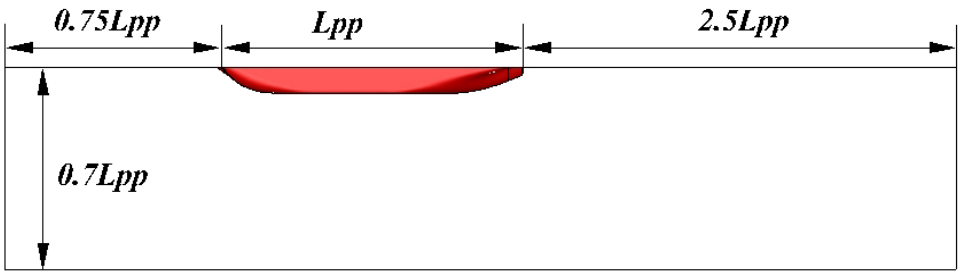

Figure 3-4 Computational domain

3.2.2. 3D Viscous Flow Grid

In case of the viscous flow computation, the 3D grid generator module of SHIPFLOW code was considered, a H-O type, mono-block, fully structured grid has been created in the limits of the computational domain (see Figure 3-5). The 3D grid is clustered, in radial direction, near the *no slip* boundary and in both radial and longitudinal direction at the extremities, enabling an accurate solution.

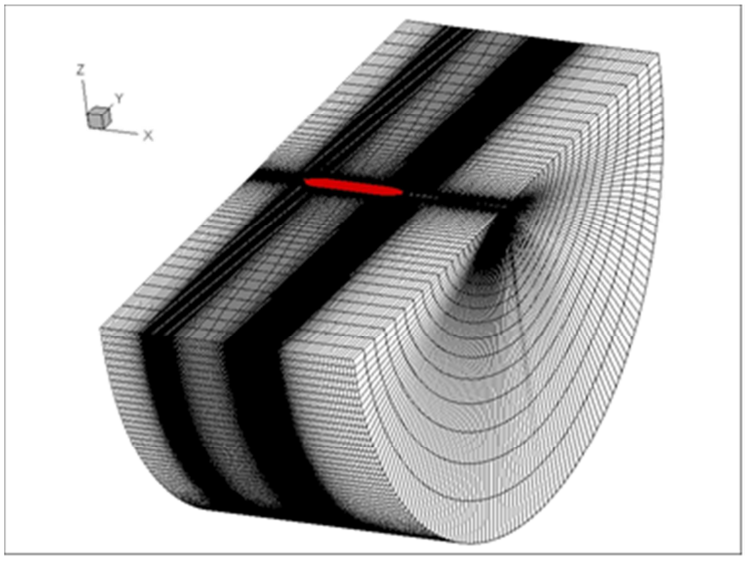

Figure 3-5 Three-dimensional grid for the whole domain of computation

As Figure 3-6 presents, the 2750000 cells generated based on an elliptical bidimensional technique are distributed between 0.5 ship length upstream, 1.0 ship length downstream and 3.0 ship length in radial direction. As in the case of potential flow computation, the origin of the coordinates system, *Oxyz*, is placed at the waterline level, at the intersection of the aft perpendicular with the Centerline. The *Ox*, *Oy* and *Oz* axes are oriented towards aft, starboard and upwards.

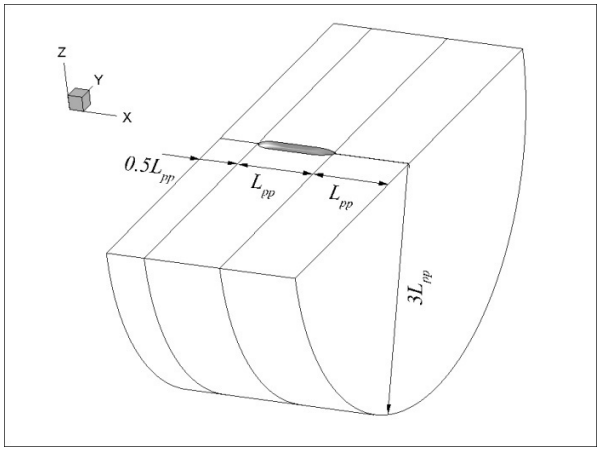

Figure 3-6 Computational domain (three dimension representation)

In order to account for the propeller and rudder effects two structured grids were created (Figure 3-7), an overlapping grid technique being used to solve the flow around the hull equipped with rudder and propeller.

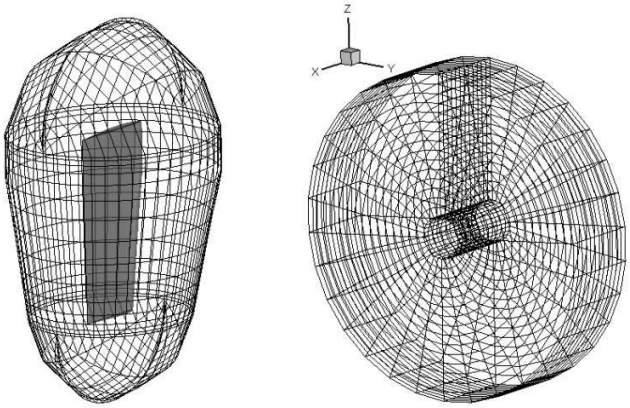

Figure 3-7 Rudder, propeller grid representation

3.3.CFD Results

The goal to solve the KVLCC2 ship manoeuvring problem can be achieved by using the described CFD techniques, a proper calibration of the numerical methods being necessary onward the calculations. In this respect, the bare hull ship resistance simulation is used in order to verify the ability of the program to accurately determine the longitudinal force, whereas the numerical simulation of static PMM tests stands for the capacity of the solver to obtain satisfactory results for the transversal force and yaw moment. For the validation process, the experimental results made public by MOERI at SIMMAN 2008 [1] have been used. The main dimensions of the 1/58 model scale KVLCC2 ship have been depicted in Table 1.1 and Table 1.2.

3.3.1. Ship Resistance

Having as a goal the validation of the numerical methodology with respect to the longitudinal force determination, the present subchapter addresses the ship resistance problem. Two approaches have been used in order to determine the model scale ship resistance and compare it with the experimental results of MOERI [1]:

- The potential flow approach in order to determine the wave resistance coefficient;
- The viscous flow approach in order to determine the viscous components of ship resistance.

3.3.1.1.Modeling Conditions

Starting from the experimental data provided by MOERI [1], at SIMMAN 2008, the 1/58 model scale was considered for the KVLCC2 tanker hull. The calculation of the model scale resistance was done for a range of eight speeds U between 0.743 to 1.0807 [m/s], for all considered speeds,

the Froude and Reynolds numbers being calculated at 11°C water temperature, as during the experimental tests. It should be mentioned that the model speed of 1.047 [m/s] corresponds to the 15.5 [Kn] full scale speed and all the calculations are done for the bare hull model with zero trim angle.

3.3.1.2.Ship Resistance Numerical Results

Table 3.1 gives the values for the viscous pressure resistance coefficient C_{PV}, friction resistance coefficient C_F, and wave resistance coefficient, C_W. The total resistance coefficient C_T, was obtained based on the following relation:

$$C_T = C_W + C_V = C_W + C_{PV} + C_F \tag{3.14}$$

The wave resistance coefficient was obtained by applying the potential flow methodology, while the viscous resistance coefficient, C_V, was determined with the viscous flow solver.

Table 3.1 Resistance coefficients (CFD numerical results)

U [m/s]	F_n	Rn	C_{PV}	C_F	C_W	C_T
0.743	0.101	3.26x106	1.14 x10-3	3.35 x10-3	4.20 x10-6	4.50 x10-3
0.8105	0.110	3.56 x106	1.13 x10-3	3.31 x10-3	8.56 x10-6	4.44 x10-3
0.8781	0.119	3.86 x106	1.12 x10-3	3.27 x10-3	1.48 x10-5	4.38 x10-3
0.9456	0.129	4.15 x106	1.11 x10-3	3.23 x10-3	2.83 x10-5	4.34 x10-3
0.9794	0.133	4.30 x106	1.10 x10-3	3.21 x10-3	3.01 x10-5	4.32 x10-3
1.0132	0.138	4.45 x106	1.10 x10-3	3.19 x10-3	3.83 x10-5	4.29 x10-3
1.0469	0.142	4.60 x106	1.10 x10-3	3.18 x10-3	4.26 x10-5	4.27 x10-3
1.0807	0.147	4.75 x106	1.09 x10-3	3.16 x10-3	5.15 x10-5	4.25 x10-3

The model scale total resistance, R_T, for the considered range of speeds between 0.743 and 1.0807 was calculated by using the total resistance coefficient, as follows:

$$R_T = C_T \cdot \frac{1}{2} \cdot \rho \cdot U^2 \cdot S \tag{3.15}$$

where ρ is the water density and S is the wetted surface of the hull.

Table 3.2 and Figure 3-8 present the model scale total resistance numerical and experimental results and the EFD-CFD comparison error.

One may see that the magnitude of the comparison error is about 7%. Since the computational results are obtained on the background of a numerical uncertainty, U_{SN}, of 4.862% for the total resistance coefficient [14], the viscous pressure resistance coefficient having the highest U_{SN}, it

can be stated that the numerical and the experimental results are in good agreement. The ability of the solver to predict the longitudinal force determination is, thus, highlighted.

Table 3.2 Comparison error (EFD-CFD) for model scale total resistance

Model Speed [m/s]	R_{T_MOERI}[N]	R_{T_CFD} [N]	*Error %*
0.743	9.58	10.25	7.00%
0.8105	11.27	12.05	6.91%
0.8781	13.10	13.99	6.81%
0.9456	15.04	16.10	7.06%
0.9794	16.07	17.19	6.98%
1.0132	17.13	18.34	7.06%
1.0469	18.22	19.50	7.05%
1,0807	19,36	20,73	7,08%

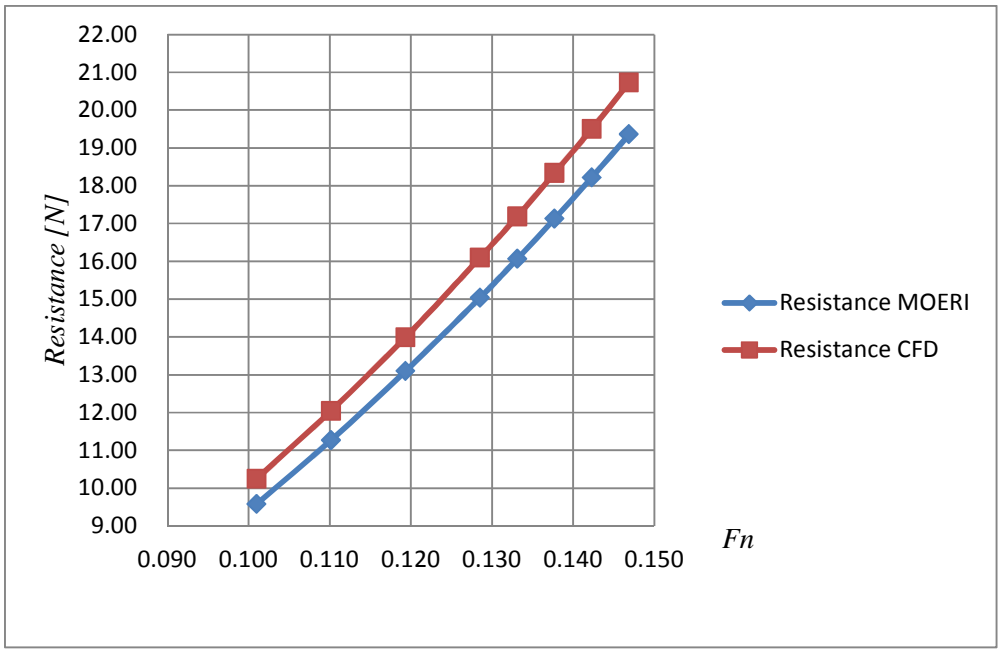

Figure 3-8 Total model ship resistance

A special attention was paid to the wave resistance coefficient. Table 3.3 and Figure 3-9 show the magnitude of C_W for the entire range of speeds between 0.743 and 1.0807, both CFD and PHP results being depicted.

The results are matching and corresponding in quality. Regarding the quantity, the values of the wave resistance coefficients are negligible. As a consequence, the two sets of results allow us to

neglect the free-surface effect in the following computations lowering, in this manner, the computational effort.

Table 3.3 Wave resistance coefficient

Fn	C_{W_CFD}	C_{W_PHP}
0.101	4.20 x10^{-6}	1,01 x10^{-6}
0.110	8.56 x10^{-6}	3,02 x10^{-6}
0.119	1.48 x10^{-5}	9,05 x10^{-6}
0.129	2.83 x10^{-5}	2,02 x10^{-6}
0.133	3.01 x10^{-5}	2,82 x10^{-6}
0.138	3.83 x10^{-5}	3,94 x10^{-6}
0.142	4.26 x10^{-5}	5,44 x10^{-6}
0.147	5.15 x10^{-5}	7,27 x10^{-6}

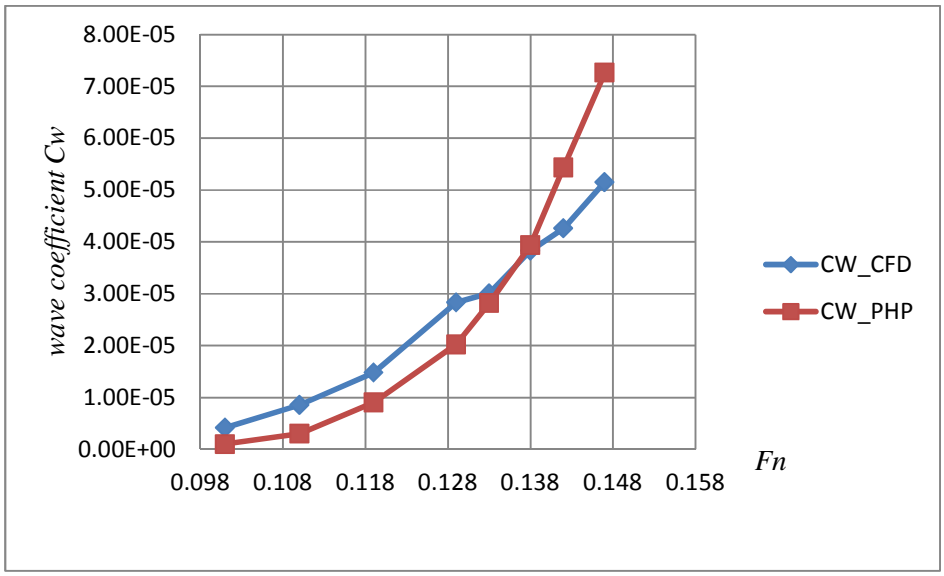

Figure 3-9 Wave resistance coefficient comparison

In the end, it may be concluded that:

- The determined CFD-EFD error, in correlation with the numerical uncertainty [14] validates the ability of the solver to determine the longitudinal force;
- The magnitude of the wave resistance coefficient permits us to neglect the free-surface effect, the viscous resistance being proven to be the main component of the KVLCC2 ship resistance.

3.3.2. Static PMM Tests

In order to solve the KVLCC2 ship manoeuvring problem, the longitudinal force, *X*, the transversal force, *Y*, and the yaw moment, *N*, that are acting on the ship hull during static manoeuvring motions (see Figure 3-10) must be accurately determined.

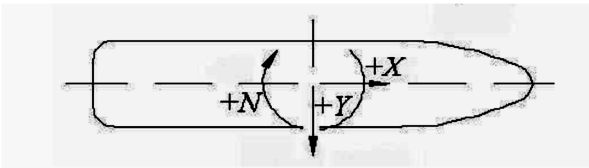

Figure 3-10 Hydrodynamic forces and moments on the ship hull

The PMM type captive model tests are one of the main experimental methods that can be applied, in a towing tank, in order to measure the hydrodynamic forces and moments resulting from different rudder and/or drift angles combinations. A PMM can be used in a static or dynamic mode of operation. For the static mode that will be numerically approached in the present research, the model is constrained to travel along a straight path at constant velocity with different drift and/or rudder angles (Figures 3-11, 3-12 and 3-13).

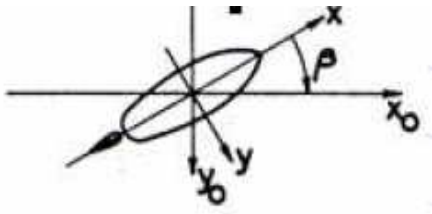

Figure 3-11 Static drift

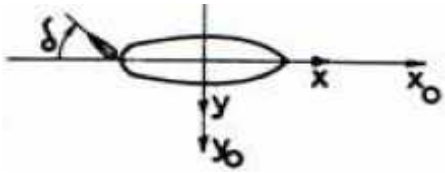

Figure 3-12 Static rudder

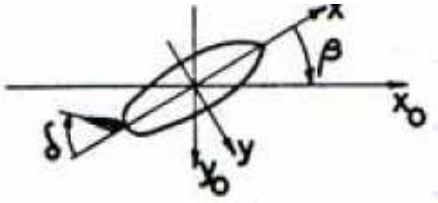

Figure 3-13 Static drift and rudder

In order to numerically simulate the static PMM tests, the viscous flow solver of the SHIPFLOW CFD code is used, a preliminary validation of the computational methodology being done based on the "static drift" and "static rudder" experimental results of MOERI [1].

3.3.2.1.Static PMM Tests Modeling Conditions

Starting from the experimental data provided by MOERI [ref], at SIMMAN 2008, the 1/58 model scale of the KVLCC2 tanker ship has been used to investigate the hydrodynamic forces and moments, taking into consideration both rudder and propeller influences.

The "static drift", "static rudder" and "static drift and rudder" virtual tests considered the propeller operating at the ship self-propulsion point, at 8.59 rps.

All the virtual PMM tests were done, in deep water, at 1.047 [m/s] model speed, the corresponding Froude and Reynolds number being equal with 0.142 and 4.6×10^6 respectively. The effects of model mass and inertia are not taken into consideration. Also, the low Froude number as well as the negligible magnitude of the wave resistance coefficient allows us to neglect the free surface effect. Thus, the viscous resistance becomes the main component of the longitudinal force to investigate during the CFD computations.

The computations have been performed for a range of drift angles from β= -12° to β=12° with 2° increment and for a range of rudder angles from δ=-40° to δ= 40° with 10° increment. The 3D grid used for the viscous flow computations is described in Chapter 3.2.2, as well as the grids used for rudder and propeller. A "body force" technique was used in order to consider the effect of the propeller which was modelled based on a lifting line approach.

3.3.2.2.Static PMM Tests Numerical Results

The theoretical methods available for the real prediction of the manoeuvring performances of the ship are not certain. Thus, the PMM tests experimental techniques are used to determine the hydrodynamic derivatives, the solution of the equations of motion in the horizontal plane giving the prediction of manoeuvring performances.

Therefore, static PMM tests are computed by the use of CFD techniques, the hydrodynamic forces and moments have been determined in order to further obtain the hydrodynamic derivatives. Prior to the numerical simulation of the "static drift and rudder" tests, the validation

of the computational methodology was done based on the "static drift" and "static rudder" experimental results of MOERI [1].

It should be mentioned that the transversal force, Y, is given by the following relation:

$$Y = Y_H + Y_R \tag{3.16}$$

where

Y_H – is the transversal forces action on the hull, in the horizontal plane;

Y_R – is the transversal forces action on the rudder, in the horizontal plane.

The hydrodynamic forces decomposition, depending the drift angle and rudder deflection angle is presented in **Appendix 3.1 Hydrodynamic forces decomposition.**

3.3.2.2.1. Static Drift

The "static drift" numerical tests were done, based on the modelling conditions presented in Chapter 3.3.2.1, for a range of drift angles extended between β = -20° to β =20° with 2° increment. During all computational tests, the rudder angle was maintained δ =0°.

With the goal to validate the numerical methodology used for the calculation of the hull transversal force, Y_H, the obtained CFD results, Y_{H_CFD}, are compared with the experimental results of MOERI, Y_{H_MOERI} (see Table 3.4 and Figure 3-14).

Table 3.4 EFD-CFD comparison error for hull transversal force during "static drift" motion

β [°]	Y_{H_MOERI}	Y_{H_CFD}	*Error %*
-20	-167.945	-160.351	4.52%
-16	-125.590	-116.479	7.26%
-12	-85.267	-78.212	8.27%
-8	-47.371	-45.496	3.96%
-6	-32.330	-30.679	5.11%
-4	-21.619	-17.931	17.06%
-2	-11.425	-7.991	30.06%
0	-0.779	0.770	-
2	10.791	9.589	11.14%
4	18.881	19.523	-3.40%
6	30.038	32.206	-7.22%
8	45.441	46.816	-3.03%
12	80.648	78.949	2.11%
16	123.035	116.892	4.99%
20	166.701	160.838	3.52%

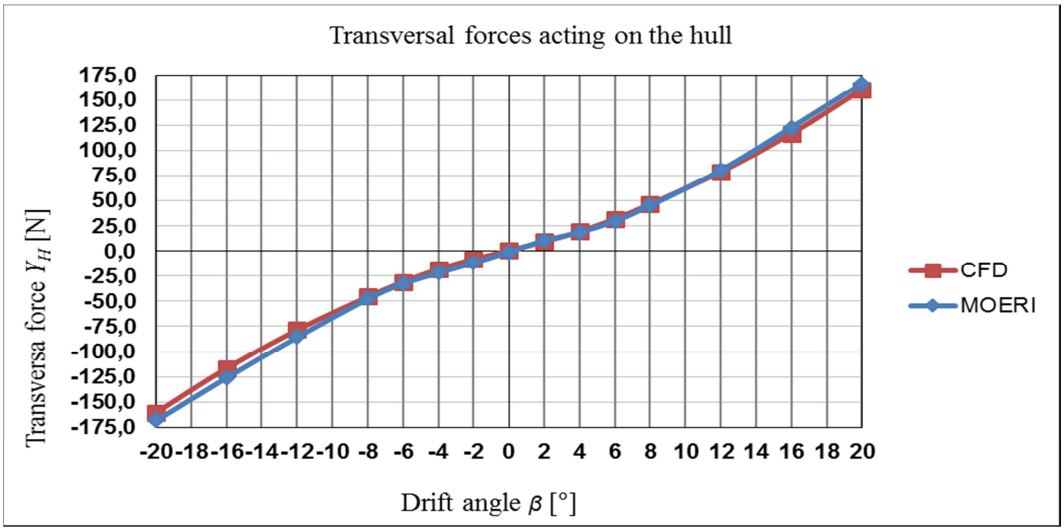

Figure 3-14 EFD-CFD comparison for hull transversal force during "static drift"

Figure 3.14 shows the qualitative agreement between the two sets of results, whereas the comparison error highlights the good ability of the viscous CFD solver with respect to the hull transversal forces. The highest errors that are registered at the smallest drift angles, β=-4°, and β=±2° can be explained by the quality of the grid. Nevertheless, the results presented for the bare hull case, for similar values of the drift angles [23], support the continuation of the study.

As a conclusion, it can be said that the CFD techniques gives a satisfactory agreement between numerical and experimental results on the hull transversal force, Y_H, especially for high drift angle.

3.3.2.2.2. Static Rudder

The "static rudder" numerical tests were done, based on the modelling conditions presented in Chapter 3.3.2.1, for a range of rudder angles extended from δ = -40° to δ =40° with 10° increment. During all computational tests, zero drift angle was maintained, β =0°. Run in conformity with the experimental results of MOERI, the "static rudder" tests were considered with the goal to validate the numerical methodology used for the calculation of the rudder transversal force, Y_R, the obtained CFD results, Y_{R_CFD}, being compared with the experimental results of MOERI, Y_{R_MOERI} (see Table 3.5 and Figure 3-15).

Although Figure 3-15 reveals the fact that the presented curves have a similar evolution, showing good qualitative agreement between the two sets of results, the comparison error displays big differences for δ=10° and δ=20° rudder deflection angle.

Table 3.5 EFD-CFD comparison error for rudder transversal force during “static rudder” motion

δ [°]	Y_{R_MOERI}	Y_{R_CFD}	Error %
-40	-16.296	-16.903	-3.722
-30	-14.748	-16.195	-9.812
-20	-11.404	-11.359	0.390
-10	-6.743	-7.934	-17.654
0	-	-	-
10	4.606	7.265	-57.734
20	10.334	15.491	-49.898
30	15.458	16.674	-7.866
40	19.499	16.959	13.027

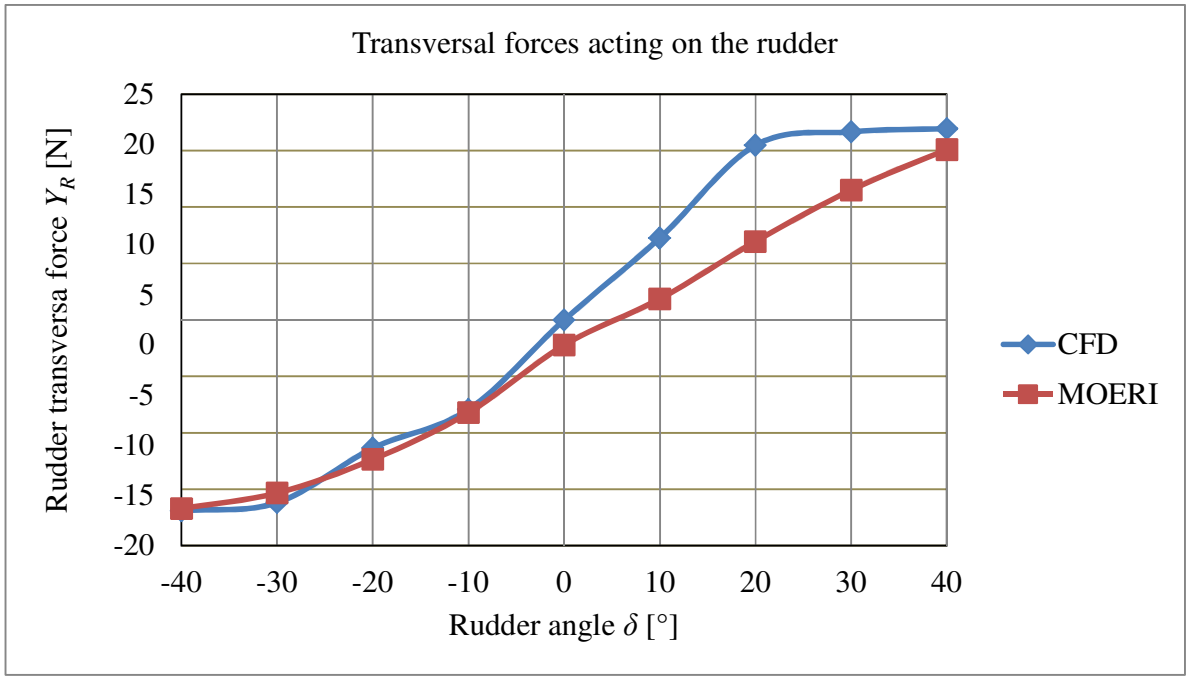

Figure 3-15 EFD-CFD comparison for rudder transversal force during “static rudder”

Still, the presented errors can be justified, the numerical solutions calculated, for Y, for $\delta = 10°$ at SIMMAN 2008 ([1], [24]), presents a numerical error of 50.1%. As well, the quality of the grid and the lack of maturity of the numerical schemes can be valid explanations.

As a conclusion, it can be said that the CFD techniques gives a satisfactory agreement between numerical and experimental results on the hull transversal force, Y_H, especially for high drift angle.

3.3.2.2.3. Static Drift and Rudder

The last computed tests were the "static drift and rudder", both rudder and propeller have been taken into consideration. For these CFD computations, all the drift/rudder angle possibilities have been considered. The drift angles were extended from β = -20° to β =20° with 2° increment, whereas the rudder deflection angles were chosen between δ = -40° to δ =40° with 10° increment.

The "static drift and rudder" tests were considered in order to determine the hydrodynamics forces and moments that will, further, be used for determining the hydrodynamic derivatives.

The obtained longitudinal *X* forces, transversal *Y* forces and yaw moments *N* acting on the hull are presented in Tables 3.7, 3.8 and 3.9 and in Figures 3-16, 3-17 and 3-18.

Table 3.6 Longitudinal X forces with drift and rudder angles influences

β/δ [°]	40	30	20	10	0	-10	-20	-30	-40
-20	-30.38	-24.38	-21.65	-20.11	-20.99	-24.19	-29.56	-36.52	-45.61
-18	-31.06	-25.33	-22.72	-21.12	-21.76	-24.74	-29.99	-36.34	-44.72
-16	-31.34	-26.36	-23.36	-21.78	-22.31	-24.92	-29.89	-35.96	-43.79
-14	-31.95	-26.52	-24.04	-22.49	-22.63	-25.20	-29.83	-35.26	-42.23
-12	-32.24	-27.81	-24.24	-22.64	-22.69	-25.19	-29.55	-34.59	-41.31
-10	-32.95	-30.76	-24.93	-22.85	-22.59	-24.90	-29.14	-34.31	-39.68
-8	-33.39	-31.29	-25.36	-23.08	-22.61	-24.51	-28.63	-33.77	-39.02
-6	-33.70	-31.44	-25.45	-23.03	-22.48	-23.95	-27.89	-33.06	-37.94
-4	-33.78	-30.39	-25.21	-22.81	-22.29	-23.28	-27.14	-31.97	-36.62
-2	-34.01	-30.04	-25.12	-22.68	-22.13	-22.84	-26.48	-30.73	-35.16
0	-34.53	-30.71	-25.31	-22.76	-22.14	-22.73	-25.94	-30.02	-33.90
2	-34.98	-31.03	-26.39	-22.95	-22.22	-22.70	-25.49	-28.83	-32.90
4	-35.92	-31.66	-26.94	-23.31	-22.48	-22.89	-25.37	-28.69	-32.44
6	-36.99	-32.84	-27.72	-23.74	-22.73	-23.10	-25.22	-29.23	-32.52
8	-37.89	-33.51	-28.73	-24.07	-22.86	-23.11	-25.15	-29.41	-32.62
10	-39.20	-34.45	-29.45	-24.29	-22.87	-22.95	-24.87	-28.87	-32.51
12	-40.63	-35.29	-29.88	-24.47	-22.97	-22.86	-24.46	-27.22	-31.72
14	-43.27	-36.61	-30.34	-24.56	-22.83	-22.65	-24.30	-26.72	-31.23
16	-43.87	-37.16	-30.90	-25.03	-22.29	-22.01	-23.67	-26.59	-31.02
18	-44.86	-37.65	-30.95	-24.77	-21.67	-21.34	-23.05	-25.95	-31.06
20	-46.19	-37.91	-30.65	-24.15	-20.76	-20.34	-21.90	-24.98	-30.67

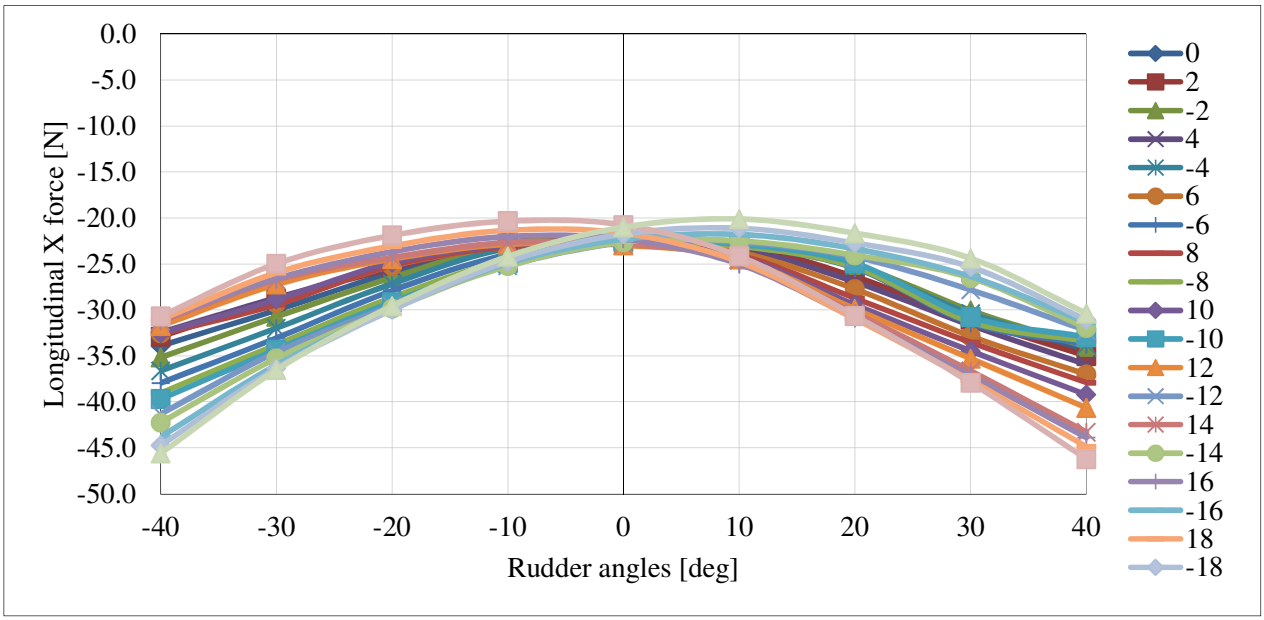

Figure 3-16 Longitudinal X forces with drift and rudder angles influences

Table 3.7 Transversal Y forces with drift and rudder angles influences

β/δ [°]	-40	-30	-20	-10	0	10	20	30	40
-20	-133.60	-136.35	-137.15	-150.95	-167.00	-183.68	-196.99	-203.89	-211.08
-18	-111.69	-115.62	-122.50	-128.87	-143.72	-158.85	-172.15	-178.33	-183.18
-16	-91.76	-94.70	-101.62	-107.54	-121.49	-135.39	-147.83	-153.99	-158.22
-14	-72.12	-76.11	-81.37	-87.36	-100.90	-115.02	-126.64	-131.75	-135.35
-12	-53.93	-55.60	-59.66	-68.25	-81.70	-96.28	-108.16	-111.93	-115.43
-10	-36.72	-33.21	-38.62	-50.07	-63.92	-78.50	-91.34	-95.57	-96.28
-8	-21.18	-17.91	-22.41	-33.88	-46.88	-61.23	-74.05	-78.99	-79.70
-6	-6.97	-4.04	-7.86	-19.27	-31.46	-45.03	-56.99	-63.22	-63.56
-4	5.46	6.20	4.10	-7.23	-18.69	-30.89	-41.63	-47.85	-48.93
-2	16.08	15.11	14.16	2.43	-8.87	-20.05	-27.57	-34.55	-35.51
0	26.22	26.52	23.92	11.81	0.19	-10.83	-16.56	-24.10	-24.28
2	36.16	36.05	31.03	21.44	9.61	-1.17	-7.13	-12.06	-13.87
4	47.91	47.08	42.23	32.73	20.12	8.96	1.89	-2.08	-2.95
6	61.72	61.79	58.61	47.12	33.63	21.67	10.18	8.25	8.93
8	77.05	76.63	74.90	63.35	49.22	36.70	24.73	20.76	22.08
10	94.54	93.55	89.73	80.40	65.94	53.02	40.77	36.60	36.65
12	113.43	111.28	104.86	97.45	83.31	70.80	60.97	59.50	54.14
14	135.54	132.75	124.65	116.03	102.40	89.86	81.63	74.87	72.81
16	156.56	154.39	149.88	136.46	123.08	110.21	102.05	97.31	91.65
18	180.96	178.76	172.91	160.41	145.57	131.54	123.27	118.12	110.93
20	208.33	204.17	197.11	185.71	169.00	153.38	138.55	139.86	132.17

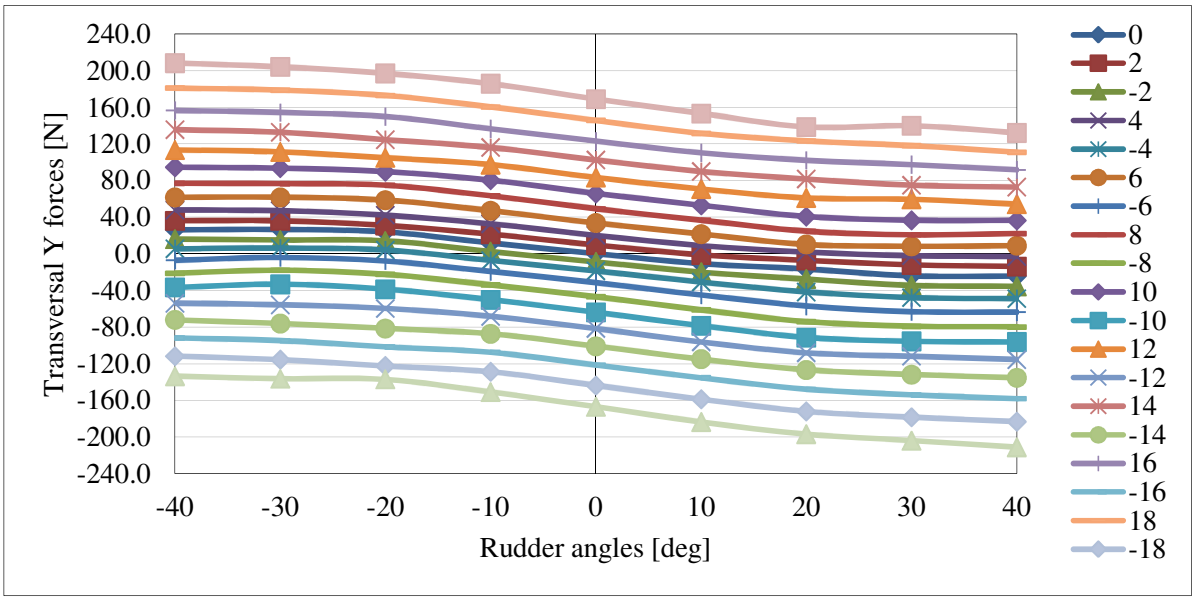

Figure 3-17 Transversal Y forces with drift and rudder angles influences

Table 3.8 Yaw moment N with drift and rudder angles influences

β/δ [°]	-40	-30	-20	-10	0	10	20	30	40
-20	-140,91	-145,66	-140,54	-165,95	-197,36	-228,99	-253,31	-265,06	-279,25
-18	-97,47	-103,08	-119,17	-124,78	-153,15	-181,28	-205,91	-216,05	-225,6
-16	-61,08	-63,97	-80,79	-86,64	-113,47	-139,21	-161,99	-172,59	-179,37
-14	-28	-33,74	-47,01	-53,65	-79,76	-106,47	-128,16	-137,27	-143,33
-12	-2,27	-4,25	-13,26	-26,06	-51,53	-79,41	-102,36	-108,52	-114,83
-10	18,72	27,03	16,42	-3,29	-29,97	-57,37	-82,06	-89,86	-92,13
-8	35,49	41,68	32,86	13,86	-10,03	-36,28	-60,58	-70,2	-70,98
-6	47,04	51,6	44,26	26,26	5,58	-18,14	-40,08	-52,5	-50,41
-4	51,23	54,04	48,83	31,93	13,71	-7,2	-26,07	-38,3	-37,52
-2	49,57	51,8	45,61	28,17	10,58	-8,24	-21,99	-34,31	-32,68
0	45,07	47,78	40,84	22,15	3,96	-13,66	-24,86	-37,94	-35,39
2	41,8	43,51	33,31	17,47	-2,37	-19,89	-31,62	-40,93	-41,13
4	42,5	43,68	33,31	16,68	-5,56	-24,37	-37,46	-45,2	-44,16
6	51,62	55,15	47,36	26,94	2,2	-19,2	-38,69	-44,81	-42,04
8	66,72	69,37	64,87	43,62	16,73	-7,01	-28,52	-37,74	-34,16
10	88,09	87,28	81,31	62,89	35,1	9,64	-13,16	-21,73	-20,65
12	111,46	106,93	97,81	82,77	55,3	31,43	14,88	12,69	-0,17
14	140,16	136,89	125,82	108,55	82,21	58,45	47,02	34,99	25,71
16	171,55	169,78	164,42	141,09	115,56	91,25	80,77	71,21	56,39
18	215,68	212,59	205,37	183,68	155,54	129,28	119,49	108,57	91,53
20	268,92	261,06	251,05	231,41	199,79	170,07	141,17	150,45	133,61

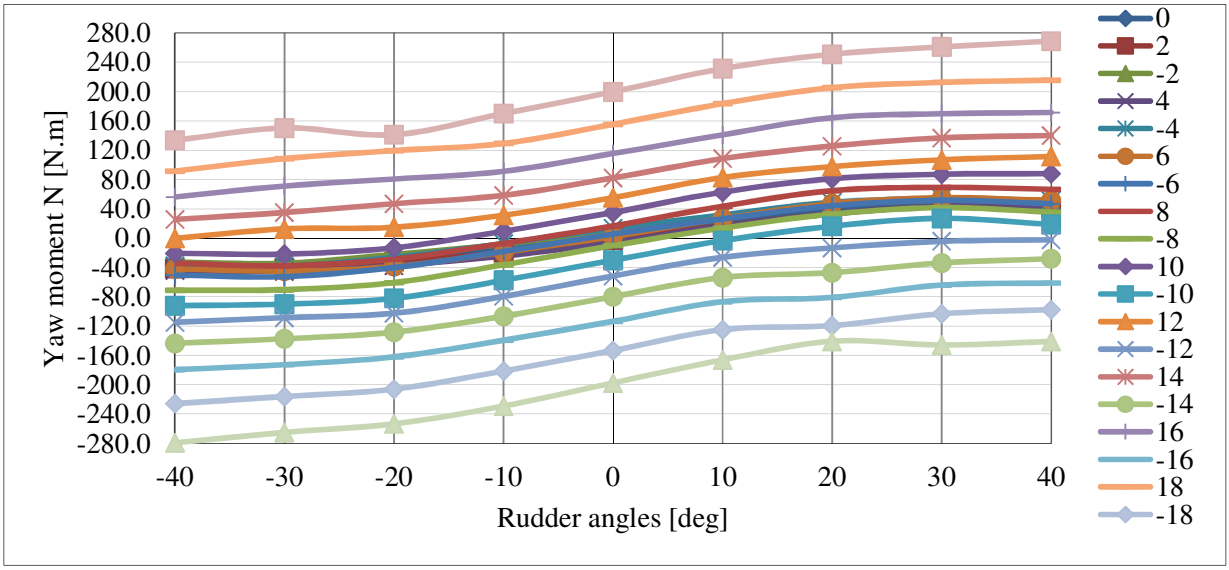

Figure 3-18 Yaw moment N with drift and rudder angles influences

Non-dimensional forces and moment acting on KVLCC2 hull model

A step forward in order to calculate the hydrodynamic derivatives essential to solve manoeuvring problem is to analyze the non-dimensional forces and moment obtained by the use of the following formulas:

$$\frac{Force}{0.5\rho U^2 L_{wL}^2} \tag{3.17}$$

$$\frac{Moment}{0.5\rho U^2 L_{wL}^3} \tag{3.18}$$

where

ρ is the water density, U is the ship speed in [m/s] and L_{wL} is length of waterline.

The obtained non-dimensional longitudinal X forces, non-dimensional transversal Y forces and non-dimensional yaw moment N, acting on the hull are presented in Tables 3.9, 3.10 and 3.11 and Figures 3-19, 3-20 and 3-21.

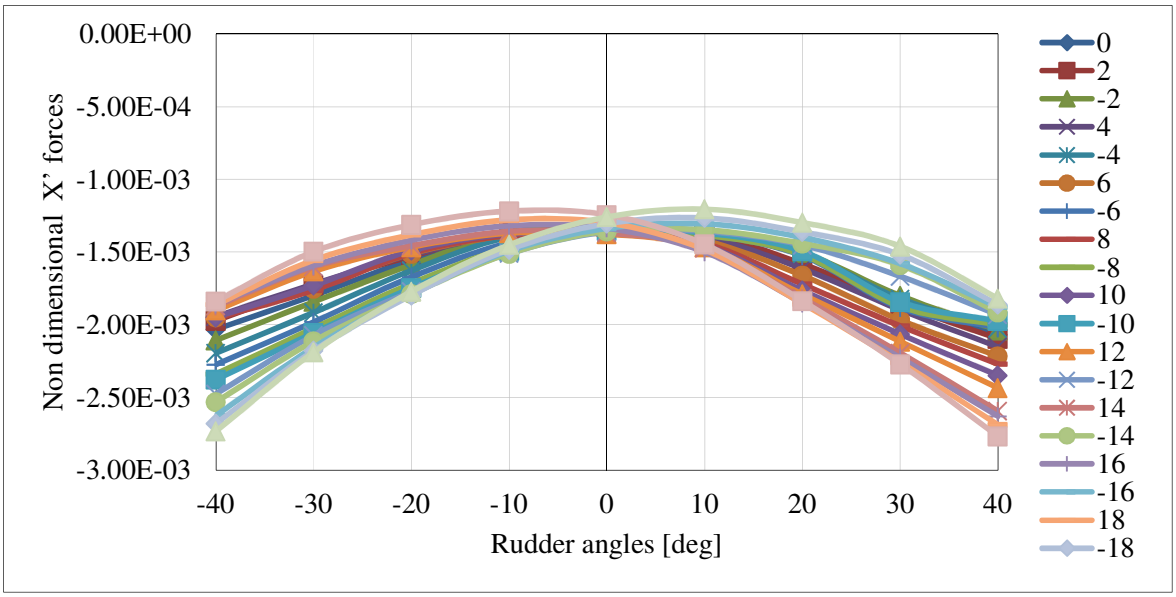

Figure 3-19 Non-dimensional longitudinal X' forces with drift and rudder angles influences

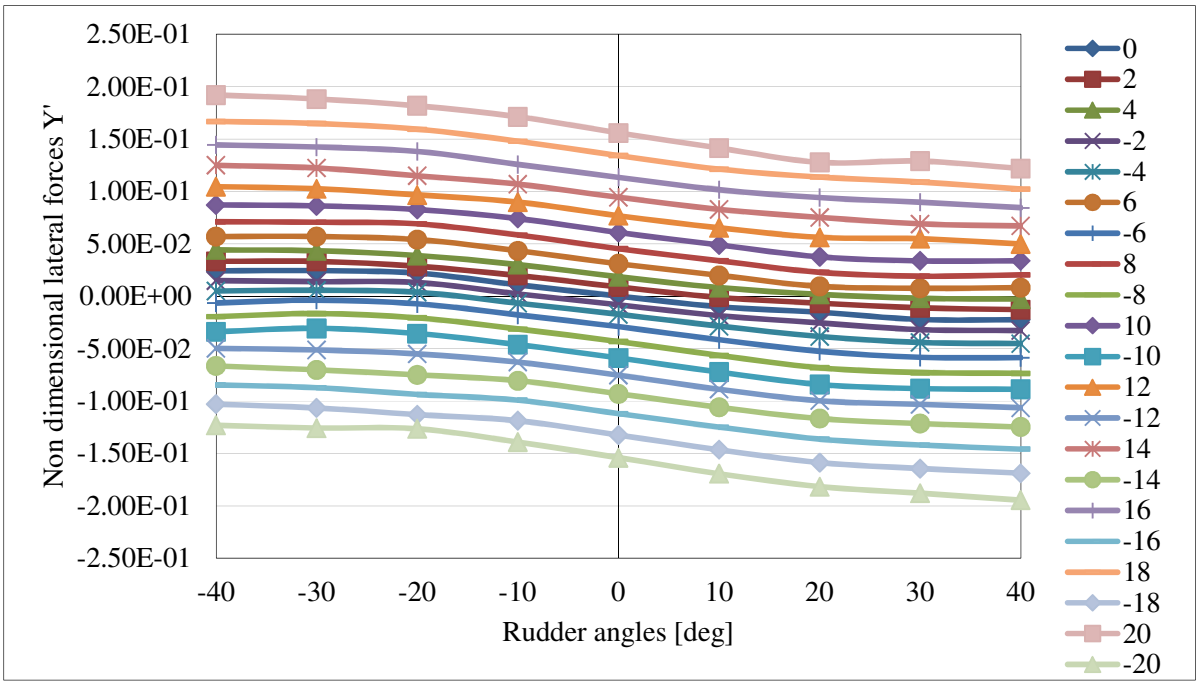

Figure 3-20 Non-dimensional lateral forces Y' with drift and rudder angles influences

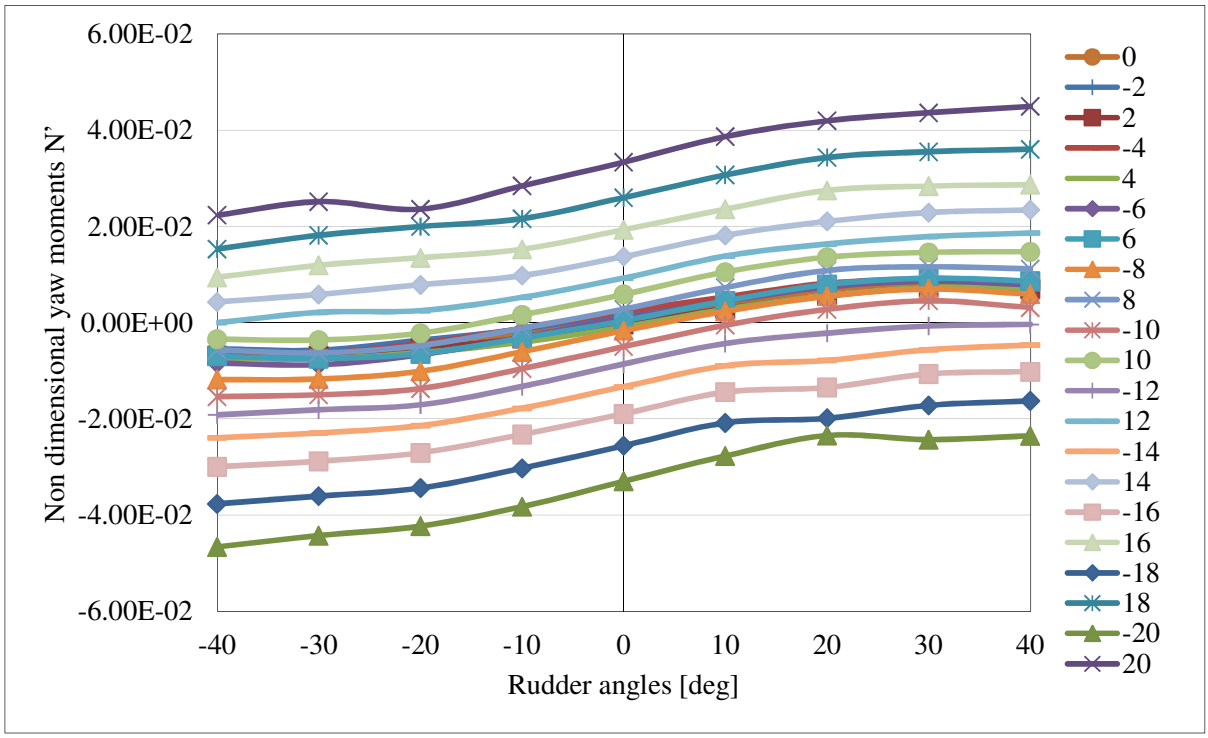

Figure 3-21 Non-dimensional yaw moments N' with drift and rudder angles influences

Table 3.9 Non-dimensional longitudinal forces X’

beta\delta	40	30	20	10	0	-10	-20	-30	-40
-20	-0,001821	-0,001461	-0,001298	-0,001205	-0,001258	-0,00145	-0,001772	-0,002189	-0,002733
-18	-0,001862	-0,001518	-0,001362	-0,001266	-0,001304	-0,001483	-0,001798	-0,002178	-0,00268
-16	-0,001878	-0,00158	-0,0014	-0,001306	-0,001337	-0,001493	-0,001791	-0,002155	-0,002625
-14	-0,001915	-0,001589	-0,001441	-0,001348	-0,001356	-0,001511	-0,001788	-0,002113	-0,002531
-12	-0,001932	-0,001667	-0,001453	-0,001357	-0,00136	-0,00151	-0,001771	-0,002073	-0,002476
-10	-0,001975	-0,001843	-0,001494	-0,00137	-0,001354	-0,001492	-0,001746	-0,002056	-0,002378
-8	-0,002001	-0,001875	-0,00152	-0,001384	-0,001355	-0,001469	-0,001716	-0,002024	-0,002339
-6	-0,00202	-0,001884	-0,001525	-0,00138	-0,001347	-0,001436	-0,001672	-0,001981	-0,002274
-4	-0,002025	-0,001822	-0,001511	-0,001367	-0,001336	-0,001395	-0,001627	-0,001916	-0,002195
-2	-0,002039	-0,0018	-0,001505	-0,001359	-0,001326	-0,001369	-0,001587	-0,001842	-0,002107
0	-0,002069	-0,001841	-0,001517	-0,001364	-0,001327	-0,001362	-0,001555	-0,001799	-0,002032
2	-0,002096	-0,00186	-0,001581	-0,001375	-0,001332	-0,001361	-0,001528	-0,001728	-0,001972
4	-0,002153	-0,001898	-0,001615	-0,001397	-0,001347	-0,001372	-0,001521	-0,00172	-0,001944
6	-0,002217	-0,001968	-0,001661	-0,001423	-0,001362	-0,001385	-0,001511	-0,001752	-0,001949
8	-0,002271	-0,002009	-0,001722	-0,001442	-0,00137	-0,001385	-0,001507	-0,001763	-0,001955
10	-0,002349	-0,002065	-0,001765	-0,001456	-0,001371	-0,001375	-0,00149	-0,00173	-0,001948
12	-0,002435	-0,002115	-0,001791	-0,001467	-0,001376	-0,00137	-0,001466	-0,001632	-0,001901
14	-0,002594	-0,002194	-0,001819	-0,001472	-0,001368	-0,001358	-0,001456	-0,001601	-0,001872
16	-0,002629	-0,002227	-0,001852	-0,0015	-0,001336	-0,001319	-0,001419	-0,001594	-0,001859
18	-0,002689	-0,002257	-0,001855	-0,001484	-0,001299	-0,001279	-0,001381	-0,001555	-0,001862
20	-0,002768	-0,002272	-0,001837	-0,001448	-0,001244	-0,001219	-0,001312	-0,001497	-0,001838

Table 3.10 Non-dimensional lateral forces Y’

beta\delta	-40	-30	-20	-10	0	10	20	30	40
-20	-0,123191	-0,125721	-0,126459	-0,139188	-0,153981	-0,169363	-0,181633	-0,187996	-0,19463
-18	-0,102986	-0,106607	-0,112952	-0,118829	-0,132521	-0,146466	-0,158736	-0,164433	-0,168907
-16	-0,084607	-0,087318	-0,093704	-0,099163	-0,112023	-0,124838	-0,136308	-0,141985	-0,145888
-14	-0,066496	-0,070183	-0,075025	-0,080553	-0,093034	-0,106056	-0,116768	-0,121477	-0,124797
-12	-0,049731	-0,051265	-0,055006	-0,062932	-0,075331	-0,088772	-0,099733	-0,103203	-0,106432
-10	-0,033862	-0,030621	-0,035606	-0,04617	-0,058934	-0,072385	-0,084218	-0,088121	-0,088777
-8	-0,01953	-0,016514	-0,020662	-0,031236	-0,043224	-0,056455	-0,06828	-0,072837	-0,07349
-6	-0,006425	-0,003729	-0,007245	-0,017772	-0,029012	-0,041518	-0,052544	-0,058297	-0,058608
-4	0,005035	0,005719	0,003784	-0,006667	-0,017229	-0,028481	-0,038381	-0,04412	-0,045117
-2	0,014825	0,013928	0,013055	0,002245	-0,008177	-0,018486	-0,025422	-0,031857	-0,032745
0	0,024181	0,024451	0,022058	0,010891	0,000173	-0,009987	-0,015269	-0,022217	-0,022384
2	0,033339	0,033241	0,028614	0,019765	0,008864	-0,001078	-0,006572	-0,01112	-0,012789
4	0,044173	0,043413	0,038934	0,03018	0,018554	0,008258	0,001745	-0,001915	-0,002716
6	0,056907	0,056974	0,054043	0,043451	0,031008	0,019978	0,009385	0,007607	0,008238
8	0,071048	0,070656	0,069066	0,058412	0,045384	0,033841	0,022799	0,019142	0,020359
10	0,087169	0,086257	0,082739	0,074131	0,060804	0,048891	0,037597	0,033743	0,033795
12	0,104588	0,102608	0,096685	0,089854	0,076815	0,06528	0,056216	0,054861	0,049921
14	0,124974	0,122407	0,114936	0,106988	0,094421	0,082859	0,075266	0,069038	0,067131
16	0,144356	0,142353	0,138195	0,125826	0,11349	0,101624	0,094099	0,089724	0,084505
18	0,166858	0,164825	0,159436	0,147903	0,134223	0,121287	0,113665	0,10891	0,102286
20	0,192092	0,188258	0,181743	0,171235	0,155828	0,141427	0,127753	0,128956	0,121869

Table 3.11 Non-dimensional yaw moments N’

beta\delta	-40	-30	-20	-10	0	10	20	30	40
-20	-0,046669	-0,044299	-0,042334	-0,03827	-0,032984	-0,027735	-0,023487	-0,024343	-0,023549
-18	-0,037703	-0,036107	-0,034412	-0,030296	-0,025596	-0,020854	-0,019915	-0,017227	-0,01629
-16	-0,029977	-0,028844	-0,027073	-0,023266	-0,018963	-0,014479	-0,013503	-0,010691	-0,010208
-14	-0,023954	-0,022941	-0,021418	-0,017794	-0,01333	-0,008967	-0,007857	-0,005638	-0,00468
-12	-0,019191	-0,018136	-0,017106	-0,013271	-0,008612	-0,004355	-0,002216	-0,000711	-0,00038
-10	-0,015397	-0,015017	-0,013714	-0,009588	-0,005009	-0,00055	0,002745	0,004517	0,003128
-8	-0,011863	-0,011733	-0,010125	-0,006064	-0,001676	0,002316	0,005491	0,006966	0,005931
-6	-0,008425	-0,008774	-0,006698	-0,003032	0,000933	0,004389	0,007397	0,008623	0,007861
-4	-0,00627	-0,006401	-0,004357	-0,001203	0,002291	0,005336	0,00816	0,009031	0,008563
-2	-0,005462	-0,005735	-0,003675	-0,001377	0,001768	0,004708	0,007623	0,008656	0,008285
0	-0,005915	-0,006341	-0,004155	-0,002283	0,000661	0,003701	0,006825	0,007986	0,007531
2	-0,006874	-0,006841	-0,005285	-0,003324	-0,000396	0,002919	0,005568	0,007272	0,006985
4	-0,007379	-0,007554	-0,00626	-0,004073	-0,00093	0,002788	0,005567	0,0073	0,007103
6	-0,007026	-0,007489	-0,006466	-0,003209	0,000369	0,004503	0,007915	0,009217	0,008627
8	-0,005709	-0,006307	-0,004767	-0,001171	0,002797	0,00729	0,010842	0,011593	0,01115
10	-0,003451	-0,003632	-0,0022	0,001612	0,005866	0,010511	0,013589	0,014587	0,014723
12	-0,000028	0,002121	0,002487	0,005253	0,009241	0,013832	0,016346	0,017871	0,018627
14	0,004297	0,005847	0,007859	0,009768	0,01374	0,018141	0,021028	0,022877	0,023424
16	0,009424	0,011902	0,013499	0,015249	0,019313	0,02358	0,027479	0,028374	0,02867
18	0,015296	0,018144	0,019969	0,021605	0,025994	0,030698	0,034323	0,03553	0,036045
20	0,02233	0,025145	0,023593	0,028422	0,03339	0,038674	0,041957	0,04363	0,044943

4. MANOEUVRABILITY PERFORMANCE PREDICTION

4.1.Introduction

In this chapter, the hydrodynamics derivatives obtained from CFD-static tests and empirical relations of Clarke (1998) are applied to simulate the turning circle and Zig-Zag standard manoeuvres and to predict their characteristics, using the computer code PMMPROG performed by "Dunarea de Jos" University of Galati.

On the basis of the nonlinear form of the Abkowitz [6] mathematical model represented by the equations (2.12) and (2.16) and the hydrodynamics forces and moments obtained from CFD techniques (Tables 3.9, 3.10 and 3.11), the results for standard manoeuvres are analyzed.

Tables 4.1, 4.2 and 4.3 contain the hydrodynamics derivatives of the proposed hydrodynamic model and the calculation specific methods (relations of the Clarke or CFD-static tests).

Table 4.1 The used derivatives X

Xu point = $m - X_{\dot{u}}$	Clarke	Xvr= $X_{vr} + m$	0
Xvv= $1/2\, X_{vv}$	CFD-static tests	Xvd= $X_{v\delta}$	CFD-static tests
Xrr= $1/2\, X_{rr} + mx_G$	0	Xrd= $X_{r\delta}$	0
Xdd= $1/2\, X_{\delta\delta}$	CFD-static tests	X0= X_0	0

Table 4.2 The used derivatives Y

Yvdot= $m - Y_{\dot{v}}$	Clarke	Yrdd= $1/2\, Y_{r\delta\delta}$	0
Yrdot= $mx_G - Y_{\dot{r}}$	Clarke	Yd= Y_{δ}	Clarke
Yv= Y_v	Clarke	Yddd= $1/6\, Y_{\delta\delta\delta}$	CFD-static tests
Yvvv= $1/6\, Y_{vvv}$	CFD-static tests	Ydvv= $1/2\, Y_{\delta vv}$	CFD-static tests
Yvrr= $1/2\, Y_{vrr}$	0	Ydrr= $1/2\, Y_{\delta rr}$	0
Yvdd= $1/2\, Y_{v\delta\delta}$	CFD-static tests	Ydu= $Y_{\delta u}$	0
Yr= $Y_r - mU$	Clarke	Yvrd= $Y_{vr\delta}$	0
Yrrr= $1/6\, Y_{rrr}$	0	Y0= Y_0	0

Yrvv= $1/2\,Y_{rvv}$	0	Y0u= Y_{0u}	0

Table 4.3 The used derivatives N

Qvdot= $mx_G - N_{\dot{v}}$	Clarke	Qrdd= $1/2\,N_{r\delta\delta}$	0
Qrdot= $I_{zz} - N_{\dot{r}}$	Clarke	Qd= N_{δ}	Clarke
Qv= N_v	Clarke	Qddd= $1/6\;N_{\delta\delta\delta}$	CFD-static tests
Qvvv= $1/6\;N_{vvv}$	CFD-static tests	Qdvv= $1/2\,N_{\delta vv}$	CFD-static tests
Qvrr= $1/2\,N_{vrr}$	0	Qdrr= $1/2\,N_{\delta rr}$	0
Qvdd= $\frac{1}{2}N_{v\delta\delta}$	CFD-static tests	Qdu= $N_{\delta u}$	0
Qr= $N_r - mx_G U$	Clarke	Qvrd= $N_{vr\delta}$	0
Qrrr= $1/6\;N_{rrr}$	0	Q0= N_0	0
Qrvv= $1/2\,N_{rvv}$	0	Q0u= N_{0u}	0

4.2.Computation of the static derivatives

In order to obtain the static derivatives, it was used the computer code POLYNEW developed at "Dunarea de Jos" University of Galati [17]. This code uses as input data the non-dimensional hydrodynamic forces and moments ([18], [19]) obtained from CFD "static drift and rudder" results, which are presented in Tables 3.9, 3.10 and 3.11, depending of the drift angle (beta) and rudder angle (delta). On the basis of a regression method, the non-dimensional static hydrodynamic derivatives were determined, using POLINEW computer code. Also, the relations of the Clarke, Gedling and Hine were used in order to compute other dynamic derivatives.

The results obtained from the POLYNEW code and Clarke relations are represented below.

Table 4.4 The obtained non-dimensional derivatives X

Xu point = $m - X_{\dot{u}}$	0.019057	Xvr= $X_{vr} + m$	0
Xvv= $1/2\,X_{vv}$	-0.003020	Xvd= $X_{v\delta}$	0.030230

Xrr= $1/2\, X_{rr} + mx_G$	0	Xrd= $X_{r\delta}$	0
Xdd= $1/2\, X_{\delta\delta}$	-0.013161	X0= X_0	0

Table 4.5 The obtained non-dimensional derivatives Y

Yvdot= $m - Y_{\dot{v}}$	0.033463	Yrdd= $1/2\, Y_{r\delta\delta}$	0
Yrdot= $mx_G - Y_{\dot{r}}$	0.001826	Yd= Y_{δ}	0.003834
Yv= Y_v	-0.024232	Yddd= $1/6\, Y_{\delta\delta\delta}$	-0.009992
Yvvv= $1/6\, Y_{vvv}$	-0.222342	Ydvv= $\frac{1}{2} Y_{\delta vv}$	0.060319
Yvrr= $1/2\, Y_{vrr}$	0	Ydrr= $1/2\, Y_{\delta rr}$	0
Yvdd= $1/2\, Y_{v\delta\delta}$	-0.008225	Ydu= $Y_{\delta u}$	0
Yr= $Y_r - mU$	-0.013903	Yvrd= $Y_{vr\delta}$	0
Yrrr= $\frac{1}{6}\, Y_{rrr}$	0	Y0= Y_0	0
Yrvv= $1/2\, Y_{rvv}$	0	Y0u= Y_{0u}	0

Table 4.6 The obtained non-dimensional derivatives N

Qvdot= $mx_G - N_{\dot{v}}$	0.001672	Qrdd= $1/2\, N_{r\delta\delta}$	0
Qrdot= $I_{zz} - N_{\dot{r}}$	0.001933	Qd= N_{δ}	-0.001879
Qv= N_v	-0.008382	Qddd= $1/6\, N_{\delta\delta\delta}$	-0.003359
Qvvv= $1/6\, N_{vvv}$	0.1358568	Qdvv= $1/2\, N_{\delta vv}$	0.021757
Qvrr= $1/2\, N_{vrr}$	0	Qdrr= $1/2\, N_{\delta rr}$	0
Qvdd= $1/2\, N_{v\delta\delta}$	0.00248465	Qdu= $N_{\delta u}$	0
Qr= $N_r - mx_G U$	-0.003946	Qvrd= $N_{vr\delta}$	0

Qrrr= $1/6\ N_{rrr}$	0	Q0= N_0	0
Qrvv= $1/2\ N_{rvv}$	0	Q0u= N_{0u}	0

4.3.Description of the PMMPROG simulation computer code

This program is able to simulate the turning circle trajectory for a given rudder deflection angle ([18], [19]). Parameters such as advance, transfer, tactical diameter, steady turning radius, heading angle, angular velocity, drift angle and final ship speed during the steady state motion are presented on a time basis ([20], [21], [22]). A graphic representation of the results is performed for turning circle trajectory.

Also, the program is able to simulate Zig-Zag manoeuvres of the ship ([18], [19]), in order to obtain first overshoot angle, second overshoot angle and the time characteristics (initial turning time, advance and period).

The turning circle manoeuvre (35 deg.) and the Zig-Zag manoeuvre (20-20 deg.) were used to evaluate the manoeuvering performance of the ship, in correlation with specific IMO criteria.

4.3.1. PMMPROG Input data

The input data have been divided into three groups [21], which are presented in the following steps.

Ship data [21]**:** include particulars, such as ship length, propeller diameter, wake coefficient, thrust deduction coefficient, ship speed and two characteristics of the rudder system (rudder rate and time lag). The input ship data are represented on the following table.

Table 4.7 Ship data

Length between perpendiculars [m].....ALPP=	325,5
Number of propellers.....PROP=	1
Propeller diameter [m].....DIAM=	9,86
Wake coefficient.....WAKE=	0,447
Thrust deduction coefficient.....TDC=	0,227
Ship speed [kn].....SPEED=	15,5
Rudder rate of deflection [deg/sec]....RATE=	1
Time lag in rudder system [sec].....TLAG=	0

Effective horse power (EHP) data and open water propeller characteristics [21]**:** this group contains the open water propeller characteristics (the thrust coefficients KT, torque coefficient KQ) and the powering performance of the ship. The Michigan computer code was used in order to obtain the diagrams of the hydrodynamic characteristics of the propeller in open water condition (see **APPENDIX 4.1 Open water propeller characteristics**) and the specific thrust and torque coefficients were represented on the following table.

Table 4.8 Open water propeller characteristics data

ADVANCE COEF.	THRUST COEF.	TORQUE COEF.
J	KT	KQ
0,1	0,275	0,0285
0,2	0,24	0,0255
0,3	0,205	0,0245
0,372	0,183	0,0237
0,4	0,165	0,0195
0,5	0,125	0,016
0,6	0,08	0,012
0,7	0,035	0,0075

Concerning the powering performance data EHP, the computed results from PHP Holtrop-Mennen were introduced and presented in Table 4.9 (effective horse power-EHP, ship resistance-RES, propeller thrust-THRUST, propeller torque-TORQUE and propeller revolutions-REVS).

Table 4.9 Powering performance data

SPEED [KNOTS]	EHP [KW]	RES [KN]	THRUST [KN]	TORQUE [KN.m]	REVS [rpm]
12	7421,4	1202,2	1554,6	1988,5	56,2
12,5	8350,5	1298,6	1679,3	2149,3	58,4
13	9356,3	1399	1809,2	2314,9	60,6
13,5	10444,4	1503,9	1944,8	2490,4	62,9
14	11621,6	1613,6	2086,7	2672,4	65,1
14,5	12896,1	1728,8	2235,7	2864,5	67,4
15	14278	1850,3	2392,7	3065,6	69,8
15,5	15789,4	1980,2	2560,6	3280,5	72,2

The powering data are given for a range of speed values from 12 Knots to 15.5 Knots, where the final value represents the design speed.

The non-dimensional hydrodynamic derivatives (Tables 3.9, 3.10 and 3.11) can be stated as the last group of the input data.

4.3.2. PMMPROG Results

Coefficients in X-equation and the parameter of stability on route (C)

Three of the coefficients in the X-equation, Xu, 1/2Xuu and 1/6 Xuuu, are calculated in the computer program on the basis of the results from open water propeller and the ship effective horsepower data, and are presented in Table 4.10. The assumption used for the calculation of the coefficients was taken that the torque of propeller has been kept constant for different values of speeds (diesel engine). Also, the parameter of the stability on route (C) was determined. Is observed that this parameter is negative, as consequence the ship will be instable on route.

Remarks:

- The analysis performed in Chapter 2.5.3 on the basis of linear Abkowitz model reveals that the ship will be stable on route;
- Using CFD Technics, only the static derivatives were performed;
- Considering this uncertainty response related to the stability on route problem, in order to increase the level of accuracy, the CFD Technics for dynamic derivatives computation must be introduced in the following researches.

Table 4.10 Additional coefficients from X-equation

XU= X_u	0,0000062828
XUU= $\frac{1}{2} X_{uu}$	0,0000505696
XUUU= $\frac{1}{6} X_{uuu}$	0,0001184611

Stability on route parameter, C	-0.0000209155

Using the PMMPROG simulation code, the **turning circle parameters** with rudder deflection angle from -35 to 35, with step of 5 degree were obtained. The results are shown bellow.

TURNING CIRCLE PARAMETERS
rudder angle [deg]..... 5.0
advance -90 deg- [m]..... 2202.0
transfer -90 deg- [m]..... -1318.3
max advance [m]..... 2212.9
tactical diameter [m]..... 2891.6
time for change 90 deg [sec]... 352.0
time for change 180 deg [sec]... 606.0
max transfer [m]..... -2902.0
steady turning radius [m]..... 1408.3
steady drift angle [deg]..... -7.4
final speed [kn]..... 17.65

TURNING CIRCLE PARAMETERS
rudder angle [deg]..... -5.0
advance -90 deg- [m]..... 2202.0
transfer -90 deg- [m]..... 1318.3
max advance [m]..... 2212.9
tactical diameter [m]..... 2891.6
time for change 90 deg [sec]... 352.0
time for change 180 deg [sec]... 606.0
max transfer [m]..... 2902.0
steady turning radius [m]..... 1408.3
steady drift angle [deg]..... 7.4
final speed [kn]..... 17.65

TURNING CIRCLE PARAMETERS
rudder angle [deg]..... 10.0
advance -90 deg- [m]..... 1741.7
transfer -90 deg- [m]..... -1095.0
max advance [m]..... 1754.6
tactical diameter [m]..... 2508.5
time for change 90 deg [sec]... 283.0
time for change 180 deg [sec]... 502.0
max transfer [m]..... -2520.8
steady turning radius [m]..... 1246.5
steady drift angle [deg]..... -8.6
final speed [kn]..... 18.52

TURNING CIRCLE PARAMETERS
rudder angle [deg]..... -10.0
advance -90 deg- [m]..... 1741.7
transfer -90 deg- [m]..... 1095.0
max advance [m]..... 1754.6
tactical diameter [m]..... 2508.5
time for change 90 deg [sec]... 283.0
time for change 180 deg [sec]... 502.0
max transfer [m]..... 2520.8
steady turning radius [m]..... 1246.5
steady drift angle [deg]..... 8.6
final speed [kn]..... 18.52

TURNING CIRCLE PARAMETERS
rudder angle [deg]..... 15.0
advance -90 deg- [m]..... 1522.9
transfer -90 deg- [m]..... -978.7
max advance [m]..... 1537.0
tactical diameter [m]..... 2296.7
time for change 90 deg [sec]... 254.0
time for change 180 deg [sec]... 462.0
max transfer [m]..... -2311.7
steady turning radius [m]..... 1152.6
steady drift angle [deg]..... -9.5
final speed [kn]..... 17.88

TURNING CIRCLE PARAMETERS
rudder angle [deg]..... -15.0
advance -90 deg- [m]..... 1522.9
transfer -90 deg- [m]..... 978.7
max advance [m]..... 1537.0
tactical diameter [m]..... 2296.7
time for change 90 deg [sec]... 254.0
time for change 180 deg [sec]... 462.0
max transfer [m]..... 2311.7
steady turning radius [m]..... 1152.6
steady drift angle [deg]..... 9.5
final speed [kn]..... 17.88

TURNING CIRCLE PARAMETERS
rudder angle [deg]..... 20.0
advance -90 deg- [m]..... 1372.8
transfer -90 deg- [m]..... -886.0
max advance [m]..... 1388.4
tactical diameter [m]..... 2126.8
time for change 90 deg [sec]... 237.0
time for change 180 deg [sec]... 448.0
max transfer [m]..... -2142.6
steady turning radius [m]..... 1073.9
steady drift angle [deg]..... -10.2
final speed [kn]..... 16.03

TURNING CIRCLE PARAMETERS
rudder angle [deg]..... 25.0
advance -90 deg- [m]..... 1246.4
transfer -90 deg- [m]..... -797.2
max advance [m]..... 1263.0
tactical diameter [m]..... 1954.3
time for change 90 deg [sec]... 224.0
time for change 180 deg [sec]... 445.0
max transfer [m]..... -1970.5
steady turning radius [m]..... 992.0
steady drift angle [deg]..... -10.8
final speed [kn]..... 13.53

TURNING CIRCLE PARAMETERS
rudder angle [deg]..... 30.0
advance -90 deg- [m]..... 1129.9
transfer -90 deg- [m]..... -710.2
max advance [m]..... 1146.0
tactical diameter [m]..... 1764.5
time for change 90 deg [sec]... 212.0
time for change 180 deg [sec]... 444.0
max transfer [m]..... -1781.1
steady turning radius [m]..... 900.6
steady drift angle [deg]..... -11.4
final speed [kn]..... 10.99

TURNING CIRCLE PARAMETERS
rudder angle [deg]..... -20.0
advance -90 deg- [m]..... 1372.8
transfer -90 deg- [m]..... 886.0
max advance [m]..... 1388.4
tactical diameter [m]..... 2126.8
time for change 90 deg [sec]... 237.0
time for change 180 deg [sec]... 448.0
max transfer [m]..... 2142.6
steady turning radius [m]..... 1073.9
steady drift angle [deg]..... 10.2
final speed [kn]..... 16.03

TURNING CIRCLE PARAMETERS
rudder angle [deg]..... -25.0
advance -90 deg- [m]..... 1246.4
transfer -90 deg- [m]..... 797.2
max advance [m]..... 1263.0
tactical diameter [m]..... 1954.3
time for change 90 deg [sec]... 224.0
time for change 180 deg [sec]... 445.0
max transfer [m]..... 1970.5
steady turning radius [m]..... 992.0
steady drift angle [deg]..... 10.8
final speed [kn]..... 13.53

TURNING CIRCLE PARAMETERS
rudder angle [deg]..... -30.0
advance -90 deg- [m]..... 1129.9
transfer -90 deg- [m]..... 710.2
max advance [m]..... 1146.0
tactical diameter [m]..... 1764.5
time for change 90 deg [sec]... 212.0
time for change 180 deg [sec]... 444.0
max transfer [m]..... 1781.1
steady turning radius [m]..... 900.6
steady drift angle [deg]..... 11.4
final speed [kn]..... 10.99

TURNING CIRCLE PARAMETERS
rudder angle [deg]..... 35.0
advance -90 deg- [m]..... 1019.5
transfer -90 deg- [m]..... -616.1
max advance [m]..... 1035.2
tactical diameter [m]..... 1558.8
time for change 90 deg [sec]... 198.0
time for change 180 deg [sec]... 438.0
max transfer [m]..... -1575.7
steady turning radius [m]..... 800.9
steady drift angle [deg]..... -11.9
final speed [kn]..... 8.80

TURNING CIRCLE PARAMETERS
rudder angle [deg]..... -35.0
advance -90 deg- [m]..... 1019.5
transfer -90 deg- [m]..... 616.1
max advance [m]..... 1035.2
tactical diameter [m]..... 1558.8
time for change 90 deg [sec]... 198.0
time for change 180 deg [sec]... 438.0
max transfer [m]..... 1575.7
steady turning radius [m]..... 800.9
steady drift angle [deg]..... 11.9
final speed [kn]..... 8.80

Discussion:

- The turning circle characteristics (at 35 degree) are used in order to evaluate and check the manoeuvring performances, with regard of IMO standard manoeuvres criteria.
- The steady turning diameter is about 4.9 L_{WL} (where L_{WL} is the length of waterline). Also, the advance is about 3.1 L_{WL} and the tactical diameter is 4.8 L_{WL}. The tactical diameter is smaller than 5 L_{WL} and the advance is smaller than 4.5 L_{WL}, as a consequence the turning circle IMO criteria are fulfilled. The speed losses are about 57 % from the initial speed.

In the following table are presented the most important characteristics of the ship trajectory during the turning circle manoeuvre, with 35 degrees, in time domain: advance, transfer, speed, heading angle, drift angle and turning rate (OMEG).

Table 4.11 Turning circle at 35 degree. Estimation trajectory in deep water

TIME [sec]	RUDDER ANGLE [deg]	ADVANCE [m]	TRANSFER [m]	SPEED [Knots]	HEADING [Deg]	OMEG [Deg/Sec]	DRIFT ANGLE [Deg]
0	0	0	0	15,5	0	0	0
10	10	79,7	0,1	15,47	-0,1	-0,035	-0,3
20	20	158,9	0,2	15,29	-1	-0,131	-1
30	30	236,5	-0,2	14,87	-3,1	-0,287	-2,3
40	35	311,2	-2,7	14,25	-7	-0,48	-4
50	35	382,7	-8,8	13,74	-12,6	-0,61	-5,9
60	35	451,4	-19,9	13,38	-19,2	-0,681	-7,9
70	35	517,4	-36,5	13,13	-26,1	-0,701	-9,6
80	35	580,5	-59	12,94	-33	-0,682	-10,8
90	35	640,2	-87,3	12,8	-39,6	-0,637	-11,7

100	35	696,3	-121	12,67	-45,7	-0,583	-12,1
110	35	748,3	-159,6	12,54	-51,2	-0,533	-12,3
120	35	796,2	-202,3	12,41	-56,3	-0,493	-12,3
130	35	839,7	-248,4	12,28	-61,1	-0,465	-12,3
140	35	878,9	-297,5	12,15	-65,7	-0,447	-12,2
150	35	913,7	-348,9	12,02	-70,1	-0,435	-12,1
160	35	944,1	-402,3	11,89	-74,4	-0,429	-12
170	35	970,1	-457,2	11,76	-78,6	-0,424	-12
180	35	991,7	-513,3	11,63	-82,9	-0,421	-11,9
190	35	1008,9	-570,3	11,5	-87,1	-0,419	-11,9
200	35	1021,7	-627,6	11,38	-91,2	-0,416	-11,9
210	35	1030,2	-685,2	11,26	-95,4	-0,413	-11,9
220	35	1034,6	-742,6	11,14	-99,5	-0,41	-11,9
230	35	1034,8	-799,6	11,03	-103,6	-0,406	-11,9
240	35	1031,1	-855,9	10,92	-107,6	-0,402	-11,9
250	35	1023,5	-911,2	10,81	-111,6	-0,398	-11,9
260	35	1012,2	-965,3	10,7	-115,6	-0,394	-11,9
270	35	997,3	-1018	10,59	-119,5	-0,39	-11,9
280	35	979,1	-1069	10,49	-123,4	-0,387	-11,9
290	35	957,7	-1118,2	10,39	-127,2	-0,383	-11,9
300	35	933,3	-1165,5	10,29	-131	-0,379	-11,9
310	35	906,2	-1210,5	10,19	-134,8	-0,375	-11,9
320	35	876,4	-1253,3	10,09	-138,5	-0,372	-11,9
330	35	844,2	-1293,7	10	-142,2	-0,368	-11,9
340	35	809,8	-1331,6	9,91	-145,9	-0,365	-11,9
350	35	773,4	-1366,9	9,81	-149,5	-0,361	-11,9
360	35	735,2	-1399,5	9,73	-153,1	-0,358	-11,9
370	35	695,4	-1429,4	9,64	-156,7	-0,355	-11,9
380	35	654,3	-1456,6	9,55	-160,2	-0,352	-11,9
390	35	611,9	-1481	9,47	-163,7	-0,348	-11,9
400	35	568,5	-1502,5	9,38	-167,2	-0,345	-11,9
410	35	524,3	-1521,2	9,3	-170,6	-0,342	-11,9
420	35	479,4	-1537,2	9,22	-174	-0,339	-11,9
430	35	434,1	-1550,3	9,14	-177,4	-0,336	-11,9
440	35	388,4	-1560,6	9,06	-180,7	-0,334	-11,9
450	35	342,7	-1568,3	8,98	-184,1	-0,331	-11,9
460	35	297	-1573,2	8,91	-187,4	-0,328	-11,9
470	35	251,4	-1575,5	8,83	-190,6	-0,325	-11,9
480	35	183,2	-1567	8,83	-193,9	-0,325	-11,9

490	35	142,4	-1560	8,83	-197,1	-0,325	-11,9
500	35	102,1	-1550,8	8,83	-200,4	-0,325	-11,9
510	35	62,2	-1539,6	8,83	-203,7	-0,325	-11,9
520	35	23	-1526,3	8,83	-207	-0,325	-11,9
530	35	-15,4	-1511	8,83	-210,2	-0,325	-11,9
540	35	-53	-1493,7	8,83	-213,5	-0,325	-11,9
550	35	-89,7	-1474,6	8,83	-216,8	-0,325	-11,9
560	35	-125,4	-1453,5	8,83	-220	-0,325	-11,9
570	35	-159,9	-1430,7	8,83	-223,3	-0,325	-11,9
580	35	-193,2	-1406,1	8,83	-226,6	-0,325	-11,9
590	35	-225,1	-1379,8	8,83	-229,8	-0,325	-11,9
600	35	-255,7	-1351,9	8,83	-233,1	-0,325	-11,9
610	35	-284,8	-1322,4	8,83	-236.4	-0,325	-11,9
620	35	-312,3	-1291,5	8,83	-239,7	-0,325	-11,9
630	35	-338,2	-1259,2	8,83	-242,9	-0,325	-11,9
640	35	-362,4	-1225,6	8,83	-246,2	-0,325	-11,9
650	35	-384,8	-1190,8	8,83	-249,5	-0,325	-11,9
660	35	-405,4	-1154,9	8,83	-252,7	-0,325	-11,9
670	35	-424,1	-1118	8,83	-256	-0,325	-11,9
680	35	-440,8	-1080,2	8,83	-259,3	-0,325	-11,9
690	35	-455,6	-1041,5	8,83	-262,5	-0,325	-11,9
700	35	-468,4	-1002,1	8,83	-265,8	-0,325	-11,9
710	35	-479,2	-962,2	8,83	-269,1	-0,325	-11,9
720	35	-487,8	-921,7	8,83	-272,4	-0,325	-11,9
730	35	-494,4	-880,8	8,83	-275,6	-0,325	-11,9
740	35	-498,8	-839,7	8,83	-278,9	-0,325	-11,9
750	35	-501,1	-798,4	8,83	-282,2	-0,325	-11,9
760	35	-501,2	-798,4	8,83	-285,4	-0,325	-11,9
770	35	-501,2	-757	8,83	-288,7	-0,325	-11,9
780	35	-499,3	-715,6	8,83	-292	-0,325	-11,9
790	35	-495,1	-674,4	8,83	-295,2	-0,325	-11,9
800	35	-488,9	-633,5	8,83	-298,5	-0,325	-11,9
810	35	-480,6	-593	8,83	-301,8	-0,325	-11,9
820	35	-470,1	-552,9	8,83	-305,1	-0,325	-11,9
830	35	-457,7	-513,5	8,83	-308,3	-0,325	-11,9
840	35	-443,2	-474,7	8,83	-311,6	-0,325	-11,9
850	35	-426,7	-436,7	8,83	-314,9	-0,325	-11,9
860	35	-408,3	-399,7	8,83	-318,1	-0,325	-11,9
870	35	-387,9	-363,6	8,83	-321,4	-0,325	-11,9

880	35	-365,8	-328,7	8,83	-324,7	-0,325	-11,9
890	35	-341,9	-294,9	8,83	-327,9	-0,325	-11,9
900	35	-316,2	-262,4	8,83	-331,2	-0,325	-11,9
910	35	-288,9	-231,3	8,83	-334,5	-0,325	-11,9
920	35	-260,1	-201,6	8,83	-337,8	-0,325	-11,9
930	35	-229,7	-173,5	8,83	-341	-0,325	-11,9
940	35	-198	-146,9	8,83	-344,3	-0,325	-11,9
950	35	-164,9	-122,1	8,83	-347,6	-0,325	-11,9
960	35	-130,6	-98,9	8,83	-350.5	-0,325	-11,9
970	35	-95,1	-77,6	8,83	-354,1	-0,325	-11,9
980	35	-58,5	-58,2	8,83	-357,4	-0,325	-11,9
990	35	-21	-40,6	8,83	-360,6	-0,325	-11,9

The turning circle trajectory is shown on the following Figure 4-1.

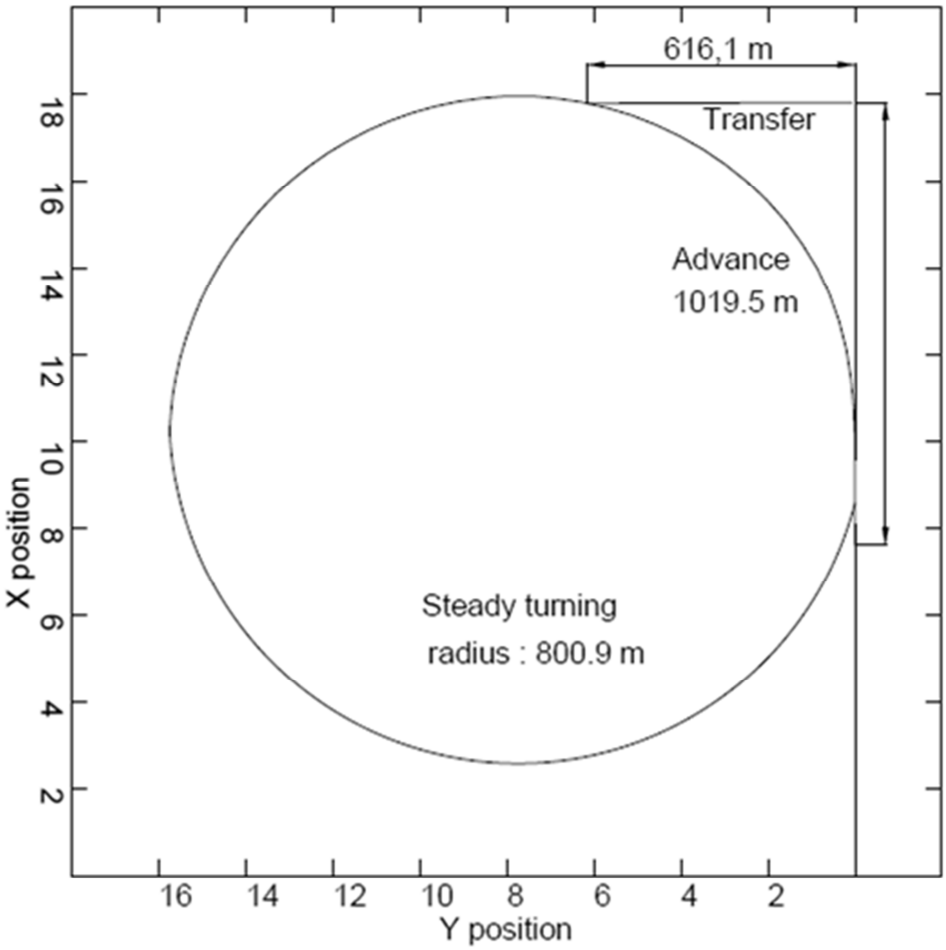

Figure 4-1 Simulation of turning circle with δ = 35 deg.

.

Zig-Zag manoeuvre

The characteristics of the Zig-Zag 20°/20 ° manoeuvres are determined and shown in Table 4.12.

Table 4.12 Zig-Zag manoeuvres characteristics

First overshoot angle (Zig-Zag 20°/20°)	18,2
Second overshoot angle (Zig-Zag 20°/20°)	13,2
Initial turning time, ta	70’
Advance (reach) Ts	295’
Period α_s	620’

The time evolution of the drift angle (psi) and rudder deflection angle (delta) during Zig-Zag 20/20 manoeuvre are show in Figure 4-2.

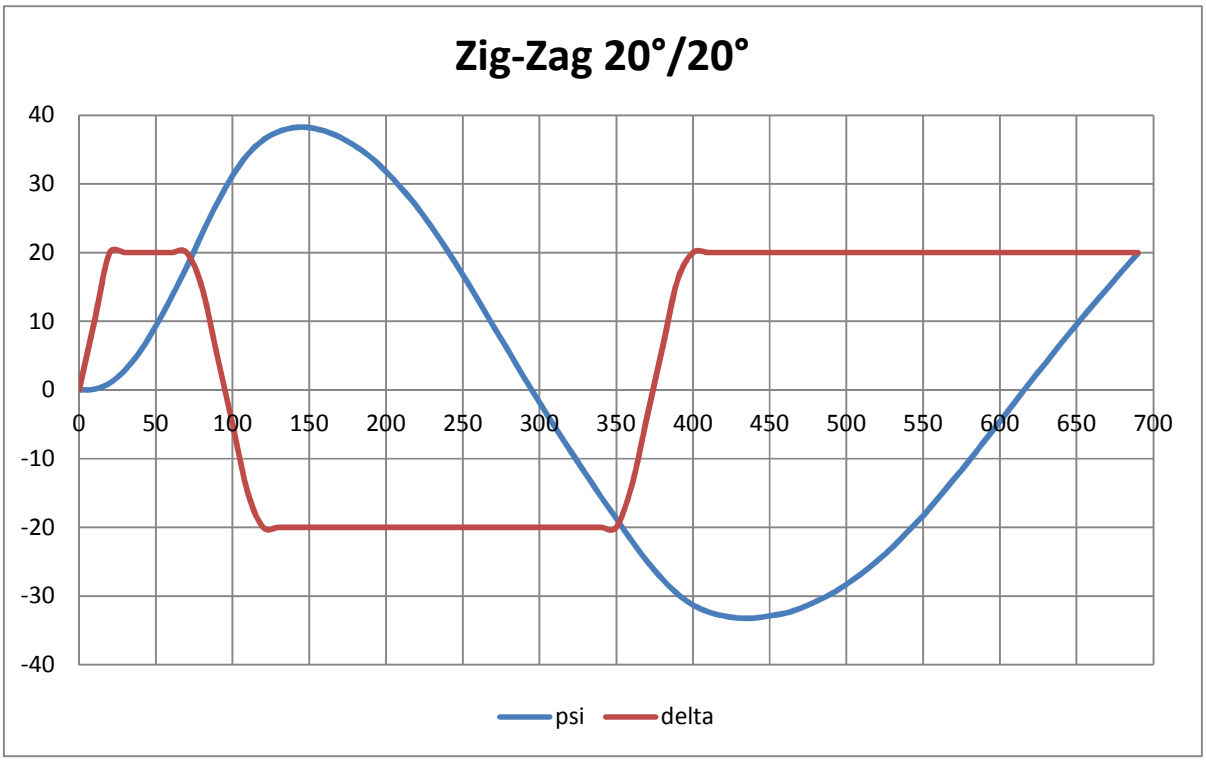

Figure 4-2 Results of the Zig-Zag manoeuvres

Discussion:

- The figure 4.2 shows unsatisfied results regarding the overshoot angles. It’s observed that the first overshoot angle is greater that the second over shoot angle. This may be caused by the absence of some important dynamic derivatives, which was not taken into account.

Standards of ship manoeuvrability: IMO Resolution A.751 (18)

In order to check the ship manoeuvring performances, the IMO standard manoeuvres criteria presented in Table 4.13 were applied.

Table 4.13 Standards of ship manoeuvrability - IMO Resolution A.751

Standard manoeuvre	Characteristics	Maximum values	Obtained values	Criteria
Turning circle	Advance (AD)	≤ 4,5 L	3,1	Passed
	Tactical diameter (TD)	≤ 5 L	4,8	Passed
Zig-Zag manoeuvre	First overshoot angle (Zig-Zag 20°/20°)	≤25’	18,2’	Passed

It is seen that all the criteria are fulfilled.

4.4. Conclusions

- The CFD is a very important tool which can be introduced into initial design stage or basic design, in order to predict the ship manoeuvring characteristics, on the basis of the static and dynamic derivatives.
- The CFD technique can be use to obtain the optimal ship manoeuvring performances, in correlation with the IMO standard manoeuvres criteria.
- The static derivatives are not sufficient to determine a good accuracy of the manoeuvring predictions, as a consequence is necessary to obtain and to use other important dynamic derivatives by means of the CFD Techniques.
- A special attention must be considered during the process of hydrodynamic derivatives estimation, using the CFD tools, due to the long time of computations and accuracy of the results.
- The simulation computer codes based on the CFD-hydrodynamic derivatives can be used in order to obtain detailed information regarding the prediction of the standard manoeuvres.

1. APPENDIX 1.1 BONJEAN CURVES NUMERICAL RESULTS

Water line [m]	X=0 [m]	X=16 [m]	X=32 [m]	X=48 [m]	X=64 [m]	X=80 [m]	X=96 [m]	X=112 [m]	X=128 [m]	X=144 [m]	X=160 [m]
0,4	0	0	2,5	5,1	7,9	11,3	15,6	19,8	22,5	22,6	22,6
0,8	0	0	4	11,2	17	23,9	32,6	40,2	44,9	45,1	45,1
1,2	0	0	4	18	26,9	37,6	50,5	61,3	67,7	68	68
1,6	0	0	7,3	25,2	37,5	52,1	69,1	82,7	90,7	91	91
2	0	0	11,9	32,9	48,7	67,3	88,3	104,5	113,8	114,1	114,1
2,4	0	0	16,7	41	60,4	83,2	108	126,5	137	137,3	137,3
2,8	0	0	21,7	49,3	72,6	99,7	128,1	148,8	160,2	160,5	160,5
3,2	0	0	26,9	58	85,2	116,8	148,6	171,3	183,3	183,7	183,7
3,6	0	0,2	32,2	66,9	98,3	134,3	169,5	193,9	206,5	206,9	206,9
4	0	2,5	37,6	76	111,9	152,3	190,6	216,7	229,7	230,1	230,2
4,4	0	4,7	43,1	85,4	125,9	170,7	211,9	239,5	252,9	253,3	253,3
4,8	0	6,9	48,7	95	140,3	189,6	233,5	262,5	276,1	276,5	276,5
5,2	0	9,1	54,3	104,8	155,2	208,8	255,3	285,5	299,3	299,7	299,7
5,6	0	10,2	60,1	114,9	170,5	228,3	277,2	308,6	322,5	322,9	322,9
6	0	10,2	65,9	125,3	186,3	248,1	299,3	331,7	345,6	346,1	346,1
6,4	0	10,2	71,8	135,9	202,4	268,2	321,6	354,9	368,8	369,2	369,3
6,8	0	10,2	75,6	146,8	219	288,6	344	378,1	392	392,4	392,5
7,2	0	10,2	76,1	158,1	235,9	309,3	366,5	401,3	415,1	415,6	415,7
7,6	0	10,2	82,3	169,7	253,2	330,1	389	424,5	438,3	438,8	438,9
8	0	10,2	88,5	181,7	270,9	351,2	411,7	447,7	461,5	461,9	462
8,4	0	10,2	94,9	194,2	288,8	372,5	434,5	470,9	484,6	485,1	485,2
8,8	0	10,2	101,5	207	307,1	393,9	457,3	494,1	507,8	508,3	508,4
9,2	0	10,2	113,5	220,3	325,7	415,6	480,2	517,3	530,9	531,4	531,6
9,6	0	10,2	127,4	234	344,6	437,3	503,1	540,5	554,1	554,6	554,8

Water line [m]	X=0 [m]	X=16 [m]	X=32 [m]	X=48 [m]	X=64 [m]	X=80 [m]	X=96 [m]	X=112 [m]	X=128 [m]	X=144 [m]	X=160 [m]
10	0	10,2	136,6	248,1	363,8	459,2	526,1	563,7	577,2	577,7	577,9
10,4	0	10,2	144,1	262,7	383,2	481,3	549,2	586,8	600,4	600,9	601,1
10,8	0	10,2	152	277,7	402,9	503,4	572,2	610	623,5	624,1	624,3
11,2	0	10,2	167,6	293,1	422,8	525,7	595,4	633,2	646,7	647,2	647,5
11,6	0	10,2	185	308,9	442,9	548	618,5	656,4	669,8	670,4	670,6
12	0	10,2	203,5	325,1	463,3	570,5	641,6	679,5	692,9	693,5	693,8
12,4	0	10,2	223	341,7	483,8	593	664,8	702,7	716,1	716,7	717
12,8	0	10,2	243,7	358,7	504,5	615,6	688	725,9	739,2	739,8	740,1
13,2	0	10,2	265,5	376	525,4	638,2	711,2	749	762,3	763	763,3
13,6	0	10,2	285,9	393,6	546,5	660,9	734,4	772,2	785,5	786,1	786,5
14	0	10,2	298	411,5	567,7	683,7	757,6	795,3	808,6	809,3	809,6
14,4	0	10,2	310,5	429,8	589,1	706,5	780,8	818,5	831,8	832,4	832,8
14,8	0	10,2	323,6	448,2	610,6	729,4	804	841,6	854,9	855,6	856
15,2	0	10,2	337,2	466,9	632,2	752,3	827,2	864,8	878	878,7	879,2
15,6	0	10,2	351,3	485,9	653,9	775,3	850,4	888	901,2	901,9	902,3
16	0	10,2	365,8	505,1	675,8	798,2	873,6	911,1	924,3	925	925,5
16,4	0	10,2	380,6	524,5	697,8	821,2	896,8	934,3	947,4	948,2	948,7
16,8	0	11	395,9	544,1	719,8	844,3	920	957,4	970,6	971,3	971,8
17,2	0	15,8	411,5	563,8	742	867,4	943,2	980,6	993,7	994,5	995
17,6	0,5	20,8	427,4	583,8	764,2	890,4	966,4	1003,7	1016,8	1017,6	1018,2
18	2,2	26,1	443,6	603,9	786,5	913,5	989,6	1026,9	1040	1040,8	1041,3
18,4	5,1	31,7	460,1	624,2	808,9	936,7	1012,7	1050	1063,1	1063,9	1064,5
18,8	8,9	37,4	476,9	644,6	831,4	959,8	1035,9	1073,2	1086,2	1087,1	1087,7
19,2	13,6	43,4	493,9	665,1	853,9	983	1059,1	1096,3	1109,4	1110,2	1110,8
19,6	19,1	49,5	511	685,7	876,5	1006,1	1082,3	1119,5	1132,5	1133,4	1134
20	25,2	55,8	528,4	706,5	899,2	1029,3	1105,4	1142,6	1155,7	1156,5	1157,2

Water line [m]	X=0 [m]	X=16 [m]	X=32 [m]	X=48 [m]	X=64 [m]	X=80 [m]	X=96 [m]	X=112 [m]	X=128 [m]	X=144 [m]	X=160 [m]
20,4	31,8	62,3	546	727,4	921,8	1052,5	1128,6	1165,8	1178,8	1179,7	1180,4
20,8	38,9	68,9	563,7	748,3	944,6	1075,7	1151,8	1188,9	1202	1202,8	1203,5
21,2	46,4	75,6	581,5	769,3	967,3	1098,9	1175	1212,1	1225,1	1226	1226,7
21,6	54,2	82,4	599,5	790,4	990,1	1122,1	1198,2	1235,2	1248,3	1249,2	1249,9
22	62,3	89,2	617,5	811,6	1012,9	1145,3	1221,3	1258,4	1271,4	1272,3	1273,1
22,4	70,6	96,2	635,7	832,8	1035,8	1170,2	1244,5	1281,6	1294,6	1295,5	1296,3
22,8	79,1	103,2	653,9	854	1058,6	1193,4	1267,7	1304,7	1317,7	1318,7	1319,4
23,2	87,8	110,3	672,2	875,3	1081,5	1216,6	1290,9	1327,9	1340,9	1341,8	1342,6
23,6	96,6	117,4	690,5	896,6	1104,4	1239,9	1314,1	1351,1	1364,1	1365	1365,8
24	105,6	119,2	708,9	918	1127,3	1263,1	1337,2	1374,2	1387,2	1388,2	1389
24,4	114,6	119,2	727,3	939,3	1150,1	1286,3	1360,4	1397,4	1410,4	1411,4	1412,2
24,8	123,7	119,2	745,7	960,7	1173	1309,5	1383,6	1420,6	1433,6	1434,5	1435,4
25,2	132,9	119,2	764,1	982,1	1195,9	1332,7	1406,8	1443,8	1456,8	1457,7	1458,6
25,6	142,1	119,2	793,7	1003,5	1218,8	1355,9	1430	1467	1479,9	1480,9	1481,7
26	151,4	119,2	825,1	1024,8	1241,7	1379,1	1453,2	1490,1	1503,1	1504,1	1504,9

Water line [m]	X=176 [m]	X=192 [m]	X=208 [m]	X=224 [m]	X=240 [m]	X=256 [m]	X=272 [m]	X=288 [m]	X=304 [m]	X=320 [m]
0,4	22,6	22,6	22,6	22,6	21,6	18,6	14,7	9,9	3,8	0
0,8	45,1	45,1	45,1	45,1	43,4	37,8	30,7	21,5	9,4	0
1,2	68	68	68	68	65,6	57,8	47,6	34,2	16	0
1,6	91	91	91	91	88,1	78,3	65,3	47,7	23,4	0,6
2	114,1	114,1	114,1	114,1	110,8	99,2	83,5	62	31,6	1,6
2,4	137,3	137,3	137,3	137,3	133,6	120,4	102,3	76,8	40,4	3,1
2,8	160,5	160,5	160,5	160,5	156,6	142	121,4	105,1	49,7	5
3,2	183,7	183,8	183,8	183,8	179,6	163,7	141	131,4	59,5	7,3
3,6	207	207	207	207	202,8	185,7	160,8	147,6	69,8	9,9
4	230,2	230,2	230,2	230,2	225,9	207,9	180,9	164,2	80,5	12,8
4,4	253,4	253,4	253,4	253,4	249,1	230,2	201,3	181,1	91,5	16
4,8	276,6	276,6	276,6	276,6	272,3	252,6	221,8	198,3	102,9	19,5
5,2	299,8	299,8	299,8	299,8	295,5	275,1	242,6	215,8	114,6	23,3
5,6	323	323	323	323,1	318,7	297,7	263,5	233,5	126,5	27,3
6	346,2	346,2	346,2	346,3	342	320,4	284,6	251,5	138,8	31,5
6,4	369,4	369,4	369,5	369,5	365,2	343,2	305,8	269,6	151,3	35,9
6,8	392,6	392,6	392,7	392,8	388,4	366	327,1	288	164	40,6
7,2	415,8	415,8	415,9	416	411,6	388,9	348,4	306,5	176,9	45,3
7,6	439	439	439,1	439,2	434,8	411,8	369,9	325,2	190	50,3
8	462,1	462,2	462,3	462,4	458,1	434,7	391,5	360,3	203,3	55,3
8,4	485,3	485,5	485,6	485,7	481,3	457,7	413,1	387,5	216,7	60,5
8,8	508,5	508,7	508,8	508,9	504,5	480,6	434,9	406,6	230,2	65,8
9,2	531,7	531,9	532	532,2	527,7	503,6	456,6	425,7	243,9	71,2
9,6	554,9	555,1	555,2	555,4	551	526,6	478,5	445	257,6	76,7
10	578,1	578,3	578,4	578,6	574,2	549,6	500,3	464,3	271,5	82,2
10,4	601,3	601,5	601,7	601,9	597,5	572,6	522,3	483,7	285,4	87,8

Water line [m]	X=176 [m]	X=192 [m]	X=208 [m]	X=224 [m]	X=240 [m]	X=256 [m]	X=272 [m]	X=288 [m]	X=304 [m]	X=320 [m]
10,8	624,5	624,7	624,9	625,1	620,7	595,7	544,2	503,1	299,5	93,4
11,2	647,7	647,9	648,1	648,4	643,9	618,7	566,3	522,7	313,5	99
11,6	670,9	671,1	671,3	671,6	667,2	641,7	588,3	542,2	327,7	104,6
12	694,1	694,3	694,6	694,9	690,4	664,8	610,4	561,9	341,8	110,1
12,4	717,3	717,5	717,8	718,1	713,6	687,8	632,5	581,5	356,1	115,7
12,8	740,4	740,7	741	741,4	736,9	710,9	654,7	601,2	370,3	121,1
13,2	763,6	763,9	764,3	764,6	760,1	733,9	676,9	621	384,6	126,5
13,6	786,8	787,1	787,5	787,9	783,4	757	699,1	640,8	398,9	131,8
14	810	810,4	810,7	811,1	806,6	780	721,3	660,6	413,2	136,9
14,4	833,2	833,6	833,9	834,4	829,9	803,1	743,6	680,5	427,5	141,9
14,8	856,4	856,8	857,2	857,6	853,1	826,1	765,9	700,3	441,8	146,6
15,2	879,6	880	880,4	880,9	876,4	849,2	788,2	720,2	456,1	151,1
15,6	902,8	903,2	903,6	904,1	899,6	872,2	810,5	740,2	470,4	155,3
16	925,9	926,4	926,8	927,4	922,8	895,3	832,9	760,1	484,7	159,1
16,4	949,1	949,6	950,1	950,6	946,1	918,3	855,3	780,1	499	162,6
16,8	972,3	972,8	973,3	973,9	969,3	941,4	877,6	800,1	513,2	165,5
17,2	995,5	996	996,5	997,1	992,6	964,4	900,1	820,1	527,5	167,9
17,6	1018,7	1019,2	1019,8	1020,4	1015,8	987,5	922,5	840,1	541,8	169,7
18	1041,9	1042,4	1043	1043,6	1039,1	1010,5	945	860,2	556,1	171,1
18,4	1065,1	1065,6	1066,2	1066,9	1062,3	1033,6	967,4	880,3	570,4	172,1
18,8	1088,3	1088,8	1089,4	1090,1	1085,5	1056,6	989,9	900,4	584,7	172,7
19,2	1111,5	1112	1112,7	1113,4	1108,8	1079,7	1012,4	920,6	599	173,1
19,6	1134,6	1135,3	1135,9	1136,6	1132	1102,7	1035	940,7	613,3	173,4
20	1157,8	1158,5	1159,1	1159,9	1155,3	1125,8	1057,5	960,9	627,7	173,5
20,4	1181	1181,7	1182,3	1183,1	1178,5	1148,8	1080,1	981,2	642,2	173,6
20,8	1204,2	1204,9	1205,6	1206,4	1201,7	1171,9	1102,7	1001,5	656,7	173,7

Water line [m]	X=176 [m]	X=192 [m]	X=208 [m]	X=224 [m]	X=240 [m]	X=256 [m]	X=272 [m]	X=288 [m]	X=304 [m]	X=320 [m]
21,2	1227,4	1228,1	1228,8	1229,6	1225	1194,9	1125,2	1021,8	671,2	173,7
21,6	1250,6	1251,3	1252	1252,8	1248,2	1218	1147,8	1042,2	685,8	173,7
22	1273,8	1274,5	1275,2	1276,1	1271,4	1241	1170,5	1062,6	700,5	173,9
22,4	1297	1297,7	1298,4	1299,3	1294,7	1264,1	1193,1	1083	715,3	174,4
22,8	1320,2	1320,9	1321,7	1322,6	1317,9	1287,1	1215,7	1103,5	730,1	175,2
23,2	1343,4	1344,1	1344,9	1345,8	1341,1	1310,2	1238,4	1124,1	745,1	176,2
23,6	1366,6	1367,3	1368,1	1369	1364,4	1333,2	1261	1144,8	760,1	177,4
24	1389,8	1390,5	1391,3	1392,3	1387,6	1356,3	1283,7	1165,4	775,3	179
24,4	1413	1413,7	1414,5	1415,5	1410,8	1379,3	1306,4	1186,2	790,5	180,8
24,8	1436,2	1437	1437,8	1438,7	1434	1402,4	1329,1	1207	805,9	183
25,2	1459,4	1460,2	1461	1461,9	1457,2	1425,5	1351,8	1227,9	821,4	185,4
25,6	1482,6	1483,4	1484,2	1485,2	1480,5	1448,5	1374,5	1248,8	837	188,2
26	1505,8	1506,6	1507,4	1508,4	1503,7	1471,6	1397,3	1269,9	852,7	191,4

2. APPENDIX 1.2 BONJEAN CURVES DRAWING

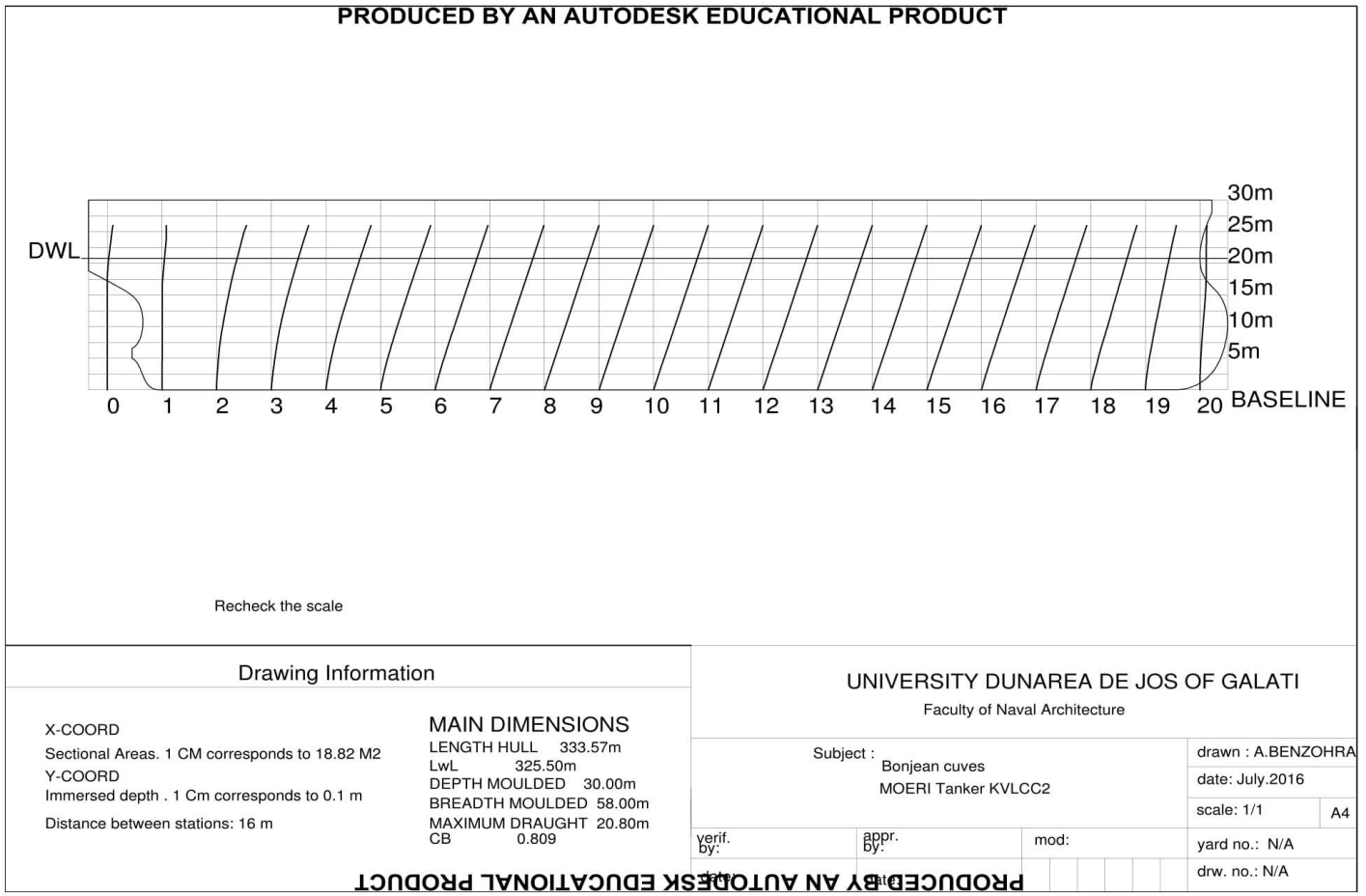

PRODUCED BY AN AUTODESK EDUCATIONAL PRODUCT

3. APPENDIX 2.1 SHIP SELECTION (REGRESSION METHOD)

Name	**ANDROMEDA**	
IMO number	9352561	
LOA	333	m
Breadth	60	m
D	N/A	m
T	22,52	m
Speed	15,5	knots
DWT	321300	t
Break power	29831,73	kW

Name	**APOLYTARES**	
IMO number	9419474	
LOA	336,17	m
Breadth	60	m
D	N/A	m
T	22	m
Speed	15,5	knots
DWT	316679	t
Break power	29340,31	kW

Name	**VLCC Tanker**	
IMO number	N/A	
LOA	330	m
Breadth	60,04	m
D	29,7	m
T	21,5	m
Speed	15,8	knots
DWT	296865	t
Break power	34643	kW

Name	**ZOURVA**	
IMO number	9679593	
LOA	333	m
Breadth	60	m
D	N/A	m
T	22,64	m
Speed	14,5	knots
DWT	318447	t
Break power	21924	kW

4. APPENDIX 2.2 RUDDER DRAWING

- Rudder Drawing -
- KVLCC 2 -
- Drawing Scale 1/200 -
Updated 02/08/2016 by A.BENZOHRA

- Rudder -
Total Area = 136.7 m²
Moving area = 111.45 m²
Moving area = 81.5%

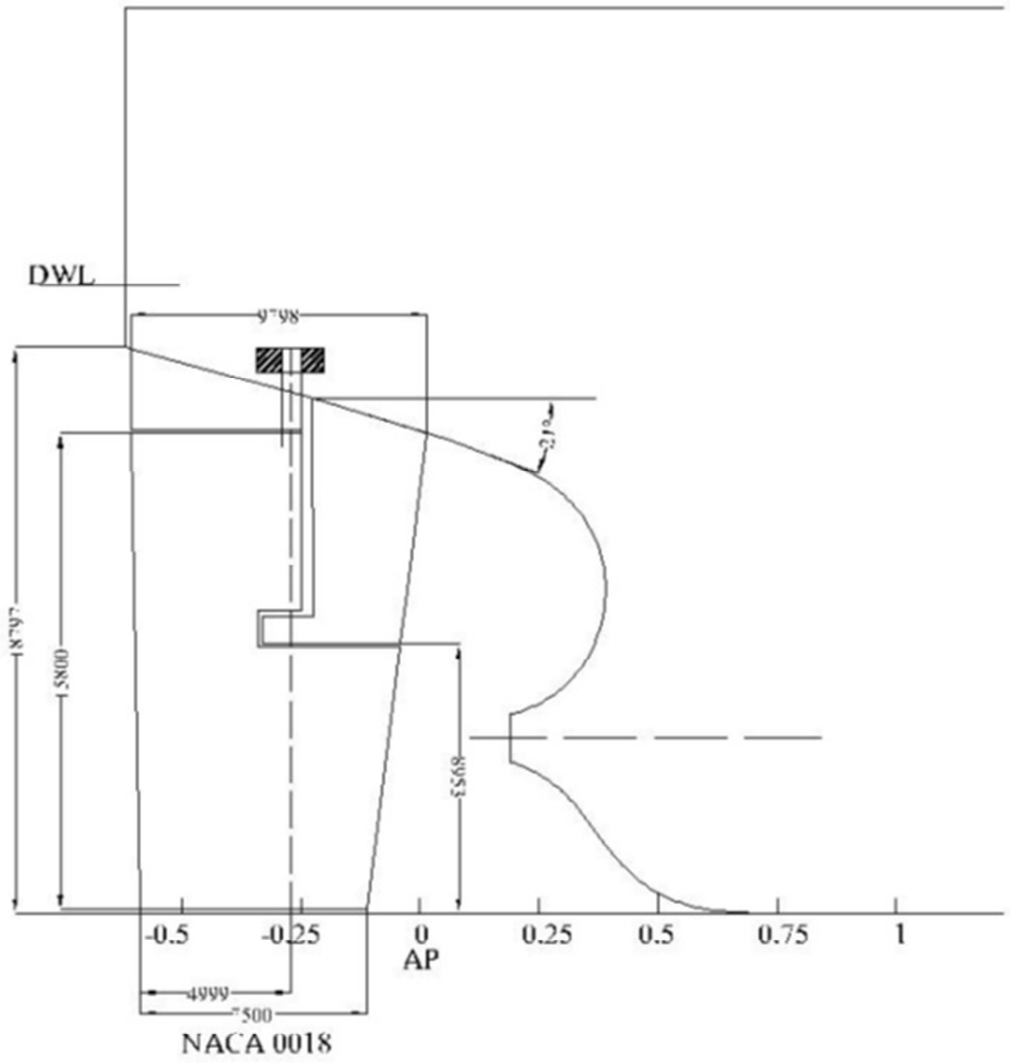

5. APPENDIX 2.3 STANDARDS FOR SHIP MANOEUVRABILITY

Standards for ship manoeuvrability principals and criteria:

Principals

The Standards for ship manoeuvrability (the Standards) should be used to evaluate the manoeuvring performance of ships and to assist those responsible for the design, construction, repair and operation of ships.

It should be noted that the Standards were developed for ships with traditional propulsion and steering systems (e.g. shaft driven ships with conventional rudders). Therefore, the Standards and methods for establishing compliance may be periodically reviewed and updated by the Organization, as appropriate, taking into account new technologies, research and development, and the results of experience with the present Standards.

Standards for ship manoeuvrability – criteria –

The criteria in the standards for ship manoeuvrability, the resolution of MSC137(76) The manoeuvrability of the ship is considered satisfactory if the following criteria are complied with:

1. ***Turning ability***

The advance should not exceed 4.5 ship lengths (L) and the tactical diameter should not exceed 5 ship lengths in the turning circle manoeuvre.

2. ***Initial turning ability***

With the application of 10° rudder angle to port/starboard, the ship should not have travelled more than 2.5 ship lengths by the time the heading has changed by 10° from the original heading.

3. ***Yaw-checking and course-keeping abilities***

The value of the first overshoot angle in the 10°/10° zigzag test should not exceed:

- 10° if L/V is less than 10 s;
- 20° if L/V is 30 s or more;
- (5 + 1/2(L/V)) degrees if L/V is 10 s or more, but less than 30 s,

Where L and V are expressed in m and m/s, respectively.

The value of the second overshoot angle in the 10°/10° zigzag test should not exceed:

- 25°, if L/V is less than 10 s;
- 40°, if L/V is 30 s or more;
- (17.5 + 0.75(L/V))°, if L/V is 10 s or more, but less than 30 s
- The value of the first overshoot angle in the 20°/20° zigzag test should not exceed 25°.

4. ***Stopping ability***

The track reach in the full astern stopping test should not exceed 15 ship lengths. However, this value may be modified by the Administration where ships of large displacement make this criterion impracticable, but should in no case exceed 20 ship lengths.

6. APPENDIX 2.4 FORCE AND TORQUE ACTING ON RUDDER ACCORDING TO BV RULES

1. GENERAL

V_{AV} : is the maximum ahead service speed, in knots, with the ship on summer load waterline; if VAV is less than 10 knots, the maximum service speed is to be taken not less than the value obtained from the following formula: $V_{min} = \frac{V_{AV} + 20}{30}$.

$V_{min} = 11.83$ knots

The maximum ahead service speed is taken equal: Vav = 15.5 knots

V_{AD} : Maximum astern speed, in knots, to be taken not less than 0.5 VAV

$V_{AD} = 0.5 V_{AV} = 7.75$ knots

A : is the Total area of the rudder blade, in m², bounded by the blade external contour, including the main piece and the part ahead of the centre line of the rudder pintle, if any.

The area of the rudder used is taken equal to A = 111.45 m² .

2. RUDDER FORCE

The rudder force C_R is to be obtained, in N, from the following formula:

$C_R = 132\ \eta_R A V^2 r_1 r_2 r_3$

Where:

η_R : Navigation coefficient taken as: $\eta_R = 1$

V : V_{AV} or V_{AD} , depending on the condition under consideration, in the following formulas it is taken as $V = V_{AV}$.

r_1 : Shape factor, to be taken equal to $r_1 = \frac{\lambda+2}{3}$

λ: Coefficient, to be taken equal to: $\lambda = \frac{h^2}{A_T}$ and not greater than 2.

h: Mean height, in m, of the rudder area to be taken equal to (see figure Geometry of rudder blade without cut-outs):

Mean height calculation formula: $h = \frac{z_3 + z_4 - z_2}{2}$

Mean height is taken equal to: h= 15.85 m

Coefficient λ is taken equal to: $\lambda = 1.84$

A_T : Area, in m², to be calculated by adding the rudder blade area A to the area of the rudder post or rudder horn, if any, up to the height h. it is taken : $A_T = 136.7\ m^2$ Hence ,

$r_1 = 1.28$

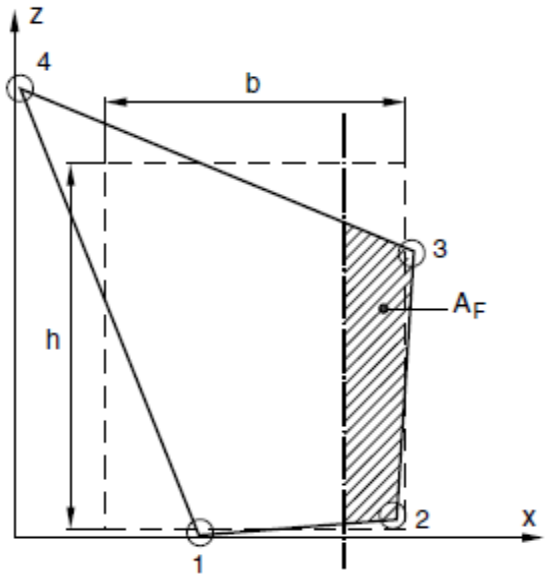

Figure6. 1Geometry of rudder blade without cut-outs

The rudder profile used is **NACA0018**.

r_2 : is a coefficient for the rudder profile.

For ahead condition it is taken equal to: $r_2 = 1.10$

For astern condition it is taken equal to: $r_2 = 0.8$

r_3 : Coefficient to be taken equal to: 0.8 for rudders outside the propeller jet (centre rudders on twin screw ships, or similar cases).

It is taken equal to $r_3 = 0.8$

2.1.Rudder force results

- The Rudder Force for Ahead motion is equal to: $C_R = 3979.69$ kN
- The Rudder Force for stern motion is equal to: $C_R = 723.58$ kN

3. RUDDER TORQUE

3.1.General

The rudder torque M_{TR}, for both ahead and astern conditions, is to be obtained, in N.m, from the following formula: $M_{TR} = C_R\ r$

r : Lever of the force C_R, in m, equal to: $r = b\left(\alpha - \frac{A_F}{A}\right)$ and to be taken not less than 0, 1 b for the ahead condition.

b : Mean breadth, in m, of rudder area to be taken equal to (see figure Geometry of rudder blade without cut-outs):

$$b = \frac{x_3 + x_4 - x_2}{2}$$

α: Coefficient to be taken equal to:

- α = 0,33 for ahead condition
- α = 0,66 for astern condition

A_F: Area, in m², of the rudder blade portion afore the centre line of rudder stock (see figure Geometry of rudder blade without cut-outs).

3.2.Rudder blade description

A rudder blade with cut-outs may have trapezoidal or rectangular contour, as indicated in figure Rudder blades with cut-outs:

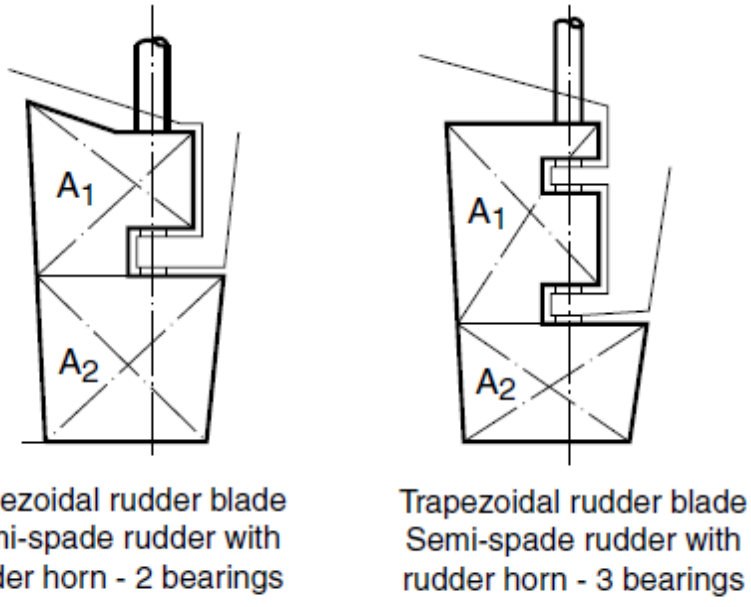

Figure6. 2 Rudder blades with cut-outs

3.3.Rudder torque calculations

The rudder torque M_{TR} , in N.m, is to be calculated with the following procedure:

The rudder blade area A is to be divided into two rectangular or trapezoidal parts having areas A_1 and A_2 , defined in figure Geometry of rudder blade with cut-outs, so that:

$A = A_1 + A_2$

The rudder forces C_{R1} and C_{R2} , acting on each part A_1 and A_2 of the rudder blade, respectively, are to be obtained, in N, from the following formulae:

- $C_{R1} = C_R \frac{A_1}{A}$
- $C_{R2} = C_R \frac{A_2}{A}$

The levers r1 and r2 of the forces C_{R1} and C_{R2} , respectively, are to be obtained, in m, from the following formulae:

- $r_1 = b_1 \left(\alpha - \frac{A_{1F}}{A_1} \right)$
- $r_2 = b_2 \left(\alpha - \frac{A_{2F}}{A_2} \right)$

Where: b_1 , b_2 : Mean breadths of the rudder blade parts having areas A1 and A2, respectively, to be determined according to previous section [b.1].

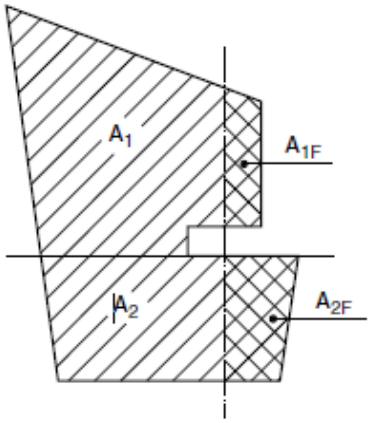

Figure6. 3 Geometry of rudder blade with cut-outs

A_{1F} , A_{2F} : Areas, in m², of the rudder blade parts, defined in figure Geometry of rudder blade with cut-outs.

α: Coefficient to be taken equal to:

- α = 0,33 for ahead condition
- α = 0,66 for astern condition

For rudder parts located behind a fixed structure such as a rudder horn, α is to be taken to:

- α = 0,25 for ahead condition
- α = 0,55 for astern condition

The torques M_{TR1} and M_{TR2}, relevant to the rudder blade parts A_1 and A_2 respectively, are to be obtained, in N.m, from the following formulae:

- $M_{TR1} = C_{R1}\, r_1$
- $M_{TR2} = C_{R2}\, r_2$

The total torque MTR Acting on rudder stock, for both ahead and astern conditions, is to be obtained, in N.m, from the following formula:

$M_{TR} = M_{TR1} + M_{TR2}$

3.4.Rudder torque results

Table 6.1: Summary for BV calculations:

Parameters		Values		
Name	Notation	Ahead	Astern	Unity
The rudder force	CR	3979688,35	723579,70	[N]
The rudder blade area	A	111,45	111,45	[m²]
The rudder blade area part 1	A1	40,22	40,22	[m²]
The rudder blade area part 2	A2	71,23	71,23	[m²]
The rudder force acting on part 1	CR1	1436187,22	261124,95	[N]
The rudder force acting on part 2	CR2	2543501,13	462454,75	[N]
The lever of the forces 1	r1	1,04	3,20	[m]
The lever of the forces 2	r2	-1,18	1,66	[m]
breadth of the rudder blade part 1	b1	7,20	7,20	[m]
breadth of the rudder blade part 2	b2	9,47	9,47	[m]
Area of the rudder blade part 1	A1F	4,23	4,23	[m²]
Area of the rudder blade part 2	A2F	26,67	26,67	[m²]
Coefficient alpha	α	0,25	0,55	--
The torque relevant to the rudder blade part 1	MTR1	1498431,77	836589,54	[N.m]
The torque relevant to the rudder blade part 2	MTR2	2996582,31	769000,80	[N.m]
The rudder torque	MTR	4495014,08	1605590,34	[N.m]

For the ahead condition only, M_{TR} is to be taken not less than the value obtained, in N.m, from the following formula: $M_{TR,MIN} = 0.1 C_R \dfrac{A_1 b_1 + A_2 b_2}{A}$ Hence:

- $M_{TR,MIN}$ = 3442965,79 N.m
- $M_{TR,MIN}$ = 3442,97 kN.m

7. APPENDIX 2.5 RUDDER HYDRODYNAMICS CALCULATION

The determination of hydrodynamic forces and torques acting on the rudder is necessary in order to calculate the diameter of the rudder stock, as well as in determining the power of the steering gear. The total torque of the rudder consists of a hydrodynamic component and a friction component among the rudder shafts. In an initial approximation, it may be considered that the friction moment may be equal to 20% of the value of the hydrodynamic moment.

In order to calculate the hydrodynamic forces acting on the rudder, may be used **the method proposed by Y.I. Voitkounsky [25]**. In principle, the hydrodynamic torques are calculated against the rudder stock, for ahead and astern ship motion, the maximum value being adopted in order to calculate the diameter of the rudder stock and to choice the steering gear. The next section contains the stages of determining the hydrodynamic torque acting on a rudder when the ship is **running ahead**.

a) The influence of the hull on the rudder characteristics is calculated, determining the wake coefficient w and the current deviation angle α_{dc}, for rudders not situated in the longitudinal symmetrical plane.

- Thus, for suspended rudders (trapezoidal or rectangular) whose upper edge is situated at a certain distance from the hull, which is less than the maximum thickness of the rudder blade (Fig. 7.1 a), the wake coefficient is determined by

$$w = \left(0.68 \cdot C_B - 0.25 + \delta w + 0.18 \cdot h_i / H\right) \cdot C_d \qquad (7.1)$$

where C_B is the block coefficient, $\delta w = -0.18$ for cruiser stern, and $\delta w = 0$ for transom stern, the coefficient C_d = 1 for rudders situated in the ship's symmetrical plane, and $C_d = C_B + 0.15$ for rudders placed at borders, while h_i and H are the dimensions shown in Fig. 7-1 a.

- For suspended rudders (trapezoidal or rectangular) whose upper edge is situated at a distance from the ship's hull which is greater than the maximum thickness of the rudder (Fig. 7-1 b), the wake coefficient w is determined by

$$w = \left[0.68 \cdot C_B - 0.43 + \delta w + 0.18 \cdot \left(2 \cdot h_i + \bar{b}\right) / H\right] \cdot C_d \qquad (7.2)$$

where $\bar{b}$ is the rudder height (Fig 7-1 b).

- For semi-suspended rudders (Fig 7-1 c) the following are used

$$w = 1 - \left\{ \left[S_{ps} \cdot (1 - w_i)^2 + S_{pi} \cdot (1 - w_s)^2 \right] / S_{pcj} \right\}^{1/2}$$

$$w_i = \left[0.68 \cdot C_B - 0.43 + \delta w + 0.18 \cdot (2h_i + b_i) / H \right] \cdot C_d \qquad (7.3)$$

$$w_s = \left[0.68 \cdot C_B - 0.43 + \delta w + 0.18 \cdot (2 \cdot h_s + b_s) / H \right] \cdot C_d$$

where S_{pcj} is the area of the rudder section placed in the propeller jet (Fig. 7-2), and the geometrical dimensions S_{pi}, S_{ps}, h_i, h_s, b_i and b_s result from Fig. 7-1 c.

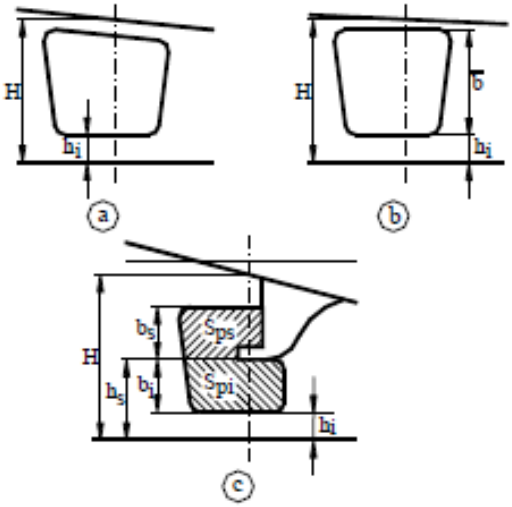

Figure 7-1 Dimensional elements accounting for the wake calculation

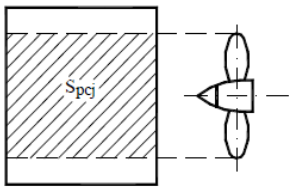

Figure 7-2 The rudder section placed in the propeller current

- for rudders which are not placed in the symmetrical plane, the flow deviation angle α_{dc}, measured in radians, is determined by the formula

$$\alpha_{dc} = 510 \cdot (A_\gamma / L) \cdot (\sin \gamma)^{1/2} \qquad (7.4)$$

where L is the ship's length, while the angle γ and the distance A_γ result from Fig. 7-3. The angle γ is measured between the symmetrical plane and the straight line (traced on the transverse body plane at the middle of the rudder height) perpendicular on the theoretical couple situated at a distance of at least one theoretic interval between couples, towards the forward from the place where the rudder is mounted. Distance A_γ is measured on the above-mentioned line, between the theoretical couple in the vicinity of the rudder stock situated on the forward and the theoretical couple situated at two theoretical intervals from it, on the ship bow.

The sign convention for the α_{dc} angle is as follows:

$\alpha_{dc} > 0$, if the rudder is situated at the starboard side;

$\alpha_{dc} < 0$, if the rudder is placed at the portside.

When the rudder is placed in the symmetric plane, the α_{dc} angle is zero (relation 7.4).

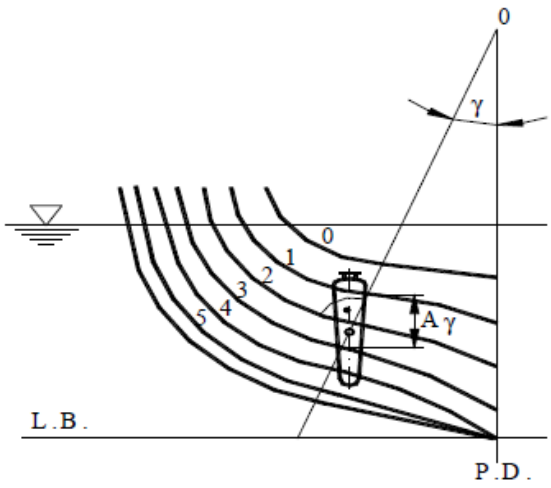

Figure 7-3 The geometrical elements γ and A_γ

b) The next step, the flow speed on the rudder (after exiting the propeller disc) is calculated by the relation

$$v_R = v_A \cdot \left[1 + \left(S_{pcj} / A_R\right) \cdot C_T\right]^{1/2}. \qquad (7.5)$$

The advance speed v_A (the inflow velocity on the propeller disc) is calculated by the formula

$$v_A = U \cdot (1 - w) .$$

C_T is the load coefficient of the propeller

$$C_T = T / \left(0{,}5 \cdot \rho \cdot v_A^2 \cdot A_0\right). \qquad (7.6)$$

T is the propeller thrust, A_0 is the area of the propeller disc, A_R is the rudder area, S_{pcj} is the area of the rudder placed in the propeller's jet, U the ship's speed measured in [m/s].

If the rudder is placed outside the propeller's jet, the flow velocity on the rudder is calculated by the formula

$$v_R = U \cdot (1 - w) \qquad (7.7)$$

where the wake coefficient w is determined on the basis of relations 7.1, 7.2 and 7.3.

c) Taking into consideration the jet rotation in the propeller's disc, the maximum deviation angle of the flow is determined (α_{r_0}, measured in degrees), by using the formula

$$\alpha_{r_0} = 686 \cdot k_Q \cdot \left(\sqrt{1 + C_T} - 1\right) / \left(k_T \cdot \sqrt{1 + C_T}\right) \qquad (7.8)$$

where k_T is the coefficient of the propeller thrust, and k_Q is the coefficient of the propeller torque. The sign convention for the α_{r_0} angle is as follows:

$\alpha_{r_0} > 0$, for the rudder behind the left propeller;

$\alpha_{r_0} < 0$, for the rudder behind the right propeller.

d) The next step is calculating the flow deviation angle, α_{em}, for the rudder section situated in the propeller's jet. According to the 8 possible situations of the rudder-propeller system positions, shown in Fig 7-4, the following calculations of the deviation angle α_{em} may be proposed:

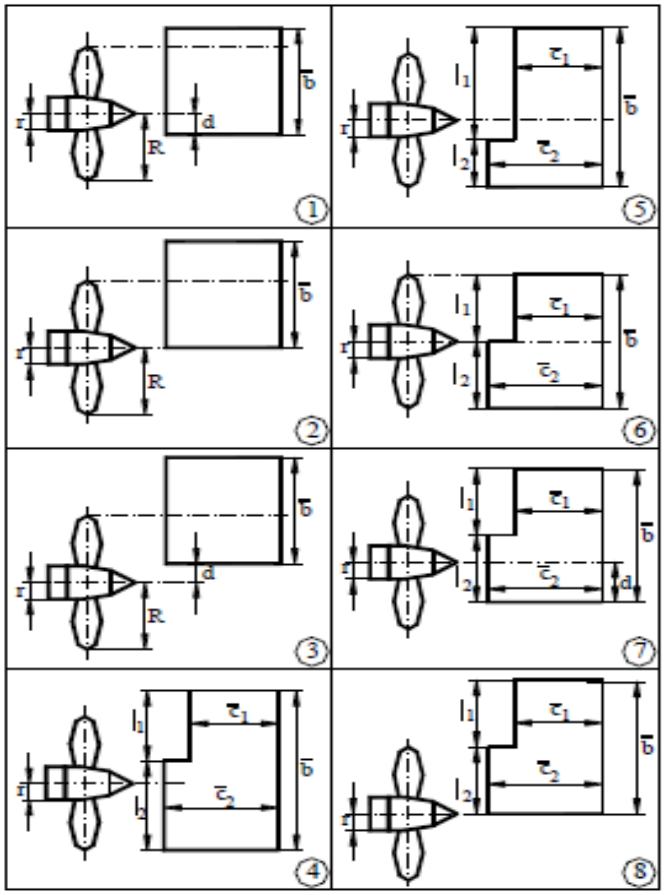

Figure 7-4 The 8 possible situations of the rudder-propeller system positions

· <u>case 1</u>

- if d > r

$$\alpha_{em} = \frac{\alpha_{r_0}}{(d+R)} \cdot \left[0.32 \cdot R - \left(1.8 - \frac{d}{R} \right) \cdot \left(\frac{d - 0.2 \cdot R}{2} \right) \right] \qquad (7.9)$$

- if d < r

$$\alpha_{em} = \alpha_{r_0} \cdot \left(0.4 \cdot R - 3.2 \cdot d^2 / R \right) / (d+R) \qquad (7.10)$$

· <u>cases 2 and 8</u>

$$\alpha_{em} = 0.4 \cdot \alpha_{r_0} \qquad (7.11)$$

· <u>case 3</u>

- if d > r

$$\alpha_{em} = 0.5 \cdot \alpha_{r_0} \cdot \left(1 - \frac{d}{R}\right) \qquad (7.12\ a)$$

- if d < r

$$\alpha_{em} = \frac{\alpha_{r_0}}{R - d} \cdot \left[0.32 \cdot R + 0.8 \cdot \left(1 + \frac{d}{R}\right) \cdot \left(\frac{0.2 \cdot R - d}{2}\right)\right] \qquad (7.12\ b)$$

· <u>cases 4, 5 and 6</u>

$$\alpha_{em} = 0.2 \cdot \alpha_{r_0} \cdot (\bar{c}_1 - \bar{c}_2) / \bar{c} \qquad (7.13)$$

· <u>case 7</u>

- if d > r

$$\alpha_{em} = \frac{\alpha_{r_0}}{(d + R) \cdot \bar{c}} \cdot \left[0.32 \cdot R \cdot \bar{c}_1 - \left(1.8 - \frac{d}{R}\right) \cdot \left(\frac{d - 0.2 \cdot R}{2}\right) \cdot \bar{c}_2\right] \qquad (7.14\ a)$$

- if d < r

$$\alpha_{em} = \alpha_{r_0} \cdot (0.4 \cdot R \cdot \bar{c}_1 - 3.2 \cdot d^2 \cdot \bar{c}_2 / R) / [(d + R) \cdot \bar{c}]. \qquad (7.14\ b)$$

In the above relations, $\bar{c}$ designates the average chord of the rudder section in the propeller jet, $\bar{c}_1$ represents the average chord of rudder section positioned in the upper part of the propeller and $\bar{c}_2$ is the average chord of the rudder section situated in the lower part of the propeller jet. The sign of the α_{em} angle depends on the sign of the α_{r_0} angle.

e) If the rudder plane is displaced laterally to the propeller stock (Fig. 7-6) by the distance y_c, then the current deviation angle (α_{em}) is corrected by multiplication with the coefficient ε_1 obtained from:

$$\varepsilon_1 = 1 - y_c / R \qquad (7.15)$$

where, R is the radius of the propeller disc.

f) The average deviation angle of the propeller jet is calculated for the entire rudder by means of the formula

$$\alpha_{re} = \varepsilon_1 \cdot \alpha_{em} \cdot S_{pcj} / A_R \,. \tag{7.16}$$

g) The deviation angle α_{cm} due to the margin effect of the propeller current is calculated by means of

$$\alpha_{cm} = -\frac{2\pi \cdot n_0 \cdot n_1}{(\lambda_1 + 2\pi \cdot n_0)} \cdot \frac{\lambda_1}{\lambda} \cdot \frac{\left(\sqrt{1+C_T} - 1\right) \cdot (\delta + \varepsilon_1 \cdot \alpha_{em})}{\sqrt{1+(S_{pcj}/A_R) \cdot C_T}} \tag{7.17}$$

where δ is the rudder angle (measured in degrees, positive to starboard), λ is the aspect ratio of the rudder $(\lambda = \bar{b}/\bar{c})$, λ_1 is the relative aspect ratio of the rudder section situated in the propeller jet (the ratio between the average height of the rudder section in the propeller jet and the average geometric chord of the rudder section situated in the propeller jet) and n_0 and n_1 are the coefficients depending on the ratios $\bar{b}/D$ and d/R (Fig. 7-5).

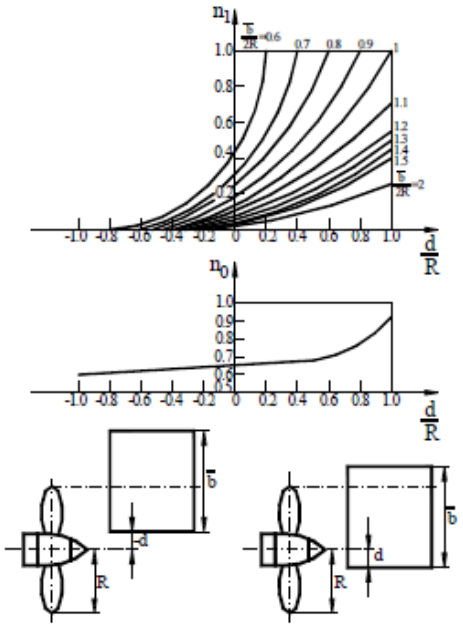

Figure 7-5 Graphical representation of coefficients n0 and n1

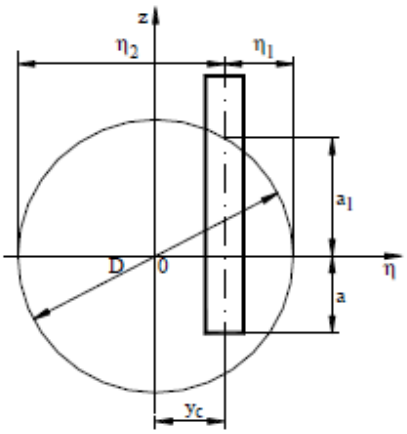

Figure 7-6 The lateral deviation of the rudder plane as compared to the propeller's revolution axis

h) The real attack angle of the rudder placed in the propeller jet, α, is calculated for imposed values of the rudder angle, δ

$$\begin{aligned} \alpha &= \delta + \Delta\alpha \\ \Delta\alpha &= \alpha_{dc} + \alpha_{re} + \alpha_{cm}. \end{aligned} \qquad (7.18)$$

The total correction $\Delta\alpha$ is an algebraic dimension (it has a sign).

i) The hydrodynamic coefficients $C_y(\alpha)$, $C_x(\alpha)$ and $C_m(\alpha)$ are calculated for the geometric aspect ratio λ_p of the rudder.

j) In case the average deviation angle of the propeller current for the entire rudder (α_{re}) is not zero, the correction of the hydrodynamic coefficient of the torque ΔC_m is calculated by means of the relation

$$\Delta C_m = -f_m \cdot \left(\frac{dC_y}{d\alpha_{cor}}\right) \cdot \left(C'_p - A_{pc}/A_R\right)^2 \cdot \frac{\bar{c}}{R} \cdot \alpha_{re} \cdot tg\alpha_{cor} \qquad (7.19)$$

where A_{pc} is the area of the compensated rudder part (situated at the front of the rudder stock) and the angle α_{re} is introduced in radians.

The C'_p coefficient takes into account the additional current on the rudder and is determined by means of the graphic in Fig. 7.7, depending on the rudder aspect ratio λ_p. The correction coefficient f_m has the following values

$$f_m = 1 \qquad \text{for } \bar{c}/R \le 1{,}75$$
$$f_m = 1{,}2 \qquad \text{for } \bar{c}/R > 1{,}75 . \tag{7.20}$$

The dimension $dC_y / d\alpha_{cor}$ represents the slope of the graphical representation of the function $C_y(\alpha_{cor})$ at the intersection point with the abscissa axis.

k) If the rudder plane is displaced laterally as compared to the propeller rotation axis, the corrections $\Delta C'_y$ and $\Delta C'_m$ are calculated for the hydrodynamic coefficients of lift and torque respectively, by means of the relations

$$\Delta C'_y = 2{,}1 \cdot \left(\Delta C'_{y1} - \Delta C'_{y2}\right) \cdot \left(\sqrt{1 + C_T} - 1\right)^2 \cdot \left(S_{pcj} / A_R\right)$$
$$\Delta C'_m = \Delta C'_y \cdot (e/\bar{c} - A_{pc} / A_R) \tag{7.21}$$

where the coefficients $\Delta C'_{y1}$ and $\Delta C'_{y2}$ are determined by means of the graphic in Fig. 1.8, function of the relative thickness $\bar{t}$ and the values η_1 / t_n and η_2 / t_n. The distances η_1 and η_2 are clarified in Fig. 7.6 The notation t_n is the maximum thickness of the rudder in the section of intersection with the horizontal plane crossing the propeller axis. Usually, for NACA profiles the ratio $e / \bar{c} = 0.38$.

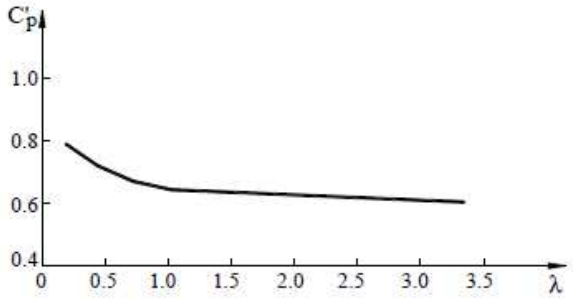

Figure 7-7 The coefficient of the additional current on the rudder, depending on the aspect ratio $C'_p = f(\lambda)$

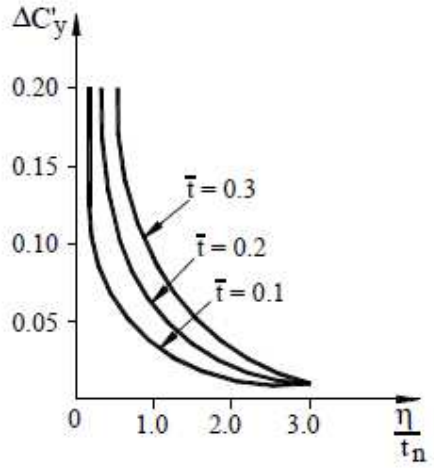

Figure 7-8 Graphical representation of the coefficient $\Delta C'_y = f(\bar{t}, \eta / t_n)$

l) The hydrodynamic coefficients of the rudder are determined by taking into account the corrections mentioned above for the attack angles α_{cor}

$$\begin{aligned} C_y^* &= C_y + \Delta C'_y \\ C_x^* &= C_{x_{cor}} \\ C_m^* &= C_m + \Delta C_m + \Delta C'_m \\ C_n^* &= C_y^* \cdot \cos\alpha_{cor} + C_x^* \cdot \sin\alpha_{cor}. \end{aligned} \tag{7.22}$$

m) Calculations are performed for the normal component of the hydrodynamic force acting on the rudder P_n, the hydrodynamic torque towards the leading edge of the rudder M and the hydrodynamic torque to the rudder stock M_r, using the formulas below, where d_0 is the distance from the rudder stock to the leading edge, v_R is the flow speed on the rudder, e is the distance from the pressure centre to the leading edge, and ρ is the water density

$$\begin{aligned} P_n &= 0{,}5 \cdot C_n^* \cdot \rho \cdot v_R^2 \cdot A_R \\ M &= 0{,}5 \cdot C_m^* \cdot \rho \cdot v_R^2 \cdot A_R \cdot \bar{c} \\ M_r &= P_n \cdot (e - d_0) \\ e &= C_m^* \cdot \bar{c} / C_n^*. \end{aligned} \tag{7.23}$$

- In order to determine the optimal distance from the rudder stock to the leading edge, $(d_0)_{optim}$, calculations are performed for at least 5 values of the distance d_0, situated between $0.15 \cdot \bar{c}$ and $0.35 \cdot \bar{c}$. The function $M_r = f(\alpha_{cor})$ is represented for each of the values of the distance from the rudder stock to the leading edge, designated by d_i (i = 1...4) in Fig. 7.9.
- In order to determine the optimal position of the rudder stock so that the torque on the stock is minimal, the linear functions $M_{r_{max}}(d_i)$ and $-M_{r_{min}}(d_i)$ are represented graphically (Fig. 7.10). At the intersection of the two lines there is the optimum point.

Knowing the optimal value of the distance from the rudder stock to the leading edge $(d_0)_{optim}$, the hydrodynamic torque to the rudder stock is calculated, for ahead speed, by means of

$$(M_r)_{optim} = k_1 \cdot k_2 \cdot P_n \cdot \lfloor e - (d_0)_{optim} \rfloor \qquad (7.24)$$

where k_1 = 1.2 is the safety coefficient for overloads, and k_2 = 1.2 is the shock safety coefficient.

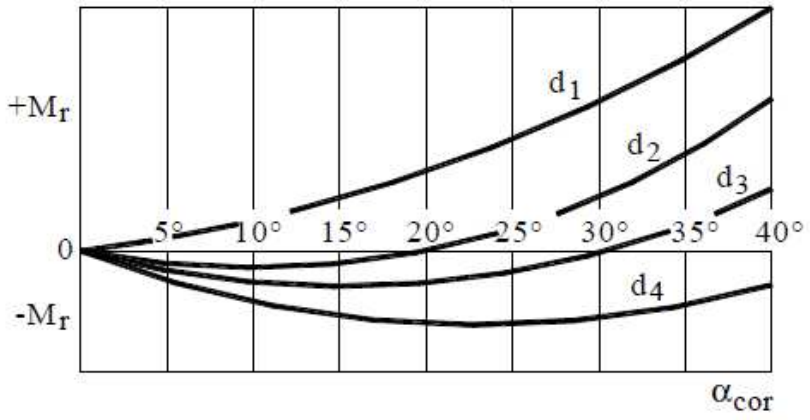

Figure 7-9 Graphical representation of the function $M_r = f(\alpha_{cor})$ for 4 values of the distance from the rudder stock to the leading edge $(d_i, \quad i = 1...4)$

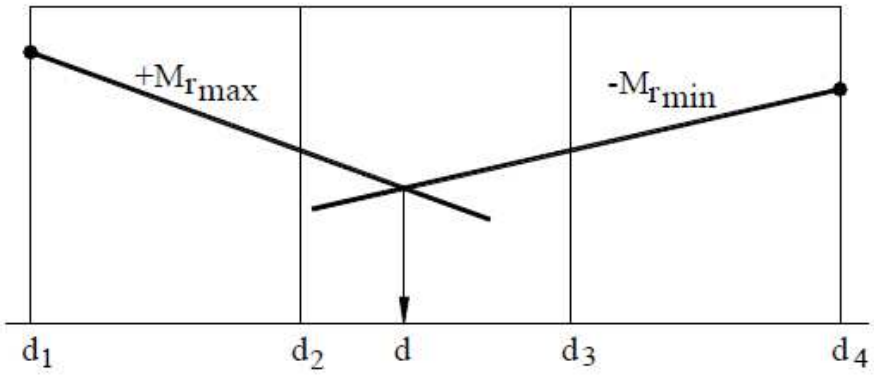

Figure 7-10 Graphical representation of the functions $M_{r_{max}}(d_i)$ and $-M_{r_{min}}(d_i)$

The forces and hydrodynamic torques are further calculated, acting on the rudder in **astern ship motion**.

n) The wake coefficient in the backwards motion w_b is calculated by

$$w_b = 0.5 \cdot w \qquad (7.25)$$

where *w* is the wake coefficient in the forward motion.

o) The flow speed on the rudder in astern motion v_{pb} is calculated by

$$v_{pb} = v_b \cdot (1 - w_b) \tag{7.26}$$

where v_b is the astern ship speed, equal with 70% … 75% of the forward ship speed.

p) The fluid's axial speed before entering the propeller disc is calculated by

$$v_{ab} = 0.35 \cdot v_{pb} \cdot (1 - k_b) \cdot \left(\sqrt{1 + C_{T_b}} - 1\right) \tag{7.27}$$

where C_{T_b} is the propeller loading coefficient in astern motion. The coefficient k_b is determined by

$$k_b = \frac{(x/R)}{\left[0.6 + (x/R)^2\right]^{1/2}} \tag{7.28}$$

where x is the distance from the propeller disc to the rudder leading edge, and R is the radius of the propeller disc.

r) The flow speed on the rudder is calculated, taking into account the influence of the propeller

$$v_{pb_1} = v_{pb} + v_{ab}\,. \tag{7.29}$$

s) The hydrodynamic coefficients $C_{yb}(\alpha)$, $C_{xb}(\alpha)$ and $C_{mb}(\alpha)$ for the aspect ratio λ closest to the real value λ_p of the designed rudder. As in backwards ship motion no corrections are applied for the real attack angle of the rudder, it is virtually equal to the rudder angle $(\alpha = \delta)$.

The coefficient C_{xb} and the attack angle α are taking into account the aspect ratio λ_p, thus reaching the values $C_{xb_{cor}}$ and α_{cor}. The values C_{yb} and C_{mb} remain unchanged.

t) The normal component of the hydrodynamic force acting on the rudder P_{nb} is calculated in backwards ship motion for the attack angles α_{cor}, together with the hydrodynamic torque to the leading edge of the rudder M_b and the hydrodynamic torque to the rudder stock M_{rb}, by means of the relations

$$\begin{aligned}
P_{nb} &= 0{,}5 \cdot C_{nb} \cdot \rho \cdot v_{Rb}^2 \cdot A_R \\
C_{nb} &= C_{yb} \cdot \cos\alpha_{cor} + C_{xb_{cor}} \cdot \sin\alpha_{cor} \\
M_b &= 0{,}5 \cdot C_{mb} \cdot \rho \cdot v_{Rb}^2 \cdot A_R \cdot \bar{c} \\
M_{rb} &= (M_b - P_{nb} \cdot d_f) \cdot k_1 \cdot k_2
\end{aligned} \tag{7.30}$$

where d_f is the distance from the rudder stock to the trailing edge of the rudder, and v_{Rb} is the speed of the flow on the rudder.

For rudders operating within the jet of the propeller, the following relation is considered

$$v_{Rb} = v_{pb_1} . \tag{7.31}$$

For rudders not operating within the propeller jet, the following equality may be used

$$v_{Rb} = v_{pb} . \tag{7.32}$$

Just like in forward ship motion, the hydrodynamic torque to the rudder stock in astern motion is amplified by the product of the safety coefficients $k_1 \cdot k_2$, for overload protection and shock.

Finally, the hydrodynamic torque to the rudder stock in ahead ship motion is compared to astern motion. The maximum value is used in order to determine the power of the steering gear, also taking into account the supplementary torque due to friction within the shafts.

8. APPENDIX 2.6 RUDDER CAVITATION CHECKING

At the design stage, the rudder cavitation checking may be performed on the basis of a theoretical method proposed by Brix ([5], [7]). This method may be applied in the domain $0{,}7D \le h_0 \le D$, where D is the propeller diameter and h_0 is the immersion of the point on the rudder.

The Brix method is based on the following steps:

- Calculate v_A the propeller inflow speed, which may be determined with formula depending of the ship speed U and the wake fraction, w.

$$v_A = U(1-w) \tag{8.1}$$

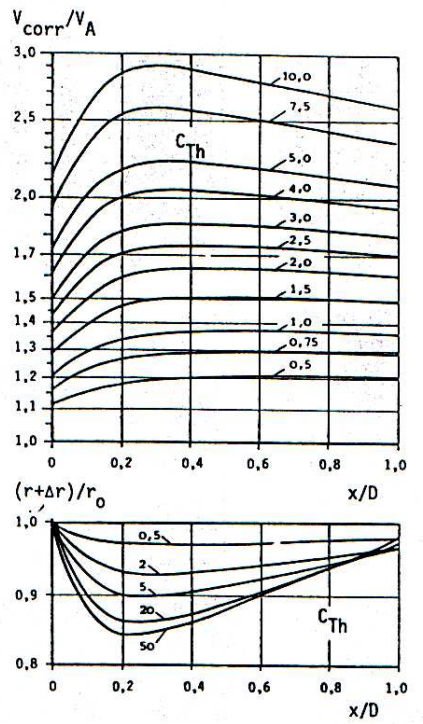

Figure 8-1 The non-dimensional mean axial slipstream speed v corr / v A and slipstream relative radius at different relative positions (x/D) and thrust loading coefficients C_T

- Determine the static pressure with the following formula:

$$q = \frac{1}{2} \cdot \rho \cdot v_A^2 \tag{8.2}$$

- Calculate the propeller disk area

$$A_0 = \pi \cdot \frac{D^2}{4} \tag{8.3}$$

- Determine the thrust loading coefficient for the propeller

$$C_{Th} = \frac{T_p}{A_0 \cdot q} \tag{8.4}$$

Where T_p is the propeller thrust coefficient .

- Determine the relative distance propeller rudder x/D where x is the distance between the propeller disk plan and the leading edge of the rudder see Figure 8-2

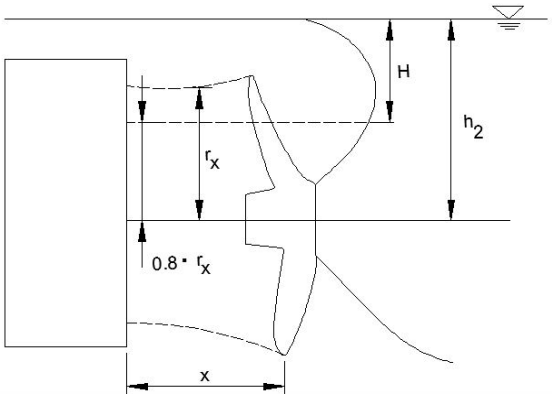

Figure 8-2 Position for rudder cavitation checking

Using Figure 8-1, it's estimated:

- The non dimensional mean axial slipstream speed $v_{corr}/v_A = f(x/D, C_{Th})$;
- Relative ratio $(r+\Delta r)/r_0 = f(x/D, C_{Th})$;
- The slipstream radius $(r + \Delta r)$ and the inflow speed to the rudder (v_{corr}).
- Correcting these values by using the following relations, in order to obtain (v_x) and (r_x)

$$v_x = (v_{corr}^2 + t \cdot U^2)/v_{corr} \tag{8.5}$$

$$r_x = (r + \Delta r) \cdot \sqrt{v_{corr}/v_x} \tag{8.6}$$

where t is the thrust suction fraction and U is the ship speed.

- Estimate the maximum axial speed at the rudder (v_{max}) with relation

$$v_{\max} = v_x + 0{,}12(v_{corr} - v_A) \tag{8.7}$$

where, v_A is the propeller inflow speed.

- Estimate the inflow angle α to the rudder in degrees using Figure 8-3 or the following equivalent relation

$$\alpha = arctg\left(4{,}3\frac{k_Q}{J^2}\cdot\sqrt{\frac{1-\overline{w}}{1-\overline{w}_{local}}}\cdot\frac{v_A}{v_{\max}}\right) \tag{8.8}$$

where k_Q is the propeller torque coefficient, J is advance coefficient, $\overline{w}$ is the mean wake fraction and $\overline{w}_{local}$ is wake fraction at the respective position.

- Determine the maximum local lift coefficient $C_{L_{1\max}}$ from Figure 8-4, depending on the ratio h_1 / r_x, where h_1 is the distance between top/bottom of rudder and propeller axis. The rudder angle $\delta = 3^\circ = 0{,}052\ rad$ is considered, as an allowance for steering rudder angles. Also $(\alpha + \delta)$ is measured in radians and *c* is the chord length of the rudder at the respective height.
- By means of Figure 8-5 determine the extreme negative pressure (p_{dyn}), as a function of $C_{L_{1\max}}$ and the type of profile; the maximum speed $v_{\max}$ is measured in [m/s], the water density ρ is considered in [t/m^3], and the extreme negative pressure results in [kPa].
- Calculate the static pressure (p_{static}) using the relation

$$p_{static} = p_0 + \rho g H \tag{8.9}$$

where p_0 = 103 kPa is the atmospheric pressure and *H* is the distance between the respective point of rudder and the water surface;

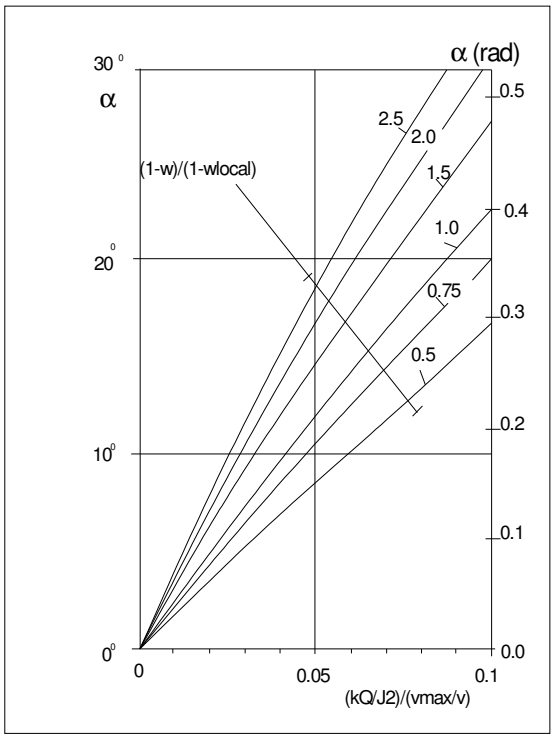

Figure 8-3 Inflow angle α due to rotation of propeller slipstream

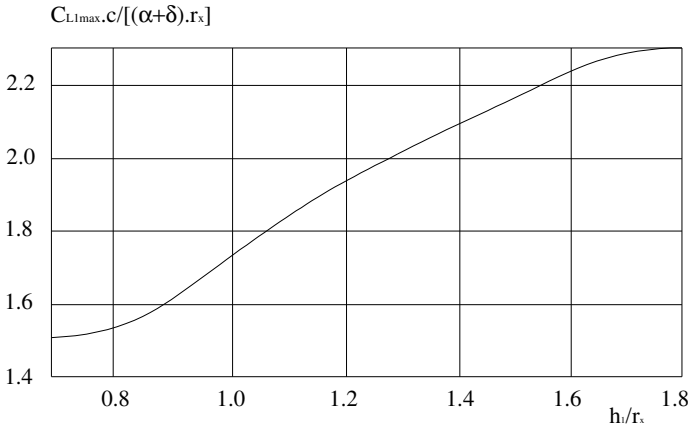

Figure 8-4 The maximum local lift coefficient

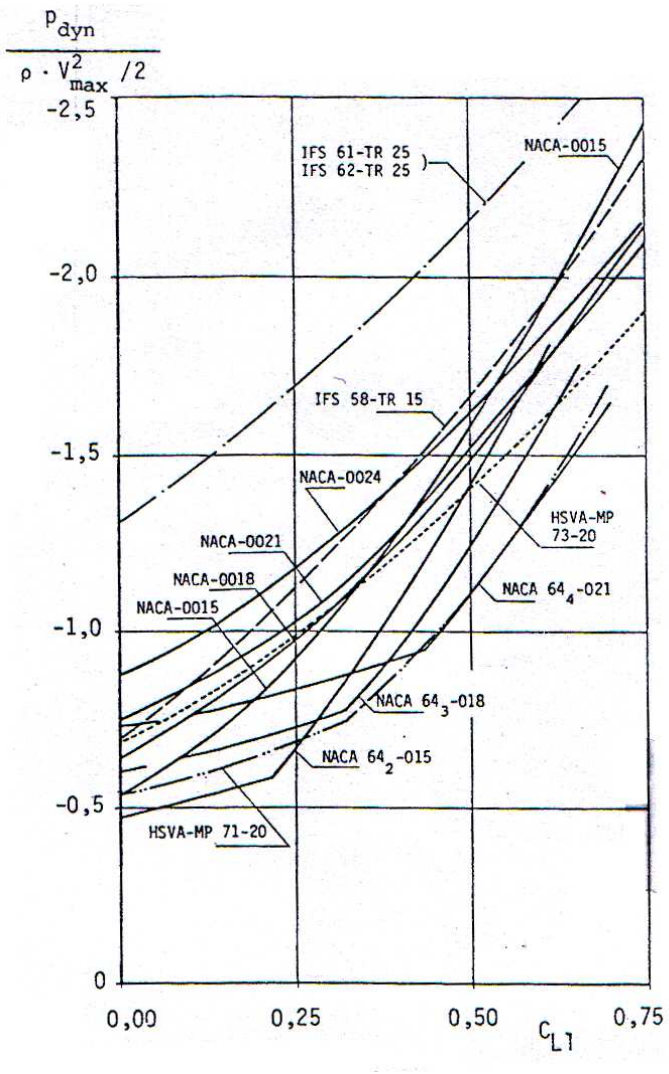

Figure 8-5 Extreme negative dynamic pressure of the suction side

- Calculate the total pressure $\left(p_{static} + p_{dyn}\right)$ on the suction side.
- If the total pressure is negative or slightly positive, the risk of cavitation on the side plating of the rudder is possible.

9. APPENDIX 3.1 HYDRODYNAMIC FORCES DECOMPOSITION

STATIC DRIFT

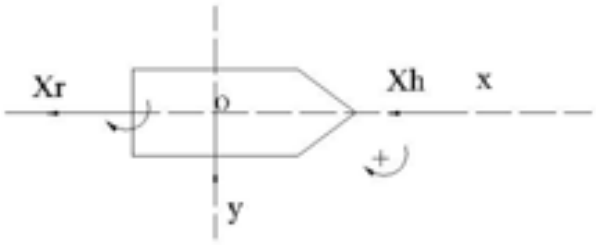

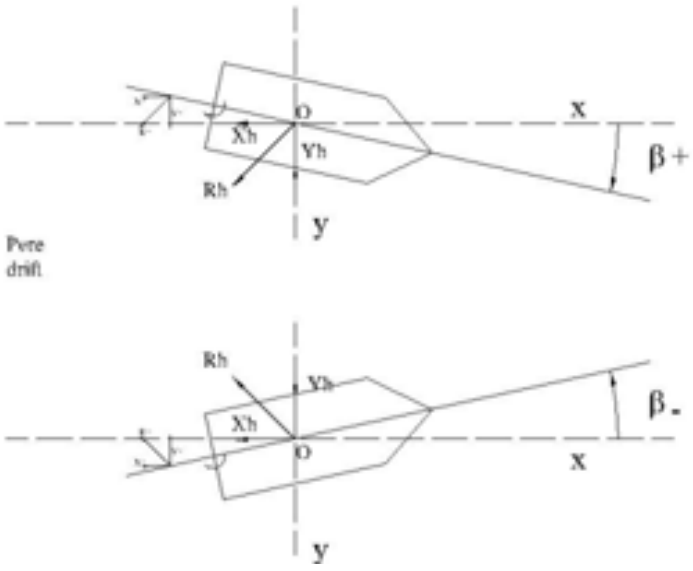

STATIC RUDDER

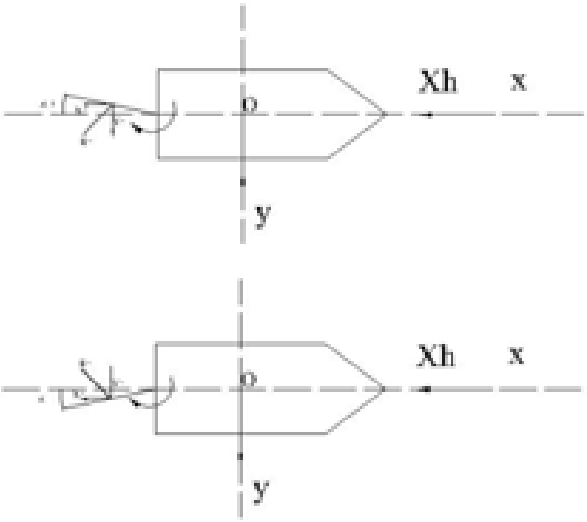

STATIC DRIFT AND RUDDER

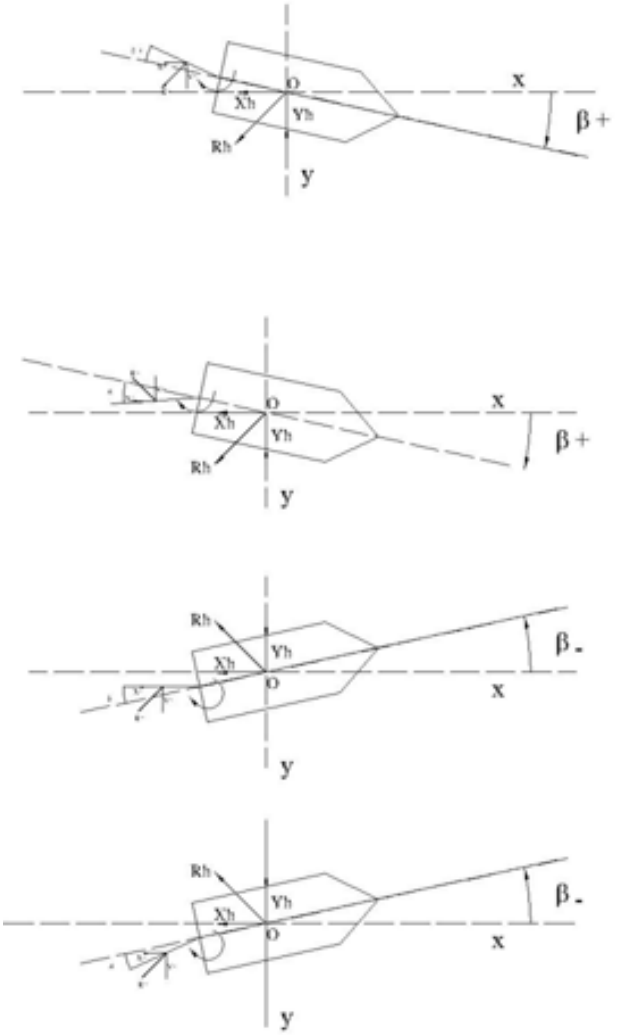

Notations:

Rh – total hydrodynamic force on the hull;

Xh – longitudinal hydrodynamic force on the hull;

Yh – lateral hydrodynamic force on the hull;

Rr – total hydrodynamic force on the rudder;

Xr – longitudinal hydrodynamic force on the rudder;

Yr – lateral hydrodynamic force on the rudder.

10. APPENDIX 4.1 OPEN WATER PROPELLER CHARACTERISTICS

MPP1.mpp

```
                    University of Michigan
          Department of Naval Architecture and Marine Engineering


        Maneuvering Prediction Program (MPP-1.3) by M.G. Parsons

          References:  Clarke,D., Gedling,P., and Hine,G.,
                       "The Application of Manoeuvring Criteria in Hull
                        Design using Linear Theory," Trans. RINA, 1983
                       Lyster, C., and Knights, H. L.,
                       "Prediction Equations for Ships" Turning Circles,"
                        Trans. NECIES, 1978-1979


         Run Identification:


         Input Verification:

              Length of Waterline LWL (m)              =    325.50

              Maximum Beam on LWL (m)                  =     58.00
```

MPP1.mpp

```
              Mean Draft (m)                           =     20.80

              Draft Forward (m)                        =     20.80

              Draft Aft (m)                            =     20.80

              Block Coefficient on LWL CB              =    0.7970

              Molded Volume (m^3)                      = 312968.50

              Center of Gravity LCG (%LWL; + Fwd)      =    3.4400
              Center of Gravity LCG (m from FP)        =    151.55

              Midships to Rudder CE XR (%LWL; + Aft)   =   49.0000
              Rudder Center of Effort XR (m from FP)   =    322.24

              Initial Ship Speed (knots)               =     15.50
              Initial Ship Speed (m/s)                 =    7.9738

              Water Type                               =  Salt@15C
              Water Density (kg/m^3)                   =   1025.87
              Kinematic Viscosity (m^2/s)              =   0.118831E-05

              Yaw Radius of Gyration K33/LWL           =    0.2500

              Water Depth to Ship Draft Ratio H/T      =   1000.00

              Steering Gear Time Constant (s)          =      2.50
```

MPP1.mpp

```
      Total Rudder Area - Fraction of LWL*T     =    0.0200

      Number of Propellers                      =         1

      Type of Single Screw Stern                =    Closed

      Submerged Bow Area - Fraction of LWL*T    =    0.0256




                  University of Michigan
 Department of Naval Architecture and Marine Engineering

Maneuvering Prediction Program (MPP-1.3) by M.G. Parsons


 *** Linear Maneuvering Criteria Option ***

  Reference:  Clarke,D., Gedling,P., and Hine,G.,
              "The Application of Manoeuvring Criteria in Hull
               Design using Linear Theory," Trans. RINA, 1983
```

MPP1.mpp

```
   Linear Maneuvering Derivatives

 Nondimensional Mass             M prime     =  0.018150
 Nondimensional Mass Moment      I sub zz    =  0.001194

 Sway Velocity Derivative        Y sub v     = -0.025383
 Sway Acceleration Derivative    Y sub v dot = -0.015313

 Yaw Velocity Derivative         N sub v     = -0.007818
 Yaw Acceleration Derivative     N sub v dot = -0.001048

 Sway Velocity Derivative        Y sub r     =  0.004811
 Sway Acceleration Derivative    Y sub r dot = -0.001202

 Yaw Velocity Derivative         N sub r     = -0.003598
 Yaw Acceleration Derivative     N sub r dot = -0.000799

 Sway Rudder Derivative          Y sub delta =  0.003834
 Yaw Rudder Derivative           N sub delta = -0.001879


   Time Constants and Gains for Nomoto"s Equation

 Dominant Ship Time Constant    T1 prime     =   52.7298
 Ship Time Constant             T2 prime     =    0.4039
 Numerator Time Constant        T3 prime     =    0.8920
 Numerator Time Constant        T4 prime     =    0.2629


   Evaluation of Turning Ability and Stability

 Inverse Time Constant          1/|T prime|  =    0.0191
 Inverse Gain Factor            1/|K prime|  =    0.0373

 Clarke"s Turning Index                    P =    0.4081
 Linear Dynamic Stability Criterion        C = 0.0000029

 Vessel is hydrodynamically open loop course stable

 Closed Loop Phase Margin with Steering Engine  =   15.8919 degrees


 Approach Speed                    =     15.50 knots

 Rudder Angle                      =     35.00 degrees

 Steady Turning Diameter           =    916.82 meters
 Tactical Diameter                 =   1114.52 meters
 Advance                           =   1002.86 meters
 Transfer                          =    533.18 meters
 Steady Speed in Turn              =      6.32 knots
```

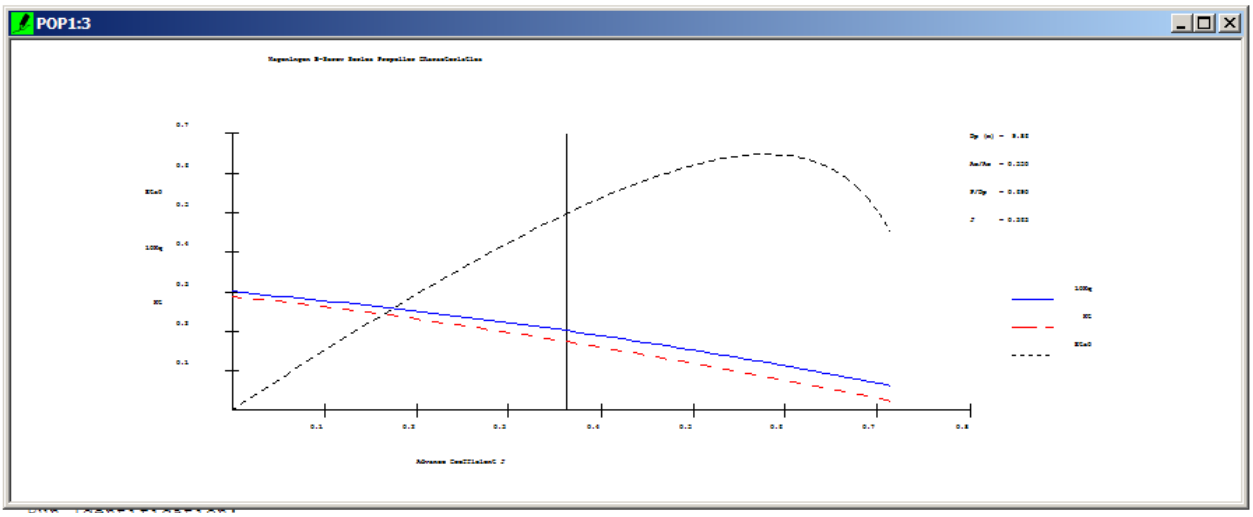
POP1:3

References

[1] Stern, F., Agdrup, K., *SIMMAN Workshop on Verification and Validation of Ship Manoeuvring Simulation Method,* Copenhagen, Denmark, April 2008.

[2] Internet document, *http://www.simman2008.dk/KVLCC/KVLCC2/kvlcc2_geometry.html*

[3] Holtrop, J., Mennen, **G.J.**, *An approximate power prediction method, International Shipbuilding Progress,* 1982.

[4] Molland, A., Turnock, S., *Marine Rudders and Control Surfaces,* Elsevier, 2007.

[5] Brix, J., *Manoeuvring Technical Manual*, Seehafen Verlag, Hamburg, 1993.

[6]Abkowitz, M.A., *Lectures on Ship Hydrodynamics-Steering and Manoeuvrability*, Report No.Hy-5, Hydro- and Aerodynamics Laboratory, Lyngby, Denmark, 1964.

[7] Obreja, C.D., *Ship manoeuvrability lecture***,** "Dunarea de Jos" University of Galati, Erasmus Mundus Ship, 2016.

[8] Strom-Tejsen, J., *A Digital Computer Technique for Prediction of Standard Maneuvers of Surface Ship*, Research and Development Report, David Taylor Model Basin, Washington, 1965.

[9] Stern, F., Agdrup, K., Kim, S.Y., Hochbaum, A.C., Rhee, K.P., Quadvlieg, F., Perdon, P., Hino, T., Broglia, R., Gorski, J., *The First Workshop on Verification and Validation of Ship Maneuvering Simulation Methods,* Experience from SIMMAN 2008.

[10] Marcu, O., Jagite, G., Ivanov, S., *Model Scale Resistance Computation for the KRISO Container Ship,* The Annals of "Dunarea de Jos" University of Galati, Fascicle XI, Shipbuilding, pp. 103-108, 2012.

[11] Marcu, O., *Contributions to the study of the flow around the bare hull*, Report of scientific research, "Dunarea de Jos" University of Galati, 2010.

[12] Marcu, O., Lungu, A., Obreja, **C.D.**, *Hydrodynamic Performance of the KVLCC2 Tanker Hull*, The Annals of "Dunarea de Jos" University of Galati, Fascicle XI, Shipbuilding, pp. 19-26, 2012.

[13] Amoraritei, M., *Ship propulsion lecture***,** "Dunarea de Jos" University of Galati, Erasmus Mundus Ship, 2016.

[14] Marcu, O., *Contributions to the study of the flow developed around the ship hull equipped with propeller and rudder,* Teza de doctorat, 2012

[15] ITTC – Recommended Procedures and Guidelines 7.5-03-01-01, *"Verification and Validation Recommended Procedures"*, 2002.

[16] ITTC – Recommended Procedures and Guidelines 7.5-02-03-01-4,*"Performance, Propulsion 1978 ITTC Performance Prediction Method"*, 1999.

[17] Frangu, R., *POLYNEW Computer Code*, "Dunarea de Jos" University of Galati, 1998.

[18] Obreja, D.C., **Nabergoj, R., Crudu, L., Păcuraru, S.,** *Identification of Hydrodynamic Coefficients for Manoeuvring Simulation Model of a Fishing Vessel*, Ocean Engineering, Vol. 37, Iss. 8-9, ISSN 0029-8018, pp. 678-687, 2010.

[19] Obreja, D.C., Nabergoj, R., Crudu, L., Păcuraru, S., *PMM Tests. Manoeuvring Simulation of a Mediterranean Fishing Vessel,* Proceedings of the 5th International Congress on Maritime Technological Innovations and Research, Barcelona, Spain, pp. 201-210, 2007.

[20] Strom-Tejsen, J., Chislett, M.S., *A Model Testing Technique and Method of Analysis for the Prediction of Steering and Manoeuvring Qualities of Surface Vessels*, Report No.Hy-7, Lyngby, Denmark, September 1966.

[21] Strom-Tejsen, J., *A Digital Computer Technique for Prediction of Standard Maneuvers of Surface Ship*, Research and Development Report, David Taylor Model Basin, Washington, December 1965.

[22] Obreja, D.C., *PMMPROG Computer Code*, Research Centre of the Naval Architecture Faculty, "Dunarea de Jos" University of Galati, 2002.

[23] Eca, L., Hoekstra, M., Toxopeus, S.L., *Calculation of the flow around the KVLCC2M*, CFD workshop Tokyo, Tokyo, Japonia, 2005.

[24] Stern, F., Agdrup, K., Kim, S. Y., Cura–Hochbaum, A., Rhee, K. P., Quadvlieg, F., Perdon, P., Hino, T., Broglia, R., Gorski J., *Experience from SIMMAN 2008–The first workshop on verification and validation of ship maneuvering simulations methods*, Journal of Ship Research, Vol. 55, No. 2, pp. 135–147, 2011.

[25] Voitkounsky, Y.I., *Spravocinik po Teoria Korablea*, Sudostroenie, Sankt Petersburg, 1985 (in Russian).